DISSERTATION

ALGAL BLOOMS IN THE ALPINE: INVESTIGATING THE COUPLED EFFECTS OF WARMING AND NUTRIENT DEPOSITION ON MOUNTAIN LAKES

Submitted by

Isabella Anna Oleksy

Graduate Degree Program in Ecology

In partial fulfillment of the requirements

For the Degree of Doctor of Philosophy

Colorado State University

Fort Collins, Colorado

Summer 2019

Doctoral committee:

Advisor: Jill S. Baron

Sarah A. Spaulding
N. LeRoy Poff
Timothy Covino

ABSTRACT

ALGAL BLOOMS IN THE ALPINE: INVESTIGATING THE COUPLED EFFECTS OF WARMING AND NUTRIENT DEPOSITION ON MOUNTAIN LAKES

While 20th century atmospheric nitrogen (N) deposition has been strongly linked to changes in diatom assemblages in high-elevation lakes, contemporaneous changes in other algae suggest additional causes. Using proxies preserved in lake sediments, we explored the origin and magnitude of changes in an alpine and subalpine lake from the end of the Little Ice Age in the 19th century to ca. 2010. We found dramatic changes in algal community structure. Diatom analyses revealed a pronounced shift from majority benthic to planktonic diatoms ca. 1950, coincident with the rise of atmospheric N deposition. Pigments representing benthic green algae have increased 200-300% since ca. 1950; diatom pigments suggest stable or slightly declining populations. Cyanophytes and cryptophytes are not abundant in the sediment record, but there has been a slight increase in some taxa since ca. 1950. While some changes began ca. 1900, the shifts in nearly all indicators of change accelerate ca. 1950 commensurate with many human-caused changes to the Earth system. In addition to N deposition, there have been marked recent increases in aeolian deposition to western mountains that contributes phosphorus. Strong increases in summer air (0.7 °C per decade) and surface water (0.2-0.5°C per decade) temperatures since 1983 have direct and indirect consequences for high elevation ecosystems. While our links between the causes of changes and the responses of mountain lake primary producers are inferred, the

drivers and their responses are indicators of changes in the Earth system that have been used to define the Anthropocene.

Algal communities (or assemblages) in historically unproductive mountain lakes are shifting, and these changes are taking place commensurate with increasing water temperatures and nutrient availability. However, the mechanisms promoting chlorophytes over bacillariophytes and the implications for ecosystem function are not well understood. We tested the effect of nutrient enrichment on the relative abundance of algal taxonomic groups in a field experiment. We also tested the interactive effects of nutrients and temperature on ecological function of chlorophyte-dominated benthic communities in a laboratory experiment. Nutrient enrichment of both nitrogen and phosphorus favored chlorophytes and led to the highest overall algal biomass. In the absence of nutrient enrichment, the relative abundance of bacillariophytes was significantly greater than chlorophytes and cyanobacteria. Nitrogen assimilation increased significantly, but net ecosystem production decreased, with warming temperatures. Collectively, our results show how chronic N deposition, permafrost thaw, P deposition, and a warming climate interact to alter both the structure and function of mountain lake algal communities.

Climate change is altering biogeochemical, metabolic, and ecological functions in lakes across the globe. Historically, high-elevation lakes in temperate regions have been unproductive due to brief ice-free seasons, a snowmelt-driven hydrograph, cold temperatures, and steep topography with low vegetation and soil cover. Observed increases in high elevation lake productivity in the Southern Rocky Mountains over the past decade led us to ask: what are the drivers behind increasing primary productivity?

We tested the relative importance of winter and summer weather, watershed characteristics, and water chemistry as drivers of phytoplankton dynamics. Boosted regression tree models were applied using data from 28 high-elevation lakes in Colorado to examine spatial, intra-seasonal, and inter-annual drivers of variability in lake phytoplankton, using chlorophyll a as a proxy. Similar to previous studies, we found that phytoplankton biomass was inversely related to the maximum snow water equivalent (SWE) of the previous winter. However, even in years with average SWE, summer precipitation extremes and warming enhanced phytoplankton biomass. Peak phytoplankton biomass consistently coincided with the warmest water temperatures and lowest nitrogen to phosphorus ratios. While links between declining snowpack, lake temperature, nutrients, and organic matter dynamics are increasingly recognized as critical drivers of change in high elevation lakes, this study identifies additional processes that will influence lake productivity as the climate continues to change. Continued changes in the timing, type, and magnitude of precipitation in combination with other global change drivers (e.g., nutrient deposition) may have consequences for production in high elevation lakes, potentially shifting these historically oligotrophic lakes toward new ecosystem states.

ACKNOWLEDGMENTS

I am grateful for financial support from the U.S. Geological Survey Western Mountain Initiative and NSF IGERT Grant No. DGE-0966346 'I-WATER: 649 Integrated Water, Atmosphere, Ecosystems Education and Research Program.'

I know it's cliché, but they say, "it takes a village," and that's especially true for alpine fieldwork. Thank you to everyone who has carried samples with me up and down the mountain, many of you countless times. Your positivity, conversations, and laughter made every 4 am wake up well worth it: In no particular order, I'd like to acknowledge: Tim Fegel, Melanie Burnett, Tyler Lampard, Ryan Davis, Maddy Dragna Davis, Kim Vincent, Jessica Johnstone, Christa Torrens, Becky Wininok-Huber, Diane Meraz, Mitch Ralson, Sam Dunn, Sydney Clark, Katie Lane, Fabio Lepori & Sybel, Alyssa Anenberg, Brian Zieger, Kristen Savage,Tim Weinmann, Georg Niedrist, Jordan Allen, Will Creed, Christie Wilkins, Jackson Ingram, Michelle Hollenkamp, Teddy Nolan, Kevin Zagorda, Jason Price, Amy McMahon, Erin Pettigrew, James Roberts, Bernie Hoyer, John Koss, John Hammond, Kelly Loria. Every single datapoint in this thesis belongs to you all, too. A special recognition goes out to Daniel Bowker, the best field companion I could ever ask for. I'll never forget our adventures in the Mummies, our philosophical musings, and our daydreams about the Utah desert. I have enough music and book recommendations to keep me entertained for a lifetime. Thank you for being my sounding board, especially in the early days of my Ph.D. when I was constantly doubting myself.

Thank you to Peter Leavitt, Heather Haig, Nicole Hayes, and Deirdre Bateson for your guidance and mentorship in paleoanalyses and for being such gracious hosts in

my two weeks in Regina, SK. Thank you to everyone who has trained me in all things analytical chemistry, especially Dan Reuss, Guy Beresford, and Claudia Boot. Thank you to my I-WATER comrades Whitney Beck, Cara Steger, Rod Lammers, Kyle Christianson. It's been so fun working with you all and I look forward to our continued collaborations as we continue to grow as scientists. Thank you Yamina Pressler for sharing your perspective and wisdom on productivity and work-life balance— you completely transformed my attitude toward my work last year (it's never too late!) and the way I approach writing.

Last, but not least, I would like to thank Jill Baron for her mentorship and tireless support the last five years. It's been an honor and a privilege to work together and to travel the world sharing our results. Thank you for taking a chance on me, and for pushing me in my writing and helping me hone my communication skills. You are a stellar example of how to be an effective leader and collaborator while also cultivating the creativity of the people with whom you work. I look forward to continuing working together for many years to come.

DEDICATION

This thesis is dedicated to family. To my mom and dad: thank you for everything you have sacrificed to give me and Ala the best life possible. Thank you for always championing my work and for encouraging me to pursue my dreams, even in the male-dominated spaces of cycling and science. I have you to thank for my eastern European work ethic that you instilled in me from a very young age. Thank you for always giving me the option to quit— even though you know I wouldn't. Even though I didn't always appreciate it at the time, I am so grateful that you pushed me in everything I did. This thesis is a product of your unconditional love and I'm forever grateful.

To Ala: thank you for being my biggest fan, my soul sister, and my continuous source of inspiration. Knowing you are only a phone call away brings me immense peace. I can't wait to live closer together and to watch you make your dreams come true, too. I love you so much.

In loving memory of Babcia Helena i Dziadek Stanislaw Oleksy, Wujek Krzysiek Fidos. Chciałbym, żebyś mnie teraz widział. Trzymam cię w sercu.

TABLE OF CONTENTS

LIST OF TABLES

LIST OF FIGURES

1. INTRODUCTION

Lakes, wetlands, and streams occupy a relatively small proportion of total land surface area on Earth, yet they play a disproportionately large role in assimilating and processing materials from the landscape (McClain et al. 2003; Tranvik et al. 2009; Clow et al. 2015). In addition to being home to a wealth of biodiversity, mountain headwater ecosystems in particular provide a myriad of ecosystem services including drinking water supply, tourism and recreational opportunities, energy production, cultural values (Grêt-Eegamey, Brunner, and Kienast 2012). In regions like the Rocky Mountains, USA, these landscapes are typically characterized by low soil organic matter and sparse plant cover. At the highest elevations, mountain landscapes are frozen much of the year, leading to hydrology that is tightly coupled to snowpack and the cryosphere more generally. With a warming climate altering timing and magnitude of snowfall and rapidly shrinking glaciers, it is important to understand how mountain headwater aquatic ecosystems are responding to these widespread climatic-driven changes so that we can better understand future changes in ecological function (Mote et al. 2005, 2018; Milner et al. 2017).

Mountain lakes are valuable systems for studying the impacts of environmental and climate change on ecological and biogeochemical functions because they are particularly sensitive to changes in the airshed (e.g., aeolian inputs, climate) (Catalan et al. 2006; Schmeller et al. 2018). Furthermore, within a relatively constrained geographic area, steep gradients cause certain factors like temperature, UV radiation, and evapotranspiration to vary predictably with elevation, allowing for space-for-time

substitutions that would elsewhere need to be performed on a large longitudinal transect at lower elevations. Littoral zones of oligotrophic mountain lakes are typically the most productive and diverse parts of the ecosystem and are effective integrators of both local and large-scale environmental heterogeneity in their ecological and biogeochemical characteristics (Zaharescu et al. 2016).

Lowland lakes in western Europe have seen human influence since the dawn of agriculture ca. 6000 years ago with an intensification of adverse impacts associated with widespread Bronze Age deforestation (Birks et al. 1988; Bradshaw, Rasmussen, and Vad Odgaard 2005). Even in the relatively remote, mountainous lakes in Europe and central Asia, humans have been agents of environmental change for thousands of years (González-Sampériz et al. 2017; Berglund 2011; Colombaroli et al. 2013). Prior to European contact in North America, land use alterations associated with agriculture and deforestation by indigenous people were extensive (Delcourt et al. 1998), but European colonialism and the industrial revolution accelerated environmental change (Köster et al. 2007; Hilfinger et al. 2001; Wohl, Lininger, and Baron 2017). In contrast to lower elevation regions, the rugged and mountainous areas of the western U.S. and the lakes therein have only recently had major Euro-American-driven influence (Vale 1998, 2002), allowing us to identify and track environmental change from its very onset, without being masked by land use change, sewage, and waves of invasive species. Western mountain lakes in North America (hereafter “western mountain lakes”) record distinct transitions between the Holocene and Anthropocene in their sediments, recording the fingerprint of widespread human disturbance of global biogeochemical cycles (Wolfe et al. 2013; Vitousek et al. 1997). These lakes were relatively pristine up until only very

recently (ca. 150 years BP), thus studying these systems gives us valuable insights into aquatic ecosystem function more generally.

Although not directly impacted by land-use change and point-source pollution, western mountain lakes are sensitive to drivers of ecosystem change originating from outside watershed boundaries. Atmospheric deposition of agricultural and industrial pollutants as well as exogenous, aeolian dust, can deposit nutrients in alpine watersheds, serving as subsidies in these otherwise nutrient-starved ecosystems (Baron 2006; Brahney, Mahowald, et al. 2015; Moser et al. 2019). In the central Rocky Mountains of Colorado, relatively low deposition rates of nitrogen (3-5 kg ha^{-1} $year^{-1}$) have altered both terrestrial and aquatic processes; a short growing season, little vegetation, and poorly developed soils result in the limited ability of alpine catchments to consume excess nitrogen compared to regions such as the north temperate United States (Williams and Baron 1996). In subalpine forests on the Colorado Front Range, foliar and soil stoichiometry have been altered, and nitrogen mineralization rates are enhanced relative to areas receiving less nitrogen deposition (Baron et al. 2000). In lakes, the onset of nitrogen deposition and associated changes in lake chemistry can be traced with lake sediment reconstructions, with algal subfossils offering insight into environmental change. Specifically, even modest levels of air pollution (and the nitrogen it delivers) increased the production of alpine lakes and changed phytoplankton species assemblages (Wolfe, Baron, and Cornett 2001; Wolfe, Van Gorp, and Baron 2003; Enders et al. 2008). In other western mountain lakes, nutrients such as phosphorus (P) associated with dust impacts, have similarly altered algal assemblages by essentially fertilizing the lakes (Brahney et al. 2014; Brahney, Ballantyne, et al. 2015).

Like the Arctic, many mountainous regions across the globe are experiencing amplified rates of warming, adding urgency to understand how warming associated climatic shifts may be impacting alpine aquatic ecosystems (Pepin et al. 2015; Palazzi et al. 2019). Arctic lakes show a distinct climate signal in sediment records resulting in altered phytoplankton ecology (Mueller et al. 2009; Smol et al. 2005). Globally, over the last 25 years, surface temperatures of seasonally ice-covered lakes have been increasing at the rate of 0.72°C decade^{-1} and lake ice cover has also decreased in duration over this same period (Sharma et al. 2019; O'Reilly et al. 2015). Locally, lake surface temperature warming rates in the southern Rocky Mountains (SRM) are slightly lower than the global average (0.13ºC decade^{-1}; Christianson et al. 2019) potentially because headwater lakes can be buffered by cryospheric inputs. Nonetheless, we can anticipate continued warming of lakes across the southern Rocky Mountains through the end of the 21st century at a rate of 0.47 ºC decade^{-1} on average (Roberts et al. 2017).

Climate change may both directly and indirectly impact lake physical structure, ecological function, and ecosystem metabolism (Thompson, Kamenik, and Schmidt 2005). Altered precipitation regimes and trends toward earlier snowmelt will further influence lake structure and function, potentially increasing lake productivity (Clow 2010; Preston et al. 2016). As the surrounding terrestrial landscape responds to these changes loading of materials into lakes as the climate continues to change may also play a role in altered ecology and biogeochemical cycling (Dong et al. 2019).

To date there has been little investigation into western mountain lakes and the interaction of climate and anthropogenic stressors on lake ecosystems. While multiple

concurrent stressors will likely impact lake production and nitrogen cycling, disentangling the effect of climatic and anthropogenic stressors on ecosystem function is notoriously difficult (Ollinger et al. 1993; Baron, Schmidt, and Hartman 2009). By combining data from paleolimnological studies, regional surveys and long-term monitoring, we can begin to understand what characteristics of lakes and the watersheds they occupy make an individual lake more resistant changes in ecosystem function, like primary production. For example, aspect and slope and position of a lake in a landscape may cause variation in a lake's sensitivity to some of these changes (Sadro, Nelson, and Melack 2012). However, the structure of the biotic community (e.g., zooplankton community composition and diversity, introduced sport fish) can also influence total lake production, but these communities also highly sensitive to climatic variation (Loewen et al, 2018). The net impact of climate change can be complicated by cross-scale interactions when drivers and responses occur at varying spatial and temporal scales, resulting in difficult to predict dynamics and nonlinear patterns (Soranno et al. 2014).

In recent decades, reports of nearshore benthic algal blooms dominated by filamentous green algae (e.g., *Spirogyra spp., Cladophora spp., Mougeoutia spp., Zygnema spp.)* are increasing, including in historically oligotrophic lakes (Kravtsova et al. 2014). These, often anecdotal, accounts include the Loch Vale Watershed, Colorado, USA, where observations of dense, filamentous green algal mats are now common, particularly in late summer and in alpine lakes and streams. Filamentous green algae can be early warning indicators of environmental change, including cultural eutrophication, acidification, or food web alterations (Turner et al. 1995; Cattaneo et al.

1995; Lambert, Cattaneo, and Carignan 2008). While cultural eutrophication is sometimes an obvious contributor to increased benthic algal growth (Hampton et al. 2011; Rosenberger et al. 2008), the cause of increase is not always so clear (Naranjo et al. 2019). The implications of changing benthic algal community composition and potentially increasing production on ecosystem function are not well understood. Further complicating the problem, benthic environments are rarely investigated in lakes as compared to streams, and Loch Vale is no exception (but see (Nydick et al. 2004). Understanding phytoplankton ecology has been a cornerstone of limnology, but benthic algal ecology in lakes has received far less attention (Cantonati and Lowe 2014).

Algae are valuable ecological indicators in aquatic ecosystems because they respond quickly and predictably to changes in environmental conditions such as flow, light, temperature, and nutrients. Their high turnover rates make them highly responsive to small changes in carbon, nitrogen, and other essential nutrients, which can have implications on food quality for higher trophic levels and downstream water chemistry. At the base of the food web, algae provide essential nutrients for grazers which propagate up through the food web supporting higher trophic levels. Investigating lakes and the algal communities within them gives scientists an integrated view of ecosystem function and allows us to gain insight both present and past environmental and climatic conditions (Smol and Cumming 2000; Bellinger and Sigee 2015).

1.1 Motivating questions

In an effort to understand consequence of multiple drivers of global change on algal communities in Rocky Mountain lakes as well as the potential mechanisms by

which these communities may be changing, in this dissertation I asked the following questions:

(1) Are benthic chlorophytes increasing in the Loch Vale watershed? If so, when did they begin to increase and can we infer the causes? (Chapter 2)?

(2) How does the taxonomic structure of the benthic algae community (e.g. diatoms, chlorophytes, cyanobacteria) change in response to nutrient additions *in situ* (Chapter 3)?

(3) What are the impacts of nutrient enrichment and temperature on ecosystem function of green algal-dominated biofilms (Chapter 3)?

(4) What are the drivers of variation of in phytoplankton dynamics across central Rocky Mountain lakes at regional, interannual, and intraseasonal scales (Chapter 4)?

1.2 Chapter descriptions

To address these questions, I collected sediments cores and analyzed major algal pigment subfossils, diatom subfossils, and geochemical proxies in order to reconstruct the paleoecology of algal communities in the subalpine Loch and alpine Sky Pond (Chapter 2). In the summer of 2017, I conducted a nutrient diffusing substrate experiment in Sky Pond in addition to a laboratory incubation in which we manipulated nutrient and temperature conditions on field-collected green algal-dominated biofilms. This allowed me to understand how nutrients and temperature individually and interactively alter algal structure and function (Chapter 3). In order to predict how the productivity of these ecosystems will change into the future, we first need to understand the current drivers of algal dynamics. To that end, I compiled three distinct datasets to

understand the drivers of phytoplankton biomass at varying spatial and temporal scales (regional, inter-annual, and intra-seasonal). These data included my own personal collections from summer 2015-2017 in Loch Vale Watershed, long-term (2008-2016) data from Niwot Ridge LTER, and a synoptic survey of Colorado Front Range lakes (2016) with data contributed by co-authors.

In the paleolimnological study (Chapter 2), I used multiple proxies preserved in lake sediments to explore the origin and magnitude of changes in an alpine and subalpine lake from the end of the Little Ice Age in the 19th century to ca. 2010. We found dramatic changes in algal community structure. In Sky Pond, diatom subfossil analyses revealed a pronounced shift from majority benthic to planktonic diatoms ca. 1950, coincident with the rise of atmospheric N deposition. Pigments representing benthic green algae have increased 200-300% since ca. 1950; diatom pigments suggest stable or slightly declining overall (planktonic and benthic) populations. Cyanophytes and cryptophytes are not abundant in the sediment record, but there was a slight increase in some taxa beginning ca. 1950. While some changes began ca. 1900, the shifts in nearly all indicators of change accelerate ca. 1950 commensurate with many human-caused changes to the Earth system. In addition to N deposition, others have noted recent increases in aeolian deposition that contributes phosphorus and strong increases in summer air (0.7 °C per decade) and surface water (0.2-0.5°C per decade) temperatures since 1983, which may have direct and indirect consequences for high elevation ecosystems. In this study, the causes of changes to mountain lake primary producers were inferred, but drivers and their responses are

indicators of changes in the Earth system that have been used to define the Anthropocene (Steffen et al., 2015).

Shifts from diatom-dominated to chlorophyte-dominated benthic communities are taking place concomitant with increasing water temperatures and nutrient availability, but the mechanisms promoting chlorophytes over diatoms and the implications for ecosystem function are not well understood. In Chapter 3, I demonstrated that nutrient enrichment of both nitrogen and phosphorus favored chlorophytes *in situ* and led to the highest overall algal biomass. In the absence of nutrient enrichment, the relative abundance of diatoms was significantly greater than green algae and cyanobacteria. In the laboratory incubations, I found that in chlorophyte-dominated periphyton, nitrogen assimilation increased significantly, but net ecosystem production decreased, with warming temperatures. These experiments offered insights into why chlorophytes are increasing in Sky Pond and The Loch; within Chapter 3, I outlined potential mechanisms that led to the algal community shift, and the potential implications for ecosystem functions like ecosystem respiration, nutrient cycling, and the balance of heterotrophic-autotrophic metabolism.

Finally, in the last chapter I shifted my focus from benthic to planktonic algal dynamics and from individual lake studies to regional surveys. We tested the relative importance of winter and summer conditions, watershed characteristics, and water chemistry as drivers or mediators of phytoplankton biomass. Boosted regression tree (BRT) models were applied to information from 28 high-elevation lakes in Colorado and from two long-term watershed monitoring programs to examine spatial, intra-seasonal, and inter-annual drivers of variability in lake phytoplankton. The results from the BRTs

were then used to inform mechanistic linear mixed effects models. We found that drivers of phytoplankton biomass here highly context and temporally dependent, with some similarities between the three models. Similar to previous studies, we found that on longer timescales (interannual) variation in phytoplankton could be explained by the maximum snow water equivalent (SWE) of the previous winter, where phytoplankton biomass was inversely related to SWE. Within a season, peak phytoplankton biomass consistently coincided with the warmest water temperatures and lowest nitrogen to phosphorus ratios. Across the region, summer precipitation and air temperature explained the most variability, illustrating the hydrological and climatic sensitivity of these lakes. While links between declining snowpack, lake temperature, nutrients, and organic matter dynamics are increasingly recognized in high elevation lakes, this study identifies additional processes that will influence phytoplankton biomass as the climate continues to change. Like other recent studies in landscape limnology, we identified the importance of considering both winter and summer conditions in structuring lake ecological dynamics. We concluded that continued changes in the timing, type, and magnitude of precipitation in combination with other global change drivers (e.g., nutrient deposition) may have consequences for basal production in high elevation lakes, potentially shifting these historically oligotrophic lakes toward new ecosystem states.

2. MULTIPLE STRESSORS INTERACT TO FORCE MOUNTAIN LAKES INTO UNPRECEDENTED ECOLOGICAL STATE

2.1 Introduction

Rapid changes in anthropogenic activities over the past century have altered the fundamental biogeochemical cycling of major elements and contaminants at local, regional and continental scales (Dubois et. al., 2018; Holtgrieve et. al., 2011; Steffen et. al., 2007; Wolfe et. al., 2013). Increasingly cited as evidence for having entered the Anthropocene, the rapid changes in the human enterprise and the environmental responses have been termed The Great Acceleration (Steffen et. al., 2015). Remote lakes in mountainous regions have chronicled responses to these regional to global scale drivers, including agriculture, urbanization, air pollution, and changes in land-use practices (Catalan et. al., 2013; Mosier et. al., 2019).

Over the past 70 years, global and regional human activities have affected the influx of energy and matter to remote mountain lakes of southern and central Rocky Mountains (Baron et. al., 2000; Brahney et. al., 2014; Leavitt et. al., 2009). Expansion of industrial fertilizer manufacturing and application, intensive livestock production, and fossil fuel combustion increased atmospheric nitrogen (N) deposition to remote watersheds by more than an order of magnitude greater than background levels (Baron et. al., 2004). In the southern and central Rocky Mountains, deposition of reactive nitrogen resulted in abrupt changes to alpine lake flora in the middle of the 20th century (Baron, 2006; Saros et. al., 2003; Wolfe et. al., 2001; Wolfe et. al., 2003). Additionally, aeolian dust from distant sources has subsidized alpine ecosystems with phosphorus

(P), and recent evidence suggests that dust deposition is increasing regionally (Clow et. al., 2016; Brahney et. al., 2014; Neff et. al., 2008).

Increased N and P availability alter the trophic state of alpine lakes. Multiple lines of evidence demonstrate modest increases in alpine lake primary productivity, altered resource response ratios, and changes in algal assemblages with increased atmospheric N deposition (Elser et. al., 2009; Nydick et. al., 2004; Nydick et. al., 2003; Saros et. al., 2003; Wolfe et. al., 2001, 2003). Phosphorus inputs from dust have increased phytoplankton and zooplankton biomasses by two orders of magnitude and altered diatom species assemblages in oligotrophic alpine lakes of the central Rocky Mountains (Brahney et. al., 2014).

Surface temperatures of seasonally ice-covered lakes have increased, including Rocky Mountain lakes, at a rate of up to 0.5 °C per decade over the past 25 years (Christianson et. al., 2019; O'Reilly et. al., 2015; Roberts et. al., 2017). Indirect effects of climate change influence the magnitude and timing of snowfall, duration of ice cover, persistence of perennial ice such as glaciers, and water residence time (Baron et. al., 2009; Preston et. al., 2016; Sadro et. al., 2018; Slemmons et. al., 2017). Warming and indirect effects of climate change also influence nutrient cycling, plankton community structure, and productivity (O'Reilly et. al., 2015; Preston et. al., 2016; Sadro et. al., 2018).

The Loch Vale Watershed in Rocky Mountain National Park, Colorado, has experienced high N deposition and strong ecosystem responses since about 1950 (Baron, 2006; Baron et. al., 2000), but deposition and lake nitrate concentrations have been relatively stable since 2000 (Mast et. al., 2014). Novel biological changes

continue, however. Phytobenthic blooms dominated by a limited set of genera (e.g. *Zygnema* spp., *Spirogyra* spp., *Nitella* spp.) in the littoral zones of both subalpine and alpine lakes are now common (Figure 1D). Historically, littoral habitats have not been well monitored, but benthic biofilms are demonstrably important sites for local nitrate assimilation (Nydick et. al., 2004, Vadeboncoeur et. al., 2001).

Lakes that have not historically been exposed to separate or coincident nutrient inputs and warming can be forced into novel ecological states (Scheffer et. al., 2001; Leavitt et. al., 2009). In this paper, we illustrate the interactive effects of global changes on two lakes in the Colorado Front Range, emphasizing changes for which there seem to be no historical precedent. Interacting forces of ecological change are now apparent in other regions (Taranu et. al., 2015; Wolfe et. al., 2013), and we posit that similar processes may be at work in Loch Vale where climatic conditions and dust inputs are changing and potentially interacting with a legacy of N deposition to alter lake autotrophic structure and function.

Using algal and biogeochemical proxies, we explored sediment geochemistry (elemental composition, stable isotopes), species composition (subfossil diatoms) and lake production and gross composition of primary producers (subfossil pigments of algae and cyanobacteria) over time in an alpine lake, Sky Pond, and a subalpine lake, The Loch. We were interested in whether contemporary assemblages of phototrophic microbes are different now than in the past, if the changes were similar between two lakes located in the same watershed, and whether changes could be attributed to nutrients and climate.

2.2 Methods

2.2.1 Study area

Sky Pond and The Loch are located in the Loch Vale watershed (LVWS), Rocky Mountain National Park, Colorado, USA (Figure 2.1). The watershed covers 6.6 km2 on the eastern slope of the Continental Divide with an elevation range from 3048-3962 m (Table 1). Data collected (1983- 2016) include meteorology, discharge, wet atmospheric deposition, and water quality (https://www2.nrel.colostate.edu/projects/lvws/). Mean (± standard deviation) annual air temperature was 1.2 (± 8.4)°C and mean annual precipitation was 106.3 (± 18.2) cm, for the period 1983-2016. Approximately 70% of annual precipitation is snow. Annual temperatures are cold enough to support permafrost above 3400 m. In 2003, 12% of the basin (77 ha) was postulated to be underlain by permafrost, while 41 additional ha were covered by glaciers and rock glaciers (Clow et. al., 2003). Locally, there were no significant temporal trends in minimum, mean, and maximum annual air temperatures, but July air temperatures increased at a rate of 0.7oC decade-1 for the period 1983-2010 (Mast et. al., 2014). The subalpine area (6% of watershed) is dominated by old-growth coniferous forests and the alpine area (11%) includes grasses, sedges, dwarf shrubs, and cushion plants (Arthur et. al., 1992). Wetlands cover less than 1% of watershed area. Much of the landscape (165 ha), particularly above treeline, is composed of talus, block slopes, and debris cones (Clow et. al., 2003).

Sky Pond (40.27814 N, -105.66837 W; 3,322 m.a.s.l) is an alpine headwater lake at the base of Taylor rock glacier. Sky Pond is small (3 ha, $1.2x10^5$ m^3), with a maximum and mean depth of 7.3 m and 4.5 m, respectively (Table 1). Multiple inlets

supply water to Sky Pond, generally flowing through talus fields below Taylor Rock Glacier as well as subsurface flow through boulder fields (Baron, 1992).

The Loch (40.2926 N, -105.65627 W; 3050 m.a.s.l.) is a subalpine lake fed by two streams, one of which flows through Sky Pond. The Loch has nearly twice the surface area (5 ha) of Sky Pond but has a maximum and average depth of 5.0 m and 1.5 m, respectively, and volume of 6.0×10^4 m^3 (Table 2.1). Due to the high area to volume ratio of The Loch, it can hold twice as much water during snowmelt compared to baseflow and lake level can fluctuate up to 1 m over the ice-free season. Sky Pond and The Loch turn over approximately 13 and 82 times per year, respectively, resulting in spring (April-June) extreme differences in residence times of between 6 (The Loch) and 39 days (Sky Pond; Baron 1992).

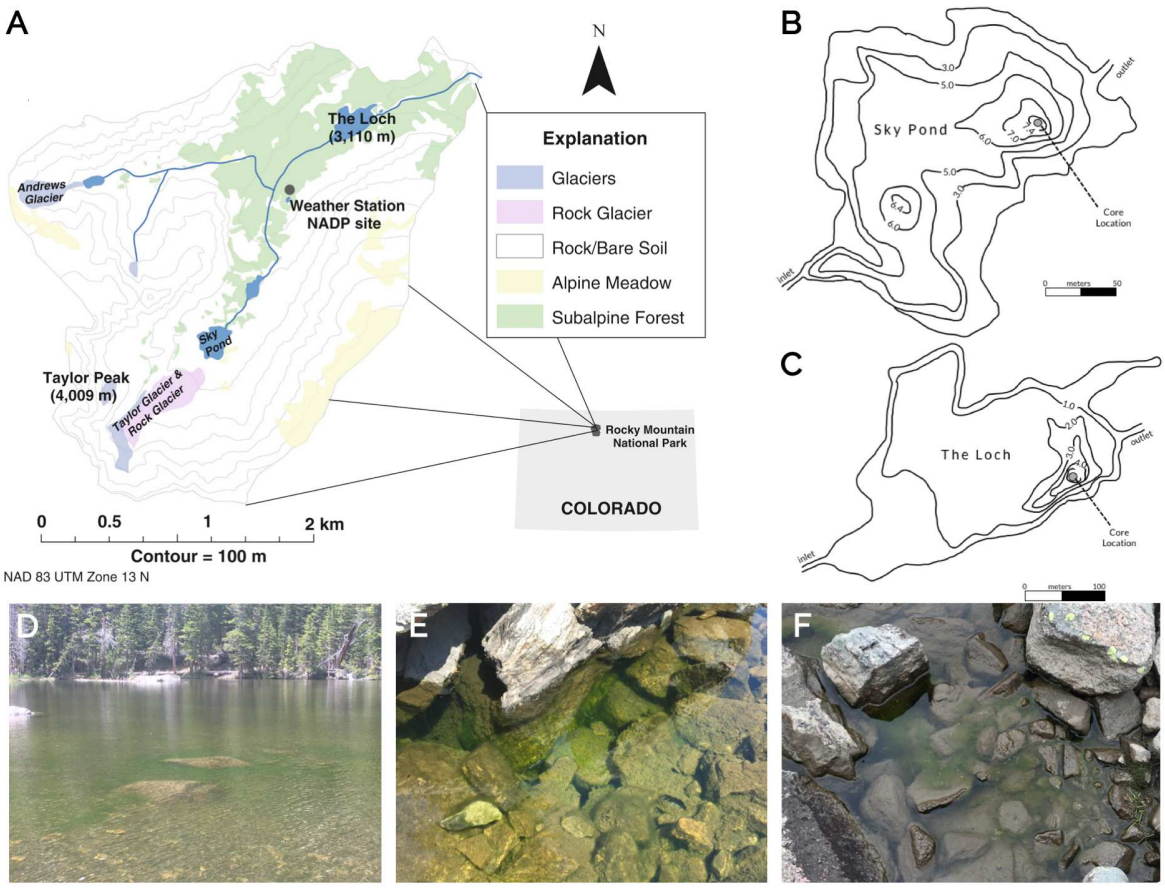

Figure 2.1. Study area, lake bathymetry, and example of a chlorophyte "bloom." Study maps showing (A) Loch Vale Watershed landcover (borrowed from Heath & Baron, 2014), (B) Sky Pond bathymetry and core location (max depth = 7.4 m), (C) The Loch bathymetry and core location (max depth= 5.0m), benthic chlorophyte "bloom" in The Loch (D) and Sky Pond (E-F), summer 2017. Contour lines are drawn at 1-meter intervals.

Both lakes are dilute, with mean summer (JJA) specific conductance <15 µS cm^{-1} (Table 1). Mean summer total N concentrations were 0.3 mg N L^{-1} for both lakes, whereas total P was 8.8 µg P L^{-1} and 10.3 µg P L^{-1} for The Loch and Sky Pond, respectively. The DIN:TP ratio was greater in The Loch at 69 compared with Sky Pond at 59. Dissolved organic carbon was low in both lakes, with a mean summer value of 1.2 mg L^{-1} in The Loch and 0.5 mg L^{-1} in Sky Pond. Chlorophyll *a*, as a measure of

biomass, was low in both lakes: 2.2 μg L^{-1} for The Loch and 5.3 μg L^{-1} for Sky Pond (Table 1).

Wet N deposition, measured at the CO98 site of the National Atmospheric Deposition Program (http://nadp.slh.wisc.edu), ranged between 3.0 and 4.5 kg N ha^{-1} yr^{-1} since 1984, with year-to-year variability largely arising from fluctuations in the amount of annual precipitation (Mast et. al., 2014). Previous paleolimnological and emissions inventory reconstructions suggest N deposition increased from a background of about 0.5 kg N ha^{-1} yr^{-1} in 1900 to 1.5 kg N ha^{-1} yr^{-1} around 1950 (Baron, 2006; Wolfe et. al., 2001). Estimated total N (wet plus dry) deposition peaked at >5.0 kg N ha^{-1} yr^{-1} before 2000 and has been relatively stable at about 3.0 kg N ha^{-1} yr^{-1} since then (Mast et. al., 2014; Morris, 2018).

Benthic blooms of chlorophytes and charophytes (*Spirogyra spp., Zygnema spp., Nitella spp.;* Figure 2.1D) have been routinely observed in large patches throughout the lake bottom of The Loch and in the littoral zones of Sky Pond since 2010. As with many limnological studies, traditional emphasis in LVWS has focused on pelagic production and food webs, while benthic production likely dominates in these shallow, oligotrophic systems (Vadeboncoeur et. al., 2001). Benthic production (epilithic, epipelic) and periphytic chlorophyll *a* were measured by Nydick et. al., (2004), who found photosynthetic rates and total biomass to be far greater than that measured for phytoplankton. Nydick et. al., (2003) described the littoral zones of The Loch and other experimental sites as characterized by large rocks and flocculant sediment but made no mention of visible attached green algae. The increase in benthic primary production and biomass was not one of the predicted ecological responses to chronic nitrogen

deposition in this watershed (Baron et. al., 2012) but is known to be a common response to low levels of P fertilization (Nydick et. al., 2003).

Analysis of species identity, relative abundance, and total biomass (as chlorophyll *a*) during 1984-1989 revealed that Sky Pond had consistently higher abundance of phytoplankton and chlorophyll *a* than did The Loch, but that both lakes exhibited strong seasonality in abundance and types of phototrophs (Spaulding et. al., 1992). Spring algal blooms were composed mainly of the diatom *Asterionella formosa*, while the cyanophyte *Oscillatoria limnetica* was common in fall blooms. During winter, planktonic cell densities were comparable to peak summer concentrations, and included *A. formosa* as well as several species of green algae that comprised a minor proportion of the planktonic flora: the chlorophytes *Coccomyxa* spp., *Chlamydomonas* sp., *Ankistrodesmus* spp., and *Chlorococcales* spp. (Spaulding et. al., 1992). Except for *Nitella spp.,* macrophytes are historically and presently rare or absent in both The Loch and Sky Pond.

Table 2.1. Watershed and summer water chemistry attributes for The Loch (subalpine) and Sky Pond (alpine) lakes. Water chemistry is reported as June-July-August surface water means for the period 2015-2017 with standard deviation shown in parentheses. Watersheds were delineated from lake outlets with the USGS StreamStats online tool (USGS, 2016) and land cover metrics were estimated using National Land Cover Database (NLCD) data 30 m resolution rasters (Homer et al. 2015).

	The Loch (*subalpine)*	**Sky Pond** *(alpine)*
Watershed Attributes		
Latitude	40.2926	40.27814
Longitude	-105.65627	-105.66837
Elevation (m)	3048	3322
Max depth (m)	5	7.2
% Barren	70%	81%
% Forest	8%	0%
% Shrub	6%	1%
% Wetland	0.2%	0.0%
Lake surface area (ha)	5.3	4.1
Watershed area (km^2)	6.8	2.2
Drainage ratio (WSA:LSA)	128.4	53.5
Water Chemistry		
Conductivity (µS/cm)	12.9 (2.3)	10.3 (2.2)
Chlorophyll *a* (µg/L)	2.2 (1.9)	5.3 (3.0)
Total N (mg/L)	0.3 (0.1)	0.3 (0.01)
NO_3-N (mg/L)	0.2 (0.1)	0.2 (0.1)
TP (µg/L)	8.8 (1.5)	10.3 (1.8)
DIN:TP (molar)	68.9 (24.6)	55.9 (16.2)
DOC (mg/L)	1.2 (0.8)	0.5 (0.2)

2.2.2 Core collection and chronology

Sediments were collected from The Loch in March 2016 using an HTH (Pylonex) gravity corer (7 cm internal diameter) through approximately 1m of ice over the deepest section of the lake (5 m). The recovered core was 20.25 cm long and included an intact

sediment-water interface. Overlying water was siphoned off the top and the core tube was capped and wrapped in aluminum foil to prevent light from stimulating algal growth. The core tube was stored upright and allowed to freeze overnight before transport to a freezer the next day. The core was later sliced longitudinally and sectioned with a sterile blade at 0.25-cm intervals in a dark, climate-controlled facility at the Institute of Environmental Change and Society (IECS), University of Regina, Saskatchewan, Canada.

Sky Pond was cored in May 2017 through ice over the deepest section of the lake (7.2 m). We used a Glew gravity corer (7.6 cm internal diameter) to obtain a 24.2-cm core, removed the overlying water, and sectioned on-site in 0.20-cm intervals using a vertical extruder (Glew, 1991). Sediment layers were transferred to WhirlPak bags, and transported on ice to Colorado State University, where they were immediately weighed, frozen, and lyophilized (48– 72 h at 0.1 Pa) for subsequent analyses.

Core chronologies were established by analysis of ^{210}Pb activities and application of constant rate of supply (CRS; Appleby and Oldfield, 1978) calculations for The Loch by Flett Research Ltd. (Winnipeg, Manitoba, Canada) and Sky Pond by the Institute of Environmental Change and Society (IECS). Dating (^{210}Pb) was conducted twice for The Loch, first using alpha spectrometry by MyCore Scientific (Ontario, Canada) and the second time with gamma spectrometry at IECS, University of Regina. Sky Pond sediments were dated with gamma spectrometry at IECS. Prior to analysis, all sediments were homogenized with a mortar and pestle. Twelve and 14 segment intervals were analyzed for The Loch and Sky Pond cores, respectively. Age estimates

for sediments deeper than the limit of ^{210}Pb dating were approximated by extrapolation of linear age–accumulation relations observed in the early 20th century.

Preliminary analysis suggested no progressive change in the activities of either ^{210}Pb or ^{137}Cs with depth in The Loch (data not shown), therefore sediment ages at this site were approximated by comparison of changes in δ^{15}N values with depth in the two lakes. Deposition of isotopically-depleted, reactive N from anthropogenic sources display coherent regional patterns of change in sedimentary N isotopes that both illustrate the onset (ca. 1880) and acceleration (ca. 1950) of atmospheric pollution (Holtgrieve et. al., 2011). A coherent change ca. 1950 in five lakes of Rocky Mountain National Park, one of which was Sky Pond, demonstrates this coherency (Wolfe et. al., 2003). Here we assumed similar rates of sediment deposition in The Loch and Sky Pond, then used cross-correlation analysis to determine the 'best fit' timing for changes in z-transformed time series of δ^{15}N. As a result of this approach, we could did not interpret N isotope stratigraphy nor interpret differences in timing between The Loch and Sky Pond; instead we focus our discussion on the timing of changes in Sky Pond and the qualitative differences between sediment proxies in The Loch and Sky Pond.

2.2.3 Elemental analyses

Stable isotope ratios and elemental composition were determined at IECS on whole dried sediment samples using a ThermoQuest DeltaPLUS XL isotope ratio mass spectrometer equipped with a continuous flow unit (Con Flo II), an automated Carlo Erba elemental analyzer as an inlet device, and following standard procedures (Savage et. al., 2004) at IECS, University of Regina. Approximately 30 mg samples were weighed in tin capsules to the nearest 0.001mg before combustion. Stable N (δ^{15}N) and

C ($\delta^{13}C$) isotopic compositions were expressed in the conventional notation: units of per mil (‰) deviation from atmospheric N_2 and an organic C standard calibrated against Vienna Pee Dee Belemnite. Sample reproducibility was < 0.25‰ and < 0.10‰ for $\delta^{15}N$ and $\delta^{13}C$ determinations, respectively.

2.2.4 Pigment analyses

Carotenoids, chlorophylls, and their derivatives were quantified in sediments as metrics of past algal and cyanobacterial abundance following standard procedures (Leavitt and Hodgson 2001) at IECS. Briefly, a 50 mg subsample of was extracted in an 80:15:5 (% by volume) mixture of acetone, methanol, and water at -12ºC. After 24 hours, pigments were filtered through a 0.2-µm pore membrane filter and dried under inert N_2 gas. After drying, pigment residues were reconstituted in a known volume of standard injection solution and analyzed on an Agilent 1100 High Performance Liquid Chromatography (HPLC) system equipped with a photodiode array detector. Individual pigments were distinguished on the basis of chromatographic position and light absorbance characteristics and compared with authentic standards of common algal and cyanobacterial pigments from DHI (Hoslholm, Denmark) and local isolates (Leavitt and Hodgson 2001). All pigment concentrations are presented as nmol pigment per g^{-1} organic carbon, a metric which is linearly correlated to annual phototroph standing stock in whole lake calibrations (Leavitt and Finlay 1994).

We quantified historical changes in a total of 21 pigments but focused our analyses on those which were abundant in sediment samples at some point in the core and show little evidence for post-depositional decay. Biomarkers include those characteristic of chlorophytes (pheophytin *b*), chlorophytes and cyanobacteria (lutein

and zeaxanthin), filamentous and colonial cyanobacteria (myxoxanthophyll), Nostocales cyanobacteria (canthaxanthin), total cyanobacteria (echinenone), cryptophytes (alloxanthin), mainly diatoms (diatoxanthin), and a combination of diatoms, chrysophytes, and some dinoflagellates (fucoxanthin). Pheophytin *a* and β-carotene are used as indicators of total primary production in lakes. Structural isomers lutein (chlorophytes) and zeaxanthin (cyanobacteria) were not separated on our HPLC system and are presented herein as a combination of chlorophytes and cyanobacteria. Labile fucoxanthin from diatoms, chrysophytes and some dinoflagellates was not used for the analysis because of obvious post-depositional degradation, as seen in many lakes (Leavitt and Hodgson 2001). The ratio of labile chlorophyll *a* to stable pheophytin *a* (preservation index) was used as a proxy of changes in the preservation down-core, although both compounds were present at high concentrations throughout the period of interest (ca. 1800 CE to present).

2.2.5 Sediment diatom enumeration

Following the method of Pite et. al., (2009), Sky Pond sediments were weighed to the nearest milligram to obtain approximately 1000 mg. Samples were hydrated with 15 mL of distilled water for 12 hours in 50 mL centrifuge tubes. Organic material was oxidized under high heat and pressure using 15 mL concentrated nitric acid in an Anton Paar microwave. Following the digestion, distilled water was added to bring the total volume to 50 mL. Samples were centrifuged at 2500 rpm for 10 minutes, decanted and filled with distilled water. This washing step was repeated until samples reached a neutral pH. The cleaned sediments were well mixed by shaking and a known volume was placed in a 50 mL centrifuge tube. Distilled water was added to make a final

volume of 30.0 mL and poured over four replicate cover slips were placed in Battarbee chambers. The cover slips were allowed to dry and were mounted on glass microslides using a high refractive mounting medium (Zrax). Permanent slides and cleaned material are archived in the University of Colorado INSTAAR Diatom Database (Accession #17121-17159); one hundred valves were identified to the genus level over a known area of the slide (Olympus BX53 microscope, 100x oil immersion objective, 1.4 NA, differential interference contrast). Identifications and habitat preference (planktonic, benthic) follow the *Diatoms of North America* project (Spaulding et. al., 2018). Results are presented as the ratio of total planktonic valve counts to benthic diatoms valve counts over time.

2.2.6 Statistical analyses

All statistical analyses were performed in R version 3.4.3 (R Core Team 2018). As our sediment cores lack annual laminations and compression of sediments can lead to uneven sampling intervals through time, we did not use simple linear regression or non-parametric approaches to assess trends in our data due to violation of model assumptions (Birks et. al., 2012). Instead, we used generalized additive models (Hastie and Tibshirani 1987; Wood 2017) to estimate trends in our response variables. Generalized additive models (GAMs) have the advantage of estimating complex, non-linear, and non-monotonic trends in time series, allowing better identification of significant change while accounting for the lack of independence that plague paleolimnological time series (Simpson 2018). All models were fit using the *gamm()* function (Wood 2004) in the *mgcv* package (Wood 2017) and were parameterized following the technical recommendations of Simpson and Anderson (2009).

We calculated the first derivative of the fitted trend using the method of finite differences to assess the timing of significant rate of change in our response variables (Ladyzhenskaya 1985). Here we accounted for uncertainty around the estimate with the simultaneous confidence interval on the derivative, calculated using simulation from the posterior distribution of the model coefficients (Simpson 2018). The onset of a period of significant change was identified as the time point when the confidence intervals on the first derivative did not include zero. Trends in seasonal air and water temperature trends from the Loch Vale Watershed long-term record were assessed using simple linear regression. We report only results that were statistically significant ($p<0.05$).

2.3 Results

2.3.1 Chronology

Analysis of ^{210}Pb and ^{137}Cs activities provided of a reliable sediment chronology for Sky Pond (Figure 2.2) but not The Loch. In Sky Pond ^{210}Pb declined in a progressive, but irregular fashion between 2 and 8 cm depth (Figure 2.2A), suggesting some sediment mixing in the surface layer and a change in sediment accumulation rates between ca. 1930 and ca. 1950 (Figure 2.2C). Overall, the ^{137}Cs profile showed good definition, with a clear peak ca. 1960 based in ^{210}Pb-established chronology, reflecting historical maxima in deposition of radioisotopes derived from open-air atomic blasts (1963). Depth-age relationships appear reliable, predictable and largely linear in Sky Pond.

There were no obvious changes in measured activity of either radioisotope in the sediments of The Loch, with very low concentration of ^{210}Pb and ^{137}Cs in all samples, likely reflecting the very low residence time of water (6 days). Sediment chronology was

instead approximated by assuming both sites received similar atmospheric influx of reactive N, and that changes in standardized (z-transformed) $\delta^{15}N$ values should be temporally coherent in the two basins, such as seen through much of the central Rocky Mountains (Figure 2.3A,B; Wolfe et. al., 2001). Historical changes in $\delta^{15}N$ values tend to be synchronous when atmospheric N influx is a high proportion of the total N budget of the lakes (Holtgrieve et. al., 2011), such as is known to be the case in the upper Loch Vale catchments (Baron and Campbell 1997; Enders et. al., 2008; Wolfe et. al., 2001, 2003).

Both Sky Pond and The Loch show similar $\delta^{15}N$ trends with depth (Figure 2.3A) and showed high correlation in the upper 6 cm of the core (Figure 2.3B; Pearson's $R = 0.9$, $p < 0.001$). We therefore assumed similar sedimentation rates in both lakes and applied the Sky Pond chronology to the Loch sediment core. We explored more complex approaches such as dynamic and parametric time warping (Bloemberg et. al., 2010; Wehrens et. al., 2015; Giorgino 2009) but low sample density at the base of The Loch core prevented carrying out these techniques. Although we are not able to make inferences concerning the difference in timing of change between lakes, we were able determine qualitative differences in response based on geochemical markers and algal pigments.

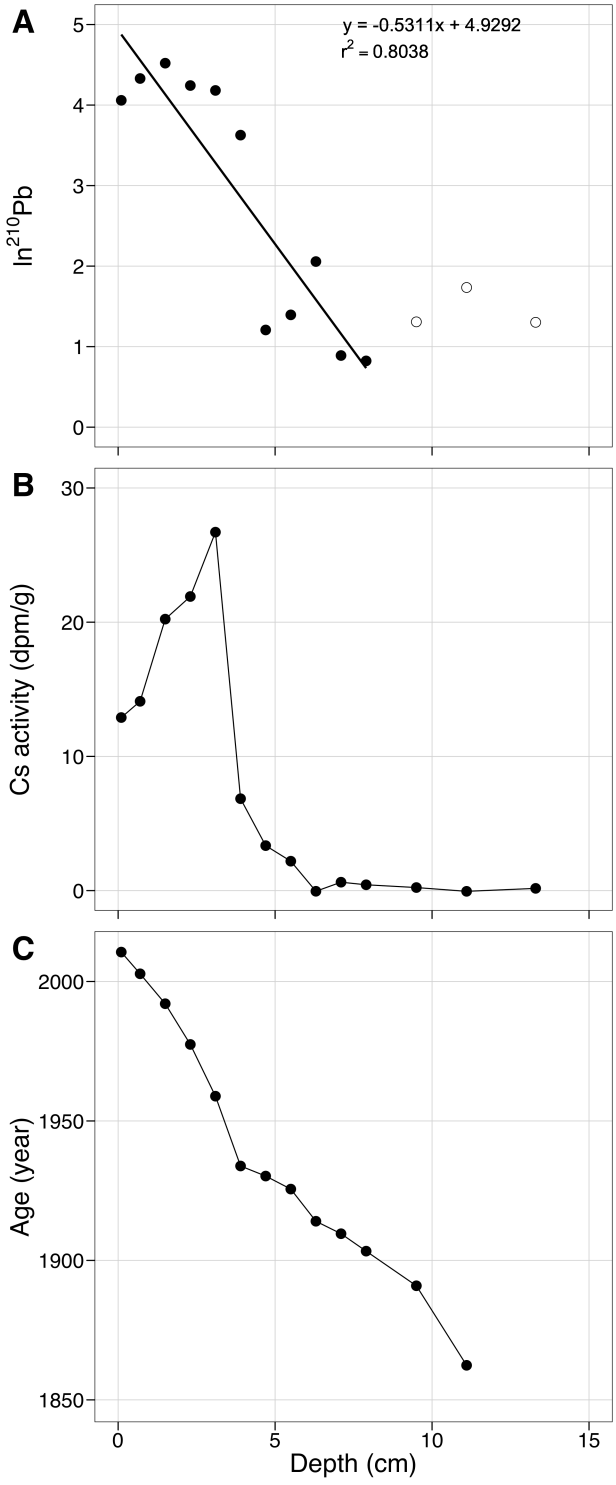

Figure 2.2. Sky Pond sediment core chronology. (A) Natural log ^{210}Pb, (B) cesium activity, and (C) estimated age by depth for Sky Pond sediments.

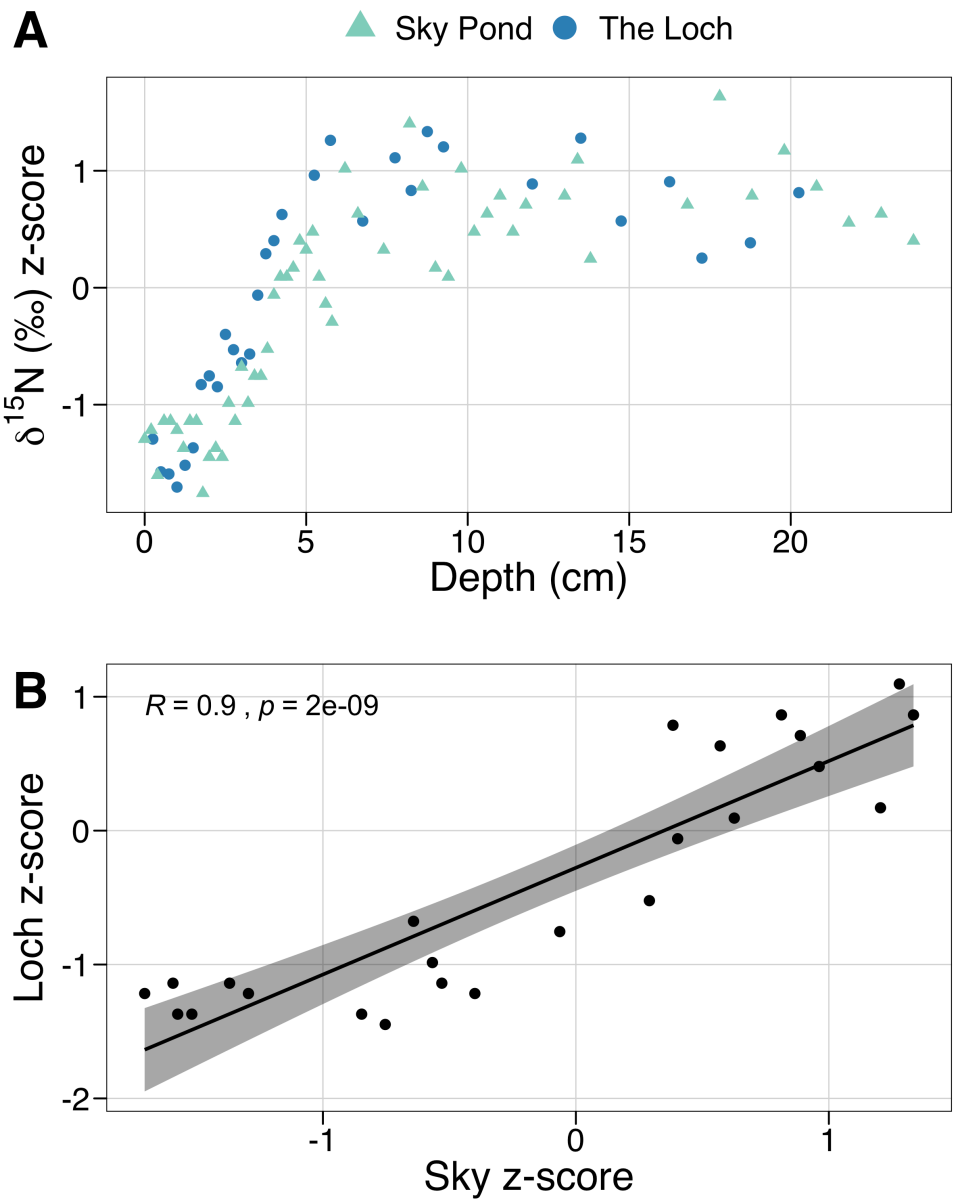

Figure 2.3. Estimated sediment age for The Loch sediments based on $\delta^{15}N$ z-scores. (A) Normalized z-scores of $\delta^{15}N$ by lake versus depth. (B) Both The Loch & Sky Pond show similar trends by depth with especially high correlations for sediment layers less than 6 cm from the top of the core (Pearson's R=0.9, $p < 0.001$).

2.3.2 Elemental analyses

The percent N in bulk sediment was generally lower in Sky Pond than in The Loch sediments (Figure 2.4A). Sediment percent N in Sky Pond was variable and averaged 0.37% ± 0.07% with no significant trend during the period of record. In

contrast, sediment percent N in The Loch was stable (0.51% ± 0.02) until mid-20th century, and then increased steadily to 0.8% in the most recent sediments. Bulk $\delta^{13}C$ values became progressively and significantly depleted mid-20th century in Sky Pond with declines in $\delta^{13}C$ values from -26‰ to -27‰ (Figure 2.4B, Appendix A2). Bulk sediment $\delta^{13}C$ values in The Loch were more enriched and varied between –23‰ and -24‰, showing little trend over time. Sediment C content increased slightly in both lakes for several hundred years, but the trend was not significant (Figure 2.4C). Until ca. 1900, C:N ratios averaged 16.5 ± 0.4 in The Loch and 9.8 ± 0.4 in Sky Pond (Figure 2.4D). There was no statistically significant change in C:N in Sky Pond; however, C:N began decreasing around mid-20th century in The Loch. Surficial C:N ratios in the cores were similar in those present in modern Sky Pond sediments.

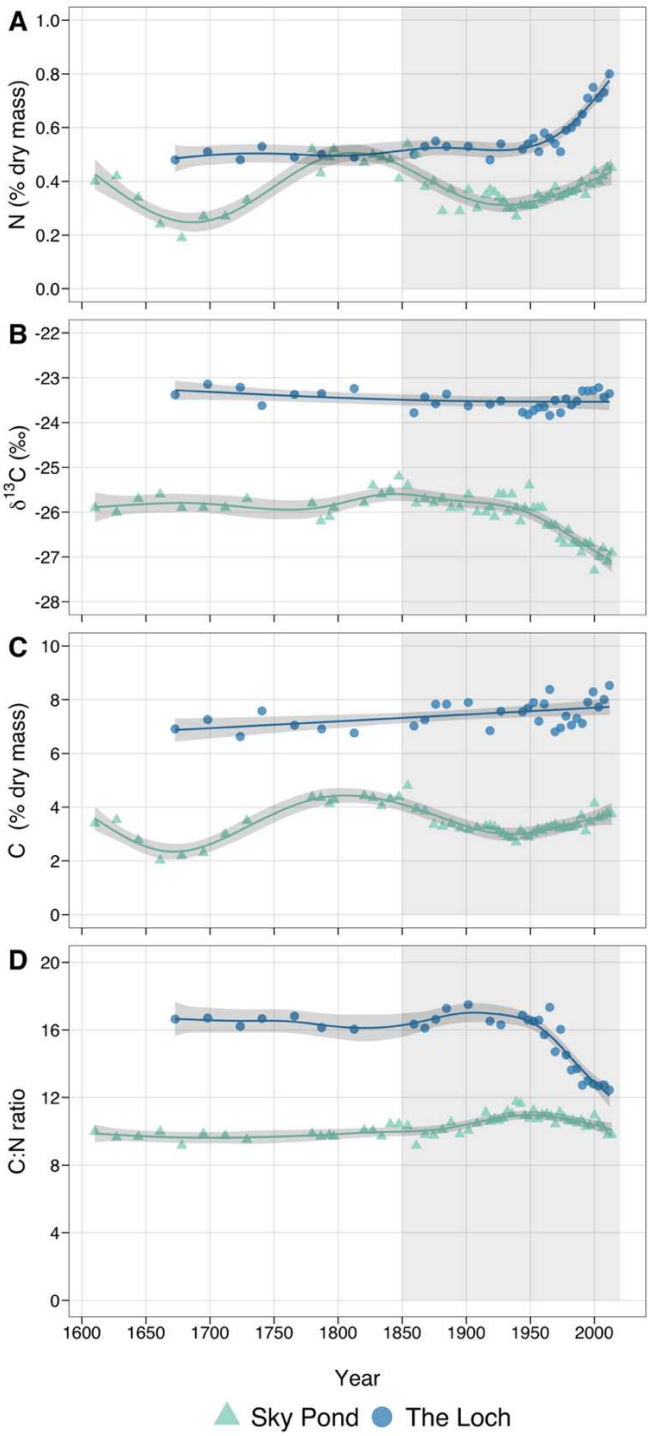

Figure 2.4. Summary of temporal trends in C, N, C:N, and $\delta^{13}C$. GAM-smoothing trends fitted are depicted with 95% confidence intervals (light grey bands) for The Loch and Sky Pond time series. Changes in (A) $\delta^{15}N$ of bulk sediment, (B) N content as a percentage of dry mass, (C) $\delta^{13}C$ or bulk sediment, (D) C content as a percentage of dry mass, and (E) C:N through time. Depths prior to ca. 1850 are extrapolated from Pb^{210} data and should be interpreted with caution.

2.3.3 Algal dynamics

Pheophytin *a* concentrations and temporal patterns were similar between the two lakes, with slightly higher values in Sky Pond. Pheophytin *a* fitted GAMs indicated a significant increase in total algal biomass in the mid-20th century and the rapid changes continue to the present (Figure 2.5A, Appendix A2). Beta-carotene, another proxy for total algal abundance, increased gradually in Sky Pond over the record (Figure 2.5B). Concentrations of this ubiquitous pigment were slightly higher in The Loch core and changes in the rate of increase of β-carotene were non-significant in Sky Pond (Appendix A2). The pigment preservation index (as chl *a*:pheophytin *a*) was stable until ca. 1970, suggesting no marked change until the most recent sediments (Appendix A1), and consistent with relatively stable concentrations of β-carotene in recently deposited sediments (Figure 2.5B).

There was a strong increase over time in green algal biomass in Sky Pond, and a smaller increase in The Loch in the 20th century, as inferred from pheophytin *b* and lutein-zeaxanthin from chlorophytes (Figure 2.5C,D). In Sky Pond, significant changes in both pheophytin *b* and lutein-zeaxanthin began ca. 1930 and continued through 1960, with highest concentrations in the most recent sediments (Appendix A2). Present-day values of lutein-zeaxanthin are similar between the two lakes, but historical concentrations in The Loch were twice as high as Sky Pond. Pheophytin *b*

concentrations in recent sediments of Sky Pond are approximately twice as high as those in The Loch.

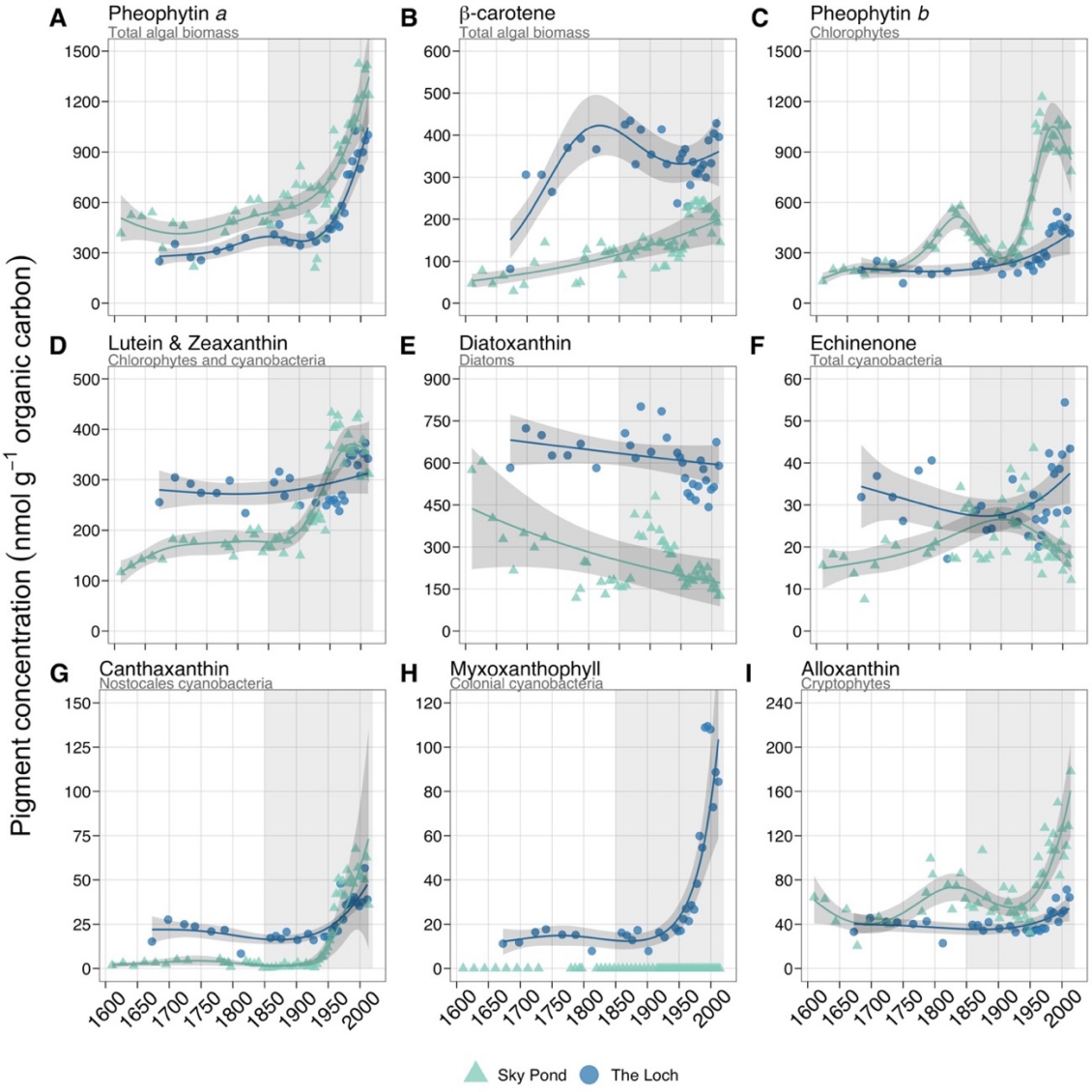

Figure 2.5. Summary of temporal trends in major algal functional groups inferred by pigment analyses. GAM-smoothing trends fitted are depicted with 95% confidence intervals for all major algal pigments in The Loch and Sky Pond time series. Pheophytin a (B) and ß-carotene (B) are proxies for total algal biomass. Pheophytin b (C) is a proxy for total chlorophyte biomass. Lutein & zeaxanthin (D) are indicative of both chlorophytes and cyanobacteria. Diatoxanthin (E) is a proxy for total diatom biomass. Echinenone (F), canthaxanthin (G), and myxoxanthophyll (H) are proxies for various cyanobacteria (total, Nostocales, and filamentous and colonial, respectively). Alloxanthin (I) is proxy for total cryptophytes. All pigments are standardized to nmol pigment per unit organic carbon. Depths prior to ca. 1850 are extrapolated from Pb^{210} data and should be interpreted with caution.

Diatoxanthin, the chemically stable biomarker for diatom abundance, did not increase with time, and in fact showed a linear decrease over the period of record in both lakes (Figure 2.5E). While the decreasing trend was significant, there was no significant decrease or increase in the rate of change since ca. 1850. To further investigate the steeper decline in Sky Pond diatoxanthin, we analyzed of diatom subfossils in Sky Pond sediments and found a marked switched from benthic to planktonic species about 1950, causing a change in planktonic:benthic ratio from 0.25 prior to 1950 to >0.50 in the most recent sediments (Figure 2.6).

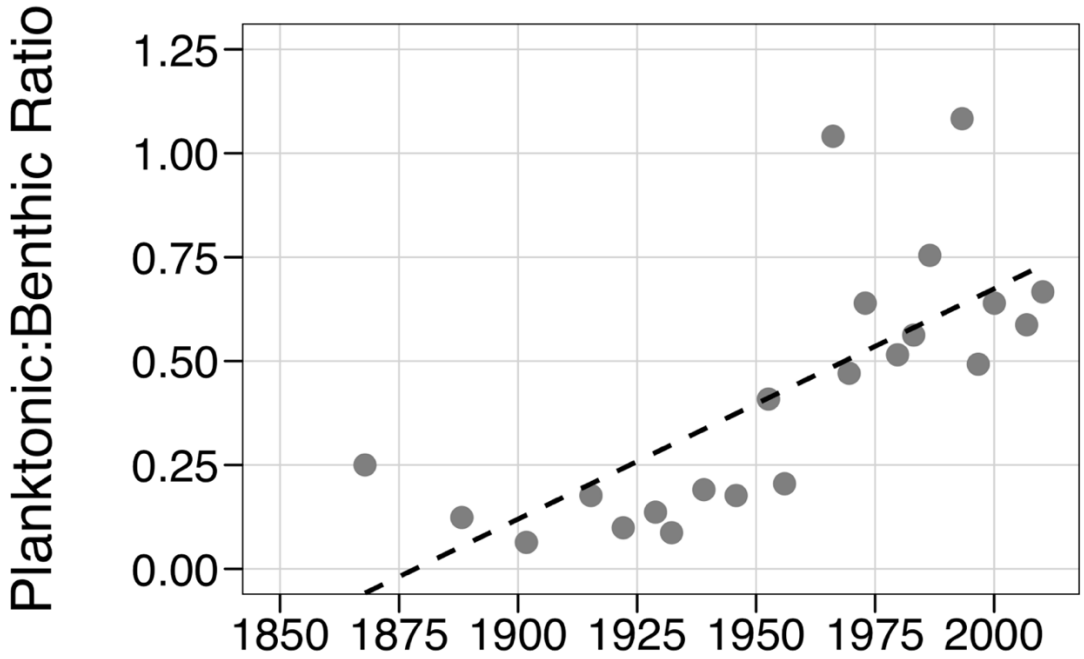

Figure 2.6. Temporal trends in the ratio of planktonic to benthic diatom valve counts in Sky Pond sediments since 1850. There was a significant positive trend ($F_{(1,20)}$=22.69, R^2 = 0.53, p = 0.0001) in P:B with a shift toward more planktonic than benthic species, with an inflection point ca. 1950.

Marked differences in historical patterns of abundance were seen in other phototrophic groups. Concentrations of pigments from cyanobacteria revealed

differences in historical composition of phototrophic prokaryotes both within and between lakes, with an order of magnitude difference in some pigments in Sky Pond compared to The Loch. Total cyanobacteria (as echinenone; Figure 2.5F) had contrasting hyperbolic patterns between lakes over the record, but both lakes showed a marked increase in abundance of Nostocales beginning mid 20th century (canthaxanthin; Figure 2.5G). Colonial cyanobacterial (as myxoxanthophyll; Figure 2.5H) increased six-fold in The Loch but were undetectable in Sky Pond sediments. Alloxanthin, representing cryptophytes, increased in concentration in Sky Pond commensurate with Nostocales and total cyanobacteria, but this pattern was not found in The Loch (Figure 2.5I). Overall, low concentrations for echinenone, canthaxanthin, myxoxanthophyll, and alloxanthin compared to green algal pigment proxies suggest that these functional groups historically and presently comprised a relatively minor proportion of the algal community of both lakes.

2.4 Discussion

Our sediment records showed limited environmental change in response to the Little Ice Age, continental industrialization and the development of agriculture on the Great Plains, all of which occurred prior to 1900. Instead, the data suggest environmental forcing since the mid-20th century may have introduced unprecedented change in the structure of autotrophic communities in remote mountain lakes. The concentrations of pigments that represent green algae increased 200-300% in both lakes and they continue to increase to the present day. This contrasts sharply with the diatom pigments and those representing total algal biomass, both of which changed little. Mid-20th century ecosystem changes were clearly indicated by sharp increases in

abundance of chlorophytes, a shift from benthic to planktonic diatoms, and declines in C:N ratios.

These changes in autotrophic structure coincide with documented chronic deposition of reactive atmospheric N (Wolfe et. al., 2001), but also increased inputs of P (Stoddard et. al., 2015), rapid regional warming (Baron et. al., 2009; McGuire et. al., 2012), and hydrological changes (Clow 2010; McCabe and Clark 2005). Although our arguments are only correlative, a combination of these drivers appear to have moved these historically ultra-oligotrophic systems into a new, mesotrophic state.

2.4.1 Contrasts between lakes

Both lakes had similar patterns for diatoms, chlorophytes, and overall phototrophic production in the sediment record, but there were notable differences between alpine Sky Pond and the subalpine Loch. Bulk organic matter $\delta^{13}C$ values in Sky Pond were consistently more depleted than those from The Loch. The alpine lake is dominated by autochthonous C fixation and receives little terrestrial organic carbon (Baron et. al., 1991). The Loch, which is surrounded by coniferous forests, had enriched bulk $\delta^{13}C$ sediment values and, prior to ~1950, higher C:N ratios indicative of terrestrial organic matter loading. The depleted $\delta^{13}C$ values for Sky Pond sediments and enriched $\delta^{13}C$ values for The Loch sediments are consistent with patterns observed in dissolved organic carbon fulvic acids in a previous study (Baron et. al., 1991). The $\delta^{13}C$ signal in The Loch remained within the historical range of variability (-23 $\pm$ 0.2‰) over the record but $\delta^{13}C$ values declined significantly by ~2‰ starting ca. 1950 in Sky Pond sediments. The decrease may reflect increased autotrophic production and use of respired CO_2 for photosynthesis (Bunting et. al., 2016; Bunting et. al., 2007). Coincident with the decline

in bulk $\delta^{13}C$ values for Sky Pond, Enders et. al., (2008) reported a significant enrichment in $\delta^{13}C_{n}$-C_{21} in *n*-alkanes preserved in the sediments of the same lake, which they postulated came from green lichen exudates in the catchment. A more plausible explanation is the increase in production by green algae (which share the same *n*-alkane signal), evidenced by observed increases in lutein, zeaxanthin, and chlorophyll *b* (Castañeda et. al., 2009).

Beginning ca.1950, the C:N of The Loch sediments decreased to ratios that are more characteristic of *in situ* primary production (C:N = 6-12), and similar to those observed in contemporary Sky Pond sediments (Meyers and Ishiwatari 1993). The C:N of Sky Pond sediments fluctuated very little in our sediment core, and only moderately over the past 4000 years (Wolfe et. al., 2001). Bulk sediment N content increased from 0.5% to 0.8% in The Loch beginning ca. 1950, possibly reflecting increased algal production in both The Loch and upstream Sky Pond. Elevated modern production by planktonic diatoms during spring snowmelt in Sky Pond maintains high cell numbers in spite of rapid hydrologic flushing during this season (McKnight et. al., 1990). Sky Pond may therefore subsidize The Loch with additional N-rich autochthonous organic matter.

2.4.2 Benthic vs. pelagic dynamics

Benthic diatoms have been found to dominate undisturbed shallow, oligotrophic, high-elevation lakes like those examined in this study (Spaulding et. al., 2015). Diatom analyses from Sky Pond, however, revealed a pronounced shift from benthic to pelagic diatoms ca. 1950 (Figure 2.6). The shift is coincident with the rise in atmospheric N deposition. Total diatom production did not increase, but the added N to the water column is postulated to have stimulated mesotrophic and planktonic *A. formosa* and

other mesotrophic taxa (Figure 2.5E). Other possible causes include warming and the introduction of trout to historically fishless mountain lakes.

In Sky Pond, changes in the proportion of planktonic diatoms to benthic diatoms (Figure 2.6) was coeval with an increase in benthic chlorophytes (Figure 2.5C,D). Such a pronounced change may reflect either competitive replacement under an altered nutrient or climatic regime or the exploitation of an opened benthic niche following loss of diatom phytobenthos. In a 10,000-year paleolimnological record from the Arctic, investigators found that chlorophytes were more sensitive to climatic variation than diatoms and were consistently the predominant algal taxa during warm periods such as the Holocene Thermal Maxima (Florian et. al., 2015). In warmer climates, preferential warming in shallow zones where light penetrates to dark sediments may occur, benefitting algal groups with higher thermal optima such as chlorophytes (Spaulding et. al., 2015; DeNicola 1996; Raven and Geider 1988; Trochine et. al., 2011).

Benthic algae are generally less sensitive to water-column nutrient additions than planktonic algae, thus the observed increase in benthic production in Sky Pond illustrates that warming may also play a key role in the trajectory of autotrophic structural change (Blumenshine et. al., 1997; Vadeboncoeur et. al., 2001). However, previous experiments revealed that additions of both N and P increased densities of benthic chlorophytes and cyanophytes even when ambient N levels were already high, suggesting that nutrients can both stimulate benthic production and change benthic community assemblages (Nydick et. al., 2003). Other competitive factors that may favor green algae over diatoms include a higher tolerance to UV-B radiation (Holzinger and 2009) and more efficient nutrient uptake (Litchman and 2007; Thomas et. al., 2017). We

cannot easily distinguish among these possibilities from our results, but the observed shift from diatom production from littoral to pelagic habitats and replacement by benthic green algae is without precedent in the Loch Vale Watershed. These structural changes in autotrophic communities are likely linked to changing climatic conditions, especially warmer summers (see below).

Fish introduction to these historically fishless lakes was previously ruled out as a contributing factor in diatom assemblage shifts (Wolfe et. al., 2003), but it is plausible that fish may have contributed to an increase in chlorophytes. Trout were stocked to Sky Pond from 1931-1939, and The Loch beginning in 1914 (Rosenlund and Stevens 1990) and both lakes maintain reproducing populations. Fish can increase nutrient availability by harvesting aquatic instars of terrestrial insects and excreting nutrient rich fecal pellets that can sink to the lake bottom (Schindler et. al., 1993; Leavitt et. al., 1994). However, while fish were stocked to both lakes, benthic chlorophyte pigments (pheophytin b, lutein-zeaxanthin) increased during the 1930s only in Sky Pond and there was no similar response in The Loch. Thus, while trout stocking may have influenced benthic chlorophytes in one lake, stocking cannot account for the coherent change in ecosystem state seen in both Sky Pond and The Loch.

2.4.3 Beyond nitrogen deposition – nutrient and climate interactions

Previous ecosystem and experimental studies in the Colorado Front Range and elsewhere uncovered the effect of N fertilization on lake ecosystems (Baron et. al., 2000; Nydick et. al., 2003; Saros et. al., 2005; Elser et. al., 2009). The advent of atmospheric N deposition shifted phytoplankton toward P-limitation and benefitted mesotrophic planktonic diatoms (Elser et. al., 2009A, B). Asterionella formosa, in

particular, thrives in high N, low P environments (Saros et. al., 2005; Saros et. al., 2011). The effects of N deposition on lake trophic state have since been widely reported from many locations in the Northern Hemisphere (Bergström and Jansson 2006; Elser et. al., 2009B). While N deposition increased mid-20th century, both wet and estimated total N deposition have been relatively stable since 2000 (Baron, 2006; Mast et. al., 2014; Morris 2018), thus N deposition alone is unlikely to be the sole cause of the changes we found in the sediment record. Additional forces, in conjunction with a legacy of N deposition, are altering phototrophic communities.

There is evidence of increased P deposition to the Rocky Mountains from sediment records, analyses of dust in winter snowpack, and long-term and spatial patterns of lake and stream data (Neff et. al., 2008; Clow et. al., 2016; Brahney et. al., 2013; Stoddard et. al., 2016). Increased weathering of apatite, a P-bearing mineral, or increased delivery of apatite particles from beneath thawing ice features may also be a source of the nutrient (Price et al. 2017). While we do not have long-term total P records for our lakes, recent values of 7-12 µg/L suggest moderate P availability, and the current TN:TP molar ratio of 60-70 is similar to values reported from collections in 2006 (Elser et. al., 2009B).

Air and water temperatures have increased worldwide and in the Rocky Mountains since the 1980s (National Climate Assessment 2018, O'Reilly et. al., 2014, Mast et. al., 2014). In the Loch Vale Watershed, summer air temperatures have warmed 0.21 °C decade^{-1} (June August, 1984-2017, Figure 2.7A). However, over the same period, surface water temperatures in The Loch have increased at a faster rate of 0.60 °C year^{-1} (Figure 2.7B). Southern Rocky Mountain lake temperatures are projected to

increase by a similar amount (0.47°C decade^{-1}) during the 21st century (Roberts et. al., 2017).

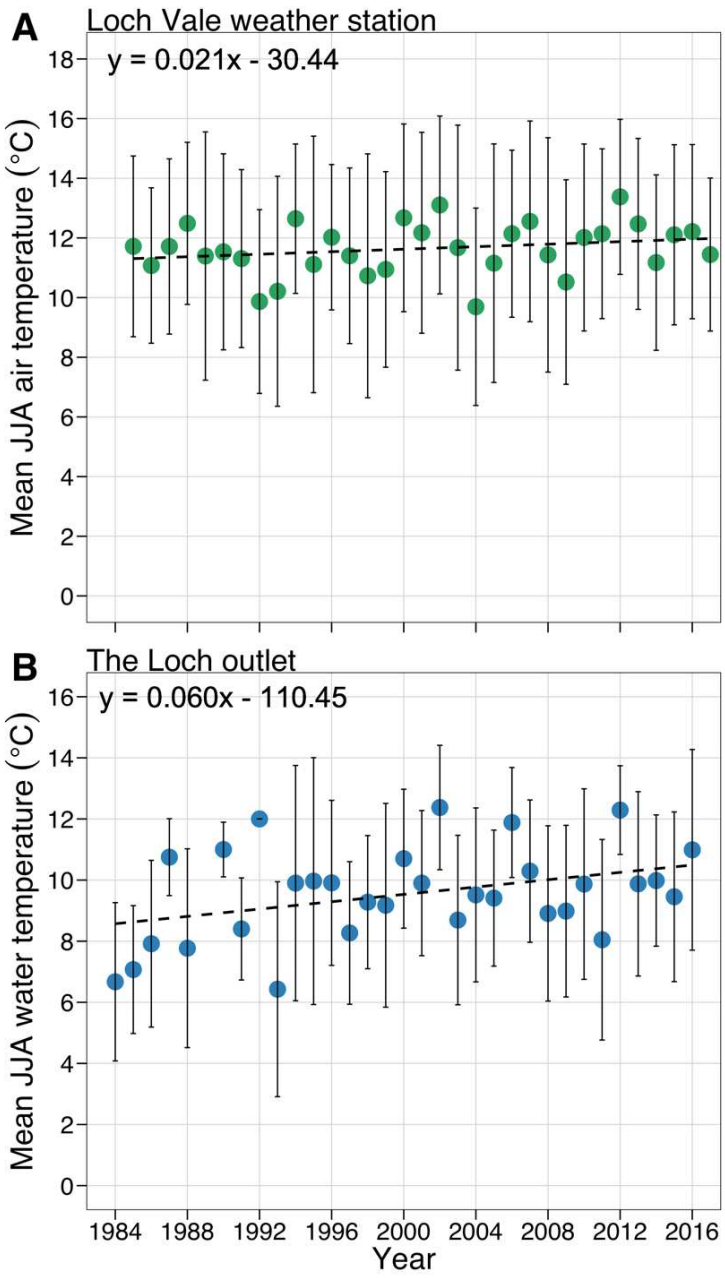

Figure 2.7. Temporal trends in mean summer and air water temperatures in Loch Vale Watershed and The Loch (subalpine lake). (A) Mean (± standard deviation) summer (July-July-August) air temperatures from the Loch weather station and (B) mean (± standard deviation) summer water temperature trends from The Loch outlet (1984-2016). The mean summer air temperature is warming at a rate of 0.021 ºC year^{-1} with slightly higher overall rates for The Loch outlet water temperatures (0.06 ºC year^{-1}). Both trends are statistically significant with $p < 0.05$.

Indirect consequences of warming, such as earlier snowmelt timing, are postulated to affect lake productivity and algal structure (Preston et. al., 2016; Sadro et. al., 2018). Warming is known to alter hydrology, which influences ice-out dates and growing season length (Agbeti and Smol, 1995; Blenckner et. al., 2002; Schindler et. al., 1990). Earlier ice-out increased algal biomass by increasing water residence times, water temperatures, and nutrient availability in other alpine systems (Preston et. al., 2016; Sadro et. al., 2018). As areas of discontinuous permafrost thaw, they release previous locked-up nutrients and increase the thickness of soil active layers, as seen in Arctic regions (Frey and McClelland 2008; Kendrick et. al., 2018; Reyes and Lougheed 2015) and in the nearby alpine Green Lakes Valley (Barnes et. al., 2014). The observed ecological changes in Loch Vale may be a result of interactions with nutrient enrichment via chronic nitrogen deposition and these changing climatic conditions.

2.4.4 Lakes on a trajectory of change

Global environmental change is altering lake ecosystems in the southern Rocky Mountains. We suggest that the onset of N deposition may have “primed the pump” that led to a cascade of ecological shifts, beginning with changes to diatom assemblages (Wolfe et. al., 2003). The dominant habitat for diatoms changed from benthic to pelagic, and the benthos is now host to abundant green algal mats. We saw unambiguous changes in community composition ca. mid-20th century, but our sediment records do not indicate a commensurate increase in lake primary production. That may follow if high elevation lakes follow similar trajectories to those from lower elevations. With abundant N in mountain lakes, small changes in phosphorus loads can have

disproportionately large effects on algal production due to Redfield ratios (Morris and Lewis 1988, Redfield 1958). The observed changes in Loch Vale are similar to those documented in Arctic lakes, where increased primary production following global warming has been inferred from increases in planktonic diatoms and changes in species composition, as well as increased abundance of green algae (Douglas et. al., 1994; Florian et. al., 2015). Like Arctic regions, alpine regions are experiencing amplified rates of air temperature change resulting in warmer lakes, particularly in the last three decades (Kraemer et. al., 2016; Kraemer et. al., 2015; Pepin et. al., 2015). While our results are inferential only, they strongly suggest a legacy of N deposition, coupled with increasing dust (including P) deposition, and rapidly changing climatic conditions, may be changing the ecosystem structure of remote mountain lakes in the southern Rocky Mountains. Our results bear witness, along with other studies, of rapid changes occurring in the mid-20th century (Dubois et. al., 2018; Wolfe et. al., 2013). Sedimentary pigment and geochemical proxies unequivocally document systemic changes in lake autotrophic structure that are suggestive of profound ecosystem shifts in recent decades. The exponential increases in green algae, a shift from planktonic to benthic algal dominance, and changes in C:N ratios are indicative of accelerating change commensurate with multiple stressors associated with global change drivers proposed by Steffen et al. (2015).

3. NUTRIENTS AND WARMING ALTER MOUNTAIN LAKE BENTHIC STRUCTURE AND FUNCTION

3.1 Introduction

Two of the most influential drivers of global change are climate warming and increases in nutrient availability (Steffen et al., 2015). For freshwater aquatic ecosystems in particular, interactions between nutrient enrichment and warming-related impacts have the potential to significantly alter the structure and function of primary producers (Cross et al., 2015). In recent decades, a substantial amount of work has been done to understand how warming and increases in nutrient loads influence algae, but the focus in lake ecosystems has traditionally been on phytoplankton with comparatively little attention paid to benthic or attached algal communities (Moss et al., 2003; Petchey et al., 2010; Winder et al., 2009; Yvon-Durocher et al., 2010).

Although benthic primary producers assimilate significant amounts of nutrients and can reach high biomass in many lakes, these communities are globally under reported and understudied, largely due to sampling difficulties and high spatial heterogeneity (Vadeboncoeur et al., 2002; Vadeboncoeur and Steinman, 2002). Benthic habitats contribute a significant proportion to whole lake metabolism and biogeochemical processes in shallow oligotrophic lakes (Sadro et al., 2011). Groundwater upwelling of nutrient fluxes at the sediment-water interface are assumed to play a larger role in explaining patterns of benthic algal biomass and nutrient assimilation (Hagerthey and Kerfoot, 1998; Périllon et al., 2017), compared to water column nutrients which have a great influence on pelagic algal dynamics (Bonilla et al.,

2005; Vadeboncoeur et al., 2001) . Upwelling or overland flow will be intercepted by the benthic autotrophs and heterotrophs (hereafter “periphyton”), assimilating nutrients in hot spots and hot moments, similar to the role of the hyporheic microbial communities in streams (McClain et al., 2003). Some hypothesize that periphyton in lakes serve as the first line of defense, intercepting nutrients that enter the lake from shallow groundwaters or overland flow before they can be used by phytoplankton (Gettel et al., 2013; Nydick et al., 2004).

Increases in benthic algal biomass and appearance of certain algal taxonomic groups (e.g., filamentous green algae) can be indicative of local-scale disturbance and nutrient loading (Hampton et al., 2011; Rosenberger et al., 2008; Schneider et al., 2014). Reports of nearshore filamentous green algae blooms are increasing in many oligotrophic lakes around the world but the causes and consequences of their dominance in some systems is not well known (Gladyshev and Gubelit, 2019). In alpine Sky Pond in Rocky Mountain National Park, Colorado, paleolimnological investigations uncovered complicated changes in autotrophic community structure over the past 50-100 years. Whole lake primary production, that was historically dominated by benthic bacillariophytes, which have been replaced in recent decades by benthic chlorophytes and planktonic bacillariophytes indicative of mesotrophic conditions (Oleksy et al. *in review*). Benthic habitats are now routinely dominated by the heterogeneously distributed genera *Spirogyra* and *Zygnema*. The observed shift from a benthic mixed diatom community to a chlorophyte-dominated community coupled with modest increases in total lake production may be indicative of altered biogeochemical cycling

and could be an early warning indicator of eutrophication (Kann and Falter, 1989; Lange et al., 2016; Nelson et al., 2013).

While multiple drivers of change are synergistically altering periphyton community structure, the mechanistic causes and the implications for ecosystem function are not well constrained. We hypothesized that a combination of the direct and indirect effects of climate change and a legacy of nitrogen deposition induced an ecological shift in both planktonic and benthic algae in Loch Vale lakes in recent decades. In addition to atmospheric nitrogen deposition, there are several other pathways that may increase nutrient loading into headwater mountain lakes in the central Rocky Mountains. Increased aeolian dust inputs, glacier and rock glacier meltwaters, increased active layer thickness of soils, and thaw of discontinuous permafrost may contribute nutrient subsidies to alpine lakes (Barnes et al., 2014; Clow et al., 2003; Leopold et al., 2015). Unlike direct atmospheric deposition, the pathways for these nutrients include shallow groundwater upwelling to lake bottoms, or overland flow to shorelines. In the Arctic, thawing permafrost and the mobilization of previously locked-up nutrients is a major driver of ecological change in aquatic systems (Frey and McClelland, 2008; Kendrick et al., 2018; Lougheed et al., 2015); similar processes may be influencing alpine lakes where thawing glaciers and rock glaciers are subsidizing headwater aquatic ecosystems with nutrients and labile carbon (Brighenti et al., 2019; Fegel et al., 2019; Saros et al., 2010). Collectively, all of these different drivers could be selecting for algal species with different life-histories, nutrient acquisition kinetics, and growth forms than historical algal populations.

Our study had two major goals. The first was to understand the nutrient limitation of benthic algae in an alpine lake. We asked how nutrient availability influenced total benthic algal biomass and the relative abundance of different algal taxonomic groups. We answered these questions with an *in situ* nutrient diffusing substrate experiment in Sky Pond, Rocky Mountain National Park. We expected additions of nitrogen and phosphorus to increase total benthic algal biomass, which is a common response in nutrient diffusing substrate (NDS) experiments in oligotrophic environments (Beck et al., 2017). However, we expected that chlorophytes would dominate when enriched with nitrogen because macroalgae such as *Spirogyra*, *Zygnema, Cladophora*, and *Mougeotia* tend to grow well in high N:P environments and under P-limitation (Frossard et al., 2014; Hawes, 1988; Middleton and Frost, 2014).

The second goal of the study was to mechanistically understand how ecosystem processes in chlorophyte-dominated periphyton respond to different temperatures and nutrient concentrations. We conducted a short-term laboratory incubation to ask how nutrients and warming individually and interactively affect ecosystem functions, including benthic nutrient uptake, dissolved organic carbon exudation, gross primary production, and ecosystem respiration.

3.2 Methods

3.2.1 Study area

Our study focused on Sky Pond (40.27814 N, -105.66837 W; 3322 m.a.s.l.), an alpine lake in the Loch Vale Watershed (LVWS), Rocky Mountain National Park (Figure 3.1). The surface area of Sky Pond is 3 ha with an approximate volume of 1.2×10^5 m^3, maximum depth of 7.3 m, and average depth of 4.5 m (Baron 1992). Multiple flowpaths

supply water to Sky Pond, generally flowing through talus fields below Taylor Rock Glacier as well as groundwater upwelling (Baron 1992). The lake is chemically dilute but has high nitrate (NO_3) concentrations from regional nitrogen deposition and glacial inputs (Table 3.1; Baron et al. 2009).

The alpine landscape surrounding Sky Pond is characterized by dwarfed trees, grasses, willows, and sedges, but vegetation in the watershed is relatively sparse (Arthur et al., 1992). Much of the landscape above treeline is composed of talus, block slopes, and debris cones (Clow et al., 2003). The majority (80%) of the bedrock in LVWS is metasedimentary biotite gneiss that includes quartz, microcline, biotite, calcite, apatite, and monazite (Mast, 1992). Above 3400 m, mean annual temperature is cold enough to support permafrost; as much as 11% of the basin is estimated to be underlain by permafrost, in addition to cryic features like rock glaciers and glaciers (Clow et al 2003). At a neighboring research station at similar elevations, permafrost was recorded in the 1970s (Ives and Fahey, 1971), but its extent and thickness has diminished significantly in recent decades (Leopold et al., 2015).

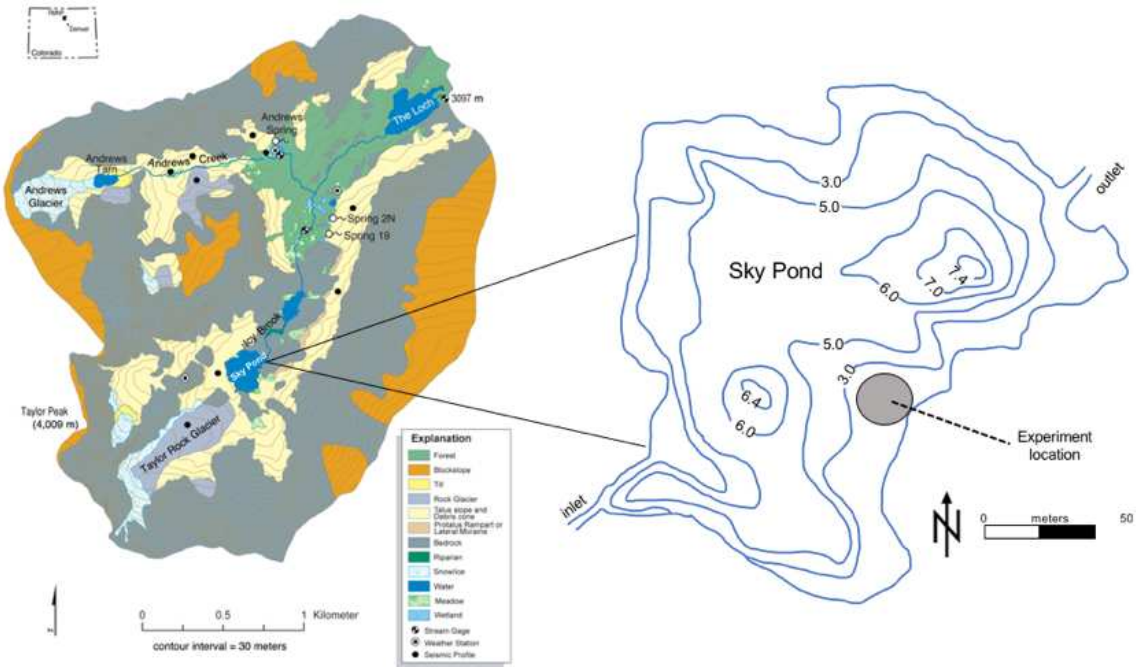

Figure 3.1. Map of Loch Vale Watershed, Rocky Mountain National Park, CO, USA with an inset of Sky Pond bathymetry (m). Location of the nutrient diffusing substrate experiment location is marked with a grey circle. Watershed map appeared originally in Clow et al., 2003 *Colorado Front Range Ground Water.*

Table 3.1. Water chemical properties for Sky Pond nutrient diffusing substrate (NDS) and incubation experimental initial conditions. Lake chemical parameters are reported as July and August means ± standard deviations for summer 2017. Littoral chemical parameters are reported as the mean of two samples taken where the NDS was deployed, at the start and end of the experiment. In the incubation experiment (n=72), the treatments received approximately 4x ambient lake DIN concentrations (N, N&P treatments) and approximately 10x ambient lake PO_4 concentrations (P, N&P treatments).

	Sky Pond environmental conditions during NDS experiment		**Laboratory incubation experiment initial conditions**			
Parameter	**Littoral**	**Lake**	**Control (Ctrl)**	**Nitrogen (N)**	**Phosphorus (P)**	**Both (N & P)**
Conductivity ($\mu S\ cm^{-1}$)	13.2	12.3	-	-	-	-
DOC ($mg\ L^{-1}$)	0.65 ± 0.05	0.52 ± 0.05	0.66 ± 0.05	0.66 ± 0.05	0.66 ± 0.05	0.66 ± 0.05
TDN (μM)	22.5 ± 1.0	14.9 ± 1.0	18.1 ± 1.1	66.6 ± 0.4	17.8 ± 0.7	66.6 ± 1.0
Chlorophyll a ($\mu g\ L^{-1}$)	-	9 ± 0.5	-	-	-	-
TP ($\mu g\ L^{-1}$)	10 ± 1	10 ± 1	-	-	-	-
PO_4 (μM)	0.8	0.8	0.8 ± 0.3	0.8 ± 0.3	8.7 ± 0.3	8.3 ± 0.3
DIN ($mg\ L^{-1}$)	0.23 ± 0.01	0.18 ± 0.01	0.18 ± 0.01	0.84 ± 0.03	0.18 ± 0.01	0.8 ± 0.03
DIN:TP (molar)	51.0	41.3	-	-	-	-
DIN:PO4 (molar)	-	-	22.4	82.5	2.1	7.6

3.2.2 Field experiment

Nutrient diffusing substrates (NDS) were built and deployed using methods outlined by Tank, Reisinger, and Rosi (2017). We filled 30 mL plastic vials with 4% agar solution and amended the treatments with no nutrients (control treatment, Ctrl), 0.5 M $NaNO_3$ (nitrogen treatment, N), 0.031 M KH_2PO_4 (phosphorus treatment, P), or 0.5 M $NaNO_3$ plus 0.031M KH_2PO_4 (nitrogen and phosphorus treatment, N & P). $NaNO_3$ was selected as the inorganic N carrier because NH_4^+ is found in low concentrations in Sky Pond and KH_2PO_4 was chosen because it is the most commonly used phosphate chemical in NDS experiments (Beck et al. 2017). Although the P additions were smaller than many other NDS manipulations, we aimed to simulate realistic P hotspots that may exist within the sediment-water interface of this lake. Diffusion tests by Lepori and Robin (2014) at similar starting concentrations confirmed that nutrients diffused at the end of the experiment at a rate of approximately 13 ± 5 µg P $hour^{-1}$.

A fritted 5.7 cm^2 glass disk was placed on top of each agar-filled vial and served as substrate for periphyton colonization. Vials were labeled, capped, randomized, and attached to six L-bars in groups of eight for a total of 48 experimental units, separated by approximately three cm space on all sides. All six L-bars were anchored to a plastic, porous tray with zip-ties and the tray was stabilized in the littoral zone of Sky Pond on the south-western shore approximately 20 m off shore and 0.75 m deep in a location where it would not be disturbed by National Park visitors. The experiment was deployed on 1 August 2017 and retrieved on 17 August 2017.

Water samples were collected for chemical analyses at the beginning and end of the experiment at the NDS deployment site in the littoral zone as well as from the mixed

layer of the epilimnion. Chemical analyses were conducted according to standard procedures for the Loch Vale program (https://www2.nrel.colostate.edu/projects/lvws/data.html). Inorganic nitrogen (NO_3^- and NH_4^+) and phosphate (PO_4^-) were measured by spectrophotometry using a flow injection analyzer (Lachat Company, Loveland, CO) at the Rocky Mountain Research Station (RMRS) Biogeochemistry Laboratory, Fort Collins, CO. Dissolved organic carbon and total nitrogen were also quantified by RMRS on a Shimadzu TOC-V Combustion Analyzer (EPA 415.1 and ASTM D5176, respectively). Total phosphorus (TP) was analyzed using persulfate digestion at High Sierra Water Laboratory (Tahoe City, CA; EPA method 365.1). Water temperature and conductivity were measured *in-situ* with a hand-held probe (Thermo Scientific Orion 3-Star). Concentrations of chlorophyll *a* were extracted with 90% acetone and analyzed using a benchtop fluorometer (Turner Designs Trilogy; EPA method 445.0).

We sampled mixed-community periphyton and chlorophyte-dominated periphyton in Sky Pond in summer 2017 to look at variation in carbon and nitrogen content. At six evenly distributed littoral sites around the lake, we sampled three patches of chlorophyte-dominated periphyton and three patches of mixed-community periphyton. We dislodged periphyton with a wire brush and used ambient lake water to rinse slurry into falcon tubes and kept on ice until we returned to the laboratory, where samples were immediately frozen. Carbon and nitrogen were analyzed on hand-ground, lyophilized samples with a LECO True-Spec CN analyzer (Leco Corp., St. Joseph, MI, USA) in the EcoCore Laboratory, Colorado State University.

Since porous fritted glass disks were used as substrata for the periphyton, microscopic taxonomic quantification identification of periphyton was not possible. We quantified total algal biomass as the sum of chlorophyll *a* and derivatives and quantified the biomass of pigments specific to certain algal groups. Fucoxanthin served as an indicator of bacillariophytes (diatoms), myxoxanthophyll for cyanobacteria, and total chlorophyll *b* for chlorophytes (green algae) (Leavitt and Hodgson, 2002; Steinman et al., 2017). All pigments were quantified on a ultra-performance liquid chromatography-ultraviolet-mass spectrometer (UPLC-UV-MS) system using a procedure modified by Fu et al. (2012) and described in Beck et al., 2019). Pigments were extracted from the disks in an 85:10:5 acetone:methanol:water solution in glass dram vials. The extractant was filtered through 0.22 micron syringe filters, and dried under N_2 gas (Steinman et al., 2017). The leftover residue in the dram vials was resuspended in a 1:1 acetonitrile:MTBE solution (Fu et al., 2012). An Acquity UPLC system with a tunable UV detector (Waters Corporation, Milford, MA) was used to measure sample UV intensities while the MS was used to confirm target pigments. We developed calibration curves from pigment standards to convert UV areas to masses (Leavitt and Hodgson, 2002); to obtain sample pigment masses, UV intensity curves were integrated using Compass Hystar data software (Bruker Corporation, Billerica, MA). Responses to treatments are presented as total areal pigment mass (μg pigment cm^{-2}).

3.2.3 Incubation experiment

Four unglazed clay 36 x 36 cm tiles (acid washed and soaked in DI water for seven days) were placed in Sky Pond in early July 2017. Each tile had approximately 25 small (surface area=5.7 cm^2) rough, porous fritted glass disks attached to them with

non-toxic aquarium sealant. The tiles were incubated in situ at a shallow bay in the lake where *Spirogyra* have grown in extensive mats in previous years (IAO *pers. obs.*). Tiles were retrieved from Sky Pond after two weeks and transported on ice back to the laboratory with minimal disturbance. Once in the laboratory, the tiles were incubated in growth chambers in an 8ºC water bath containing filtered lake water and 16:8 light dark cycle. Algae continued to grow on the fritted glass disks in the growth chambers for another week until the initiation of the experiment. Although we were not primarily interested in changes in algal structure, we used a BenthoTorch™ (bbe Moldaenke, Germany) to estimate initial and final benthic algal biomass and controlled for any changes in our observed functional responses (see "Statistical analyses").

We designed a three by four factorial experiment (temp x nutrients, respectively) for an eight-day incubation. The coldest temperature (8ºC) represented 2015-2017 mid- to late summer averages for the littoral zone of Sky Pond. The 12ºC temperature treatment represented 2015-2017 peak maximum temperature in the littoral zone. The warmest temperature treatment (16 ºC) represented a warming scenario comparable to littoral conditions in a downstream subalpine lake, The Loch.

Nutrient treatments included control (Ctrl), elevated nitrogen (N; 4x higher than ambient lake water), elevated phosphorus (P; 10x higher than ambient lake water), and elevated nitrogen and phosphorus treatments (N & P; 5 and 10x higher than ambient lake water concentrations, respectively; table 1). Due to atmospheric N deposition, ambient lake water (Ctrl) had an average NO_3-N concentration of 12 µM and an N:P molar ratio of approximately 120 (Elser et al., 2009). Each beaker contained one colonized fritted glass disk. The experiment was conducted under a 16:8 hour light:dark

cycle and all beakers were exposed to the same intensity of light. The experiment was monitored daily and we corrected for evaporative loss by supplementing with DI water.

At the conclusion of the eight-day experiment, we poured the overlying water into acid-washed Nalgene® high density polyethylene (HDPE) plastic bottles for chemical analyses and estimates of nutrient uptake (further explanation to follow). Water was filtered (Whatman GF/F) within six hours of the end of the experiment. Nitrogen uptake rates were calculated as the difference between initial dissolved nitrogen and final dissolved nitrogen concentrations divided by incubation length. Similarly, we calculated nitrogen uptake efficiency as the initial minus final nitrogen concentration multiplied by 100.

We conducted short term light-dark incubations on each of the fritted glass disks to estimate GPP and ER following methods developed by Reisinger, Tank, and Dee (2016). We estimated NEP (μg O2 cm^{-2} h^{-1}) as the increase in dissolved oxygen in the light incubation and ER (μg O2 cm^{-2} h^{-1}) as the decrease in dissolved oxygen during the dark incubation, with each glass disk representing the “ecosystem” (Eqn. 1). To conduct the light-dark incubations, we placed each fritted disk into a 50mL acid-washed falcon tube and filled the tubes with filtered lake water from a 3.75 L bucket and capped the tubes underwater to avoid air bubbles. We measured temperature and dissolved oxygen of the bucket water with a multimeter probe (Hach, Loveland CO), which served as experimental starting conditions. Falcon tubes were inverted and exposed to the same light and temperature environment as the eight-day experiment. After the light incubation, we measured the temperature and dissolved oxygen concentrations of each tube. The centrifuge tubes were refilled with a fresh batch of filtered lake water and

incubated in a dark environmental chamber at 8ºC. The light and dark incubations each ran for 3-4 hours, which was long enough to observe significant changes in dissolved oxygen concentrations. We controlled for changes in dissolved oxygen of the filtered lake water by incubating falcon tubes without glass fritted disks. Gross primary production (μg O_2 cm^{-2} h^{-1}) was calculated as:

$$GPP = NEP + ER; \quad \text{(Eqn. 1)}$$

3.2.4 Statistical analyses

All statistical analyses were performed in R version 3.4.4. (R Core Team 2018). Treatment effects were quantified for the NDS experiment using a one-way analysis of variance (ANOVA) on each individual pigment (n=4). Chlorophyll *a* concentrations were log transformed to meet the assumptions of normality. Where log- and square root-transformations did not help meet model assumptions (myxoxanthophyll, chlorophyll *b*), we used the Kruskal-Wallis followed by a Dunn test to check for pairwise comparisons using *dunnTest* function in the *FSA* package.

For the incubation experiments, responses were analyzed as a two-way analysis of covariance (two-way ANCOVA) to determine whether there were individual or interactive effects of temperature (as a factor) and nutrient treatments in terms of a continuous response variable (N uptake rates, N uptake efficiency, DOC exudation, GPP, ER, NEP), with observed changes in benthic algal biomass as a covariate. We contrasted least-squared means with Tukey-adjusted p-values to determine post-hoc significant differences among treatments (α=0.05), using the *lsmeans* package and estimated slopes using the *lstrends* package. Multiple regression analysis by the backwards stepwise procedure was used to select the minimum combination of

variables explaining the variability in key responses (e.g., N uptake rates and efficiency, DOC exudation). All plots were drawn with *ggplot2* package.

3.3 Results

3.3.1 Field data

Sky Pond is generally oligotrophic with low conductivity (13.2 μS cm^{-1}), low dissolved organic carbon concentrations (DOC; 0.52 ± 0.05 mg L^{-1}), and summer phytoplankton biomass averaging 9 ± 0.5 μg L^{-1} chlorophyll *a* during the summer of 2017. Dissolved inorganic N concentrations (DIN) were relatively high (0.18 ± 0.01 mg L^{-1}) resulting in high DIN:TP ratios. Total dissolved nitrogen (TDN), DOC, and DIN were slightly higher in littoral than pelagic habitats (Table 3.1). We analyzed carbon and nitrogen content of mixed-community periphyton and compared values to those of chlorophyte-dominated periphyton. While C:N ratios were similar between the two periphyton types (two-sample t-test; t = 1.1857, df = 24, p-value = 0.2473), chlorophyte-dominated periphyton on average had 3.3 times higher percent carbon (t = 9.1345, df = 17.565, p<0.0001) and almost three times as much nitrogen per unit dry mass (t = 8.2435, df = 19.471, p<0.0001) compared to mixed-community periphyton (Figure 3.4).

3.3.2 Field experiment - biomass and community structure

Nutrient additions had a significant effect on total amount of algal biomass as chlorophyll *a* ($F_{3,30}$=19.059, p<0.0001; Table 3.2). When both N and P were added, total biomass was highest and there was substantially more algal biomass compared to the control, N, and P treatments (Figure 3.2). The effect of N additions alone did not differ

from the no-nutrient Ctrl, and when P was added as the only nutrient addition, there was a slight decrease in algal biomass compared to the control.

We quantified the relative influence of nutrient enrichment on major algal taxonomic groups. Nutrient enrichment had a strong positive effect on chlorophyte (as chlorophyll *b*) biomass and biomass was significantly greater in the N and N & P treatments than either the no-nutrient control or P treatments ($\chi^2_{3,60}$ =23.199; p<0.0001). The opposite was observed for diatom biomass (as fucoxanthin). A one-way ANOVA revealed that the control had the highest biomass of bacillariophytes compared to all nutrient treatments ($F_{3,30}$=31.459; p<0.0001). The P treatment stimulated diatom biomass accumulation more than N and N & P treatments. Cyanobacteria biomass (as myxoxanthophyll) was uniformly low in the no-nutrient control, N, and P treatments, but was significantly higher than the control when both N and P were added together (χ^2_3 =7.337; p<0.0001). Bacillariophytes comprised the highest proportion of total algal biomass in the no-nutrient control and P treatments while chlorophytes contributed the most biomass in the nitrogen and N & P treatments (Figure 3.3).

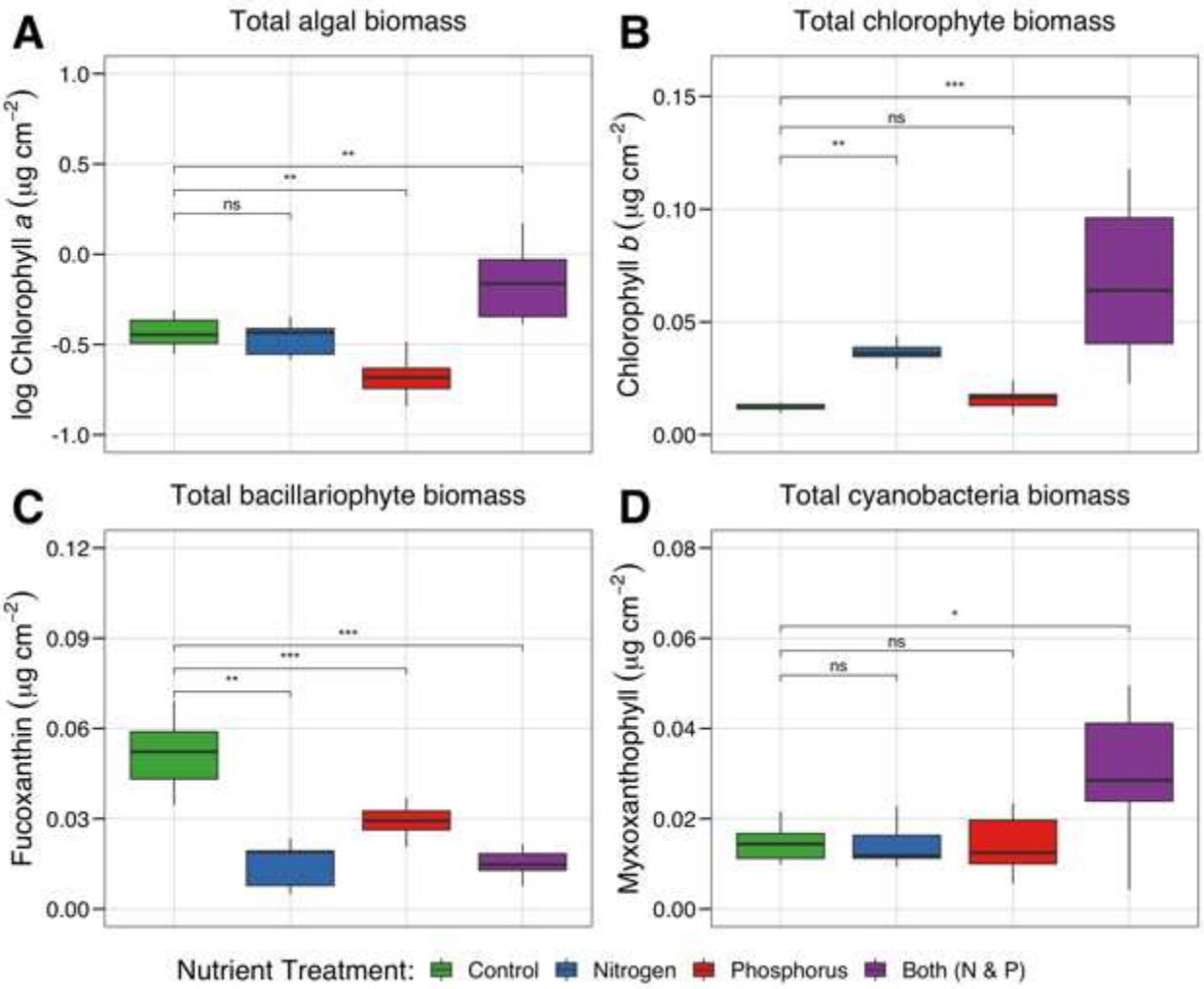

Figure 3.2 Algal biomass responses to nutrient enrichment in the nutrient diffusing substrate experiment. (A) Total algal biomass (as chlorophyll a), (B) total chlorophyte biomass (as chlorophyll b), (C) total bacillariophyte biomass (as fucoxanthin), and (D) total cyanobacteria biomass (as myxoxanthophyll). The box plots show 25-75% quantiles and the thick black lines are the median of 12 replicates in each treatment. Statistical significance across pairwise comparisons are denoted as: ns: $p > 0.05$, *: $p \leq 0.05$, **: $p \leq 0.01$, ***: $p \leq 0.001$, ****: $p \leq 0.0001$. Note difference in scale of the y-axis.

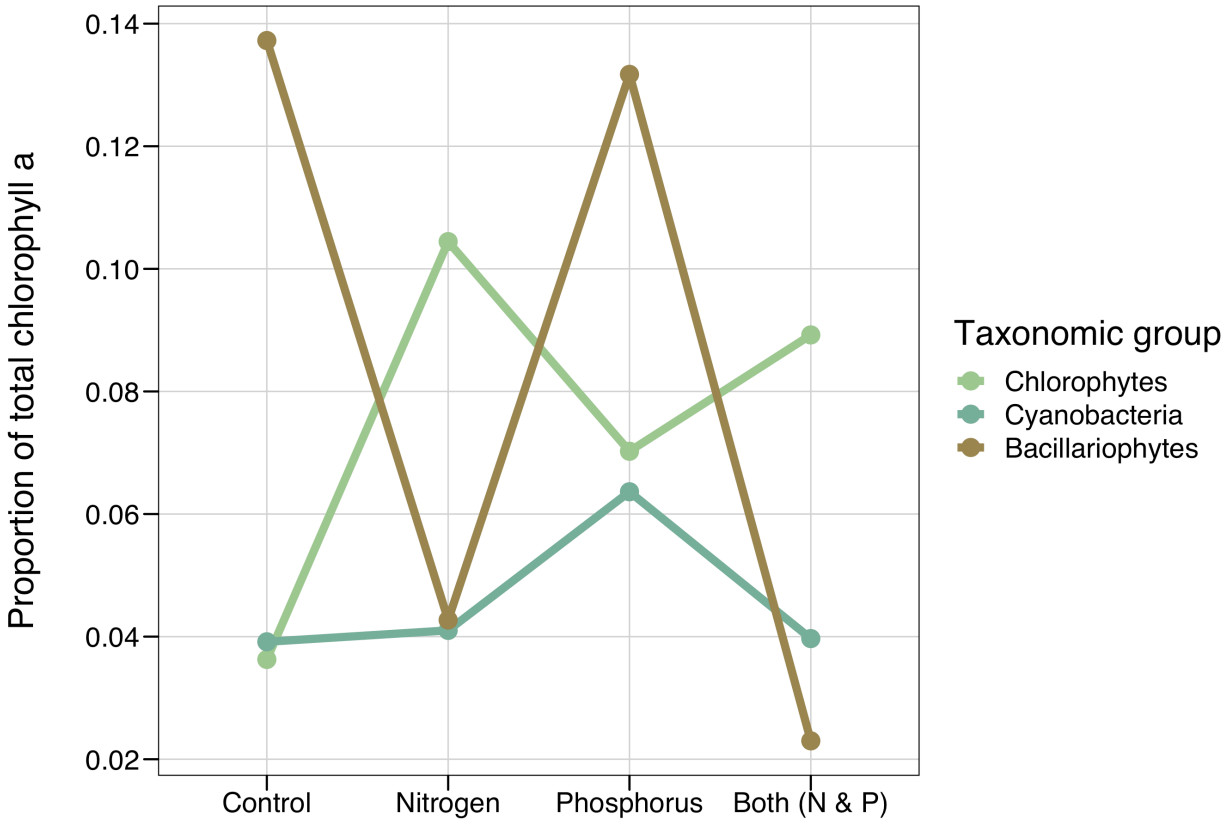

Figure 3.3 Mean chlorophyte, cyanobacteria, and bacillariophyte responses to treatments. Each taxonomic group is shown as a proportion of total algal biomass (as chlorophyll *a*).

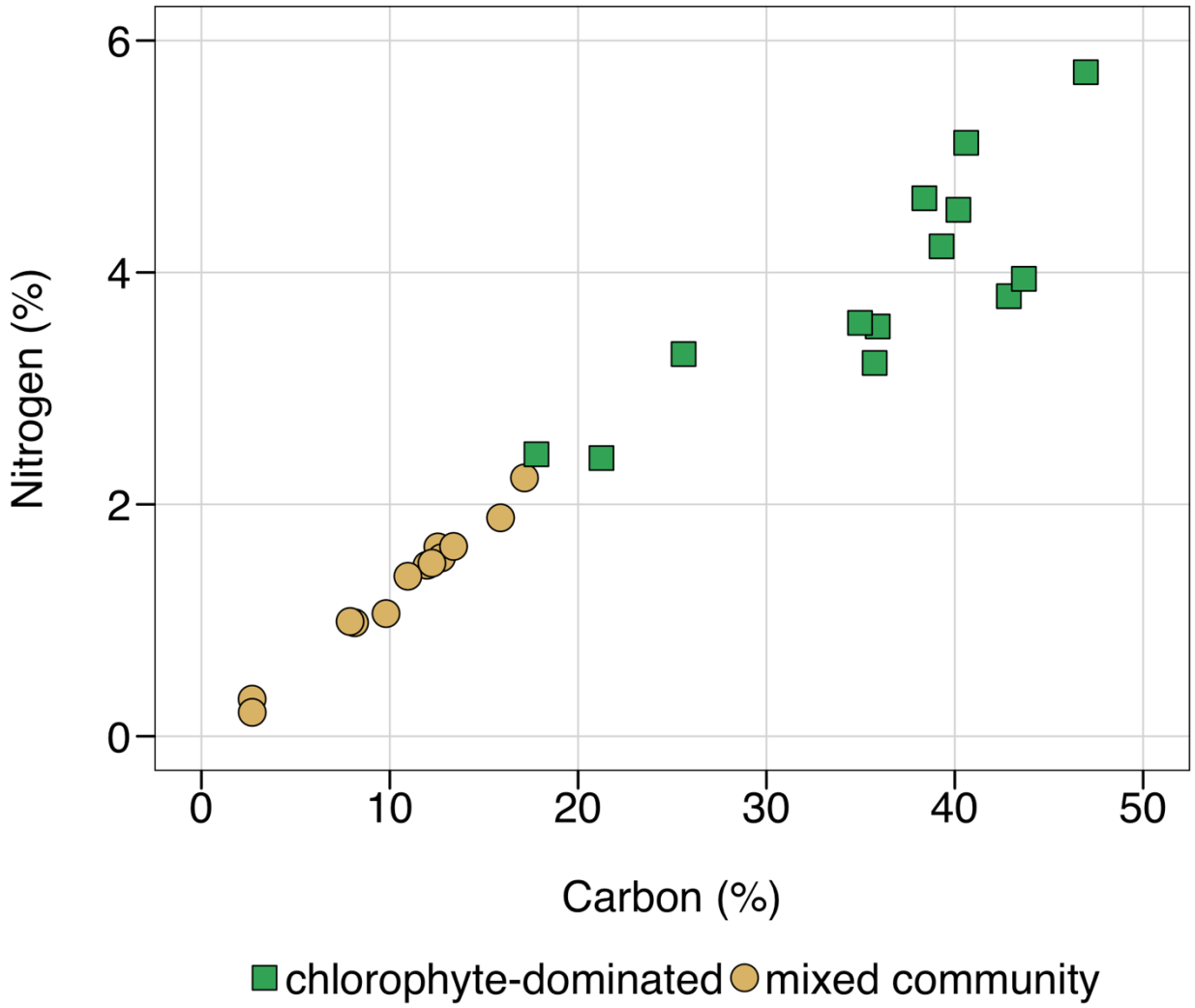

Figure 3.4. Carbon and nitrogen content (% of dry mass) of mixed biofilms (diatoms, chrysophytes, minor green algae) and green algae dominated biofilms harvested from Sky Pond in 2017.

3.3.2 Incubation experiment

Across all measured response variables, we included the small observed changes in benthic algal biomass as a covariate in our ANCOVA models but found very small effect sizes and limited explanatory power. Benthic chlorophyll *a* concentration was high in all nutrient and temperature incubations (6.9 ± 1.0 μg cm^{-2}) and varied little over the duration of the experiment.

3.3.2.1 Nitrogen dynamics

Our results demonstrated the high capacity of benthic chlorophytes to assimilate inorganic N but also showed the importance of the N:P ratio of the water in influencing rates of uptake (Figure 3.5, Figure 3.6). Controlling for changes in benthic algal chl *a,* across all experimental treatments, nutrient amendment had a large effect on TDN uptake rates ($F_{3,59}$=300.76, p<0.0001). The model also identified a significant temperature by nutrient treatment interaction ($F_{6,59}$=44.1081, p<0.0001), which is most evident in the N treatment, where TDN uptake increased as a function of increasing temperature. Total dissolved N uptake rates were similarly and consistently low across temperature treatments in the unenriched control and P treatments and insensitive to changes in temperature. However, when both N & P were added TDN uptake rates were 6-7 times higher than the Ctrl and P treatments. In the N and N & P treatments, all pairwise comparisons among temperature treatments were statistically significant, but the pattern was much starker in the N-enriched treatments where TDN uptake rates increased from 1.9, 3.0, 5.4 μM N day^{-1} in the 8, 12, and 16ºC treatments, respectively. In the N & P treatment, mean uptake rates increased from 6.1 to 7.3 μM N day^{-1} between the 8 and 12ºC treatments but then decreased slightly in the 16 ºC treatment to 6.8 μM N day^{-1}.

Since N was supplied in different quantities across treatments, investigating the percentage of initial N that was taken up (hereafter N uptake efficiency) provided some further context to describe the N-cycling dynamics. As with N uptake rates, N uptake efficiency was also highest in the N & P treatments (Figure 3.5B). The test for the main effect of nutrient treatment was significant ($F_{3,59}$ =65.8275, p<0.0001) as well as the

main effect of temperature ($F_{2,59}$ =11.0975, p<0.001), with a strong interaction between temperature and nutrient amendment ($F_{6,59}$=19.9433, p<0.0001). Temperature influenced N uptake efficiency in all nutrient treatments except the P treatment, which showed no significant pairwise differences across temperatures. When P alone was supplied, more N was taken up on average than the control in the coldest treatment but did not appear to play as big of a role at warmer temperatures. Only in the control and N treatments (when P was in low supply relative to N) did we see very large differences by temperature (Figure 3.5B). In all temperature treatments, N uptake efficiency was highest in the treatments enriched with N & P.

In spite of N concentrations approaching 10x higher than background in N and N & P treatments, the benthic communities still assimilated up to 88% of available inorganic N at 16ºC. At low TDN:PO4 molar ratios of 25, most NO_3^- was assimilated (figure 6). In a multiple regression analysis on NO_3^- assimilation, we found 69.8% of the variation could be explained by the main effects of temperature and nutrient treatments , but an additional 10.3% of variation was explained by the interaction between initial N:P ratio and temperature. Nitrate uptake efficiency was significantly lower at 8ºC and 12ºC compared to 16 ºC. Slope coefficients were -0.53, -0.40, -0.14 for 8, 12, and 16ºC, respectively. The slopes for 8 and 12ºC were not statistically different (p=0.1227) but

both were significantly steeper than the slope across all nutrient treatments at 16ºC ($p<0.001$).

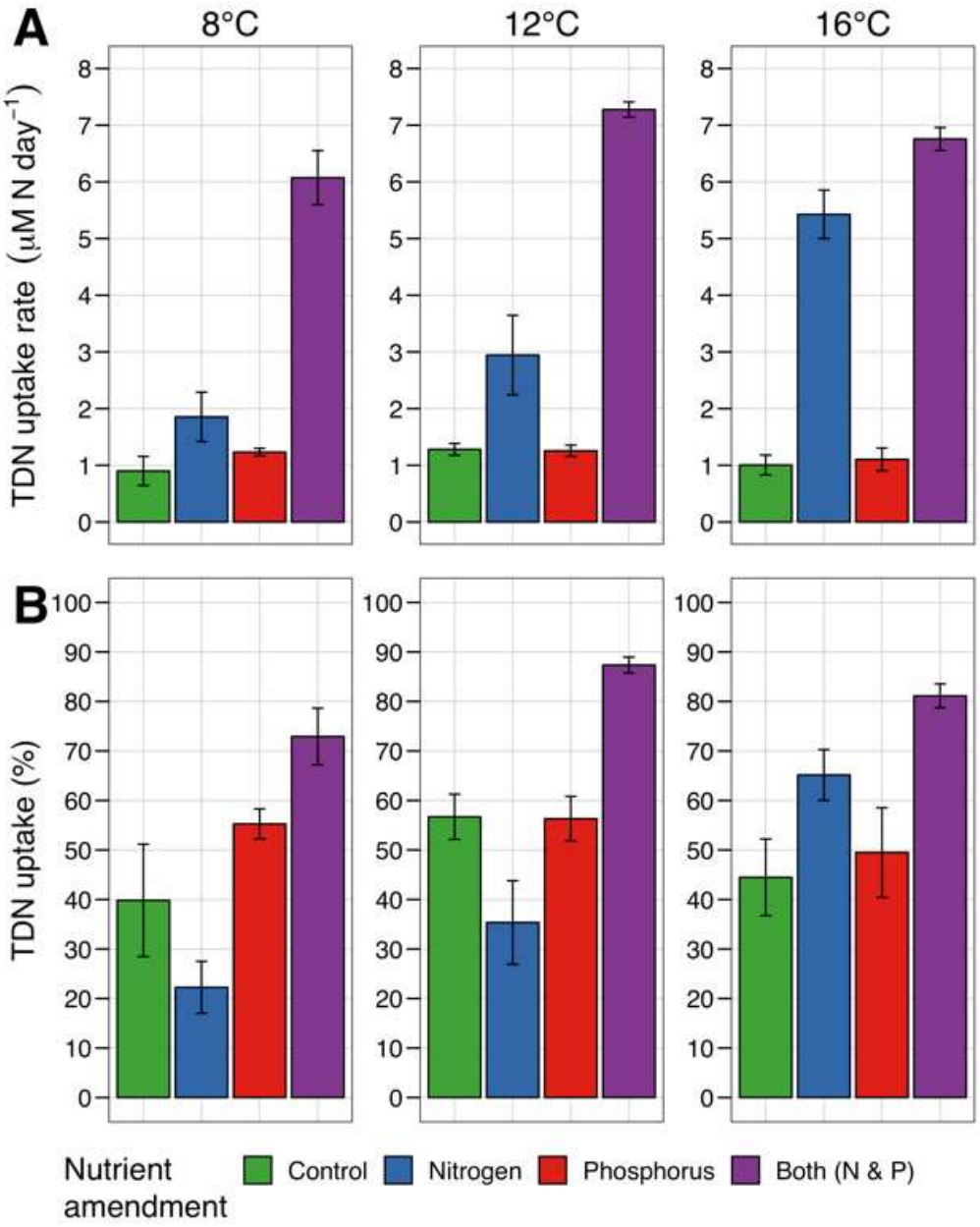

Figure 3.5. (A) Total dissolved N (TDN) uptake rates (µM day^{-1}) and (B) percentage of initial TDN assimilated across each temperature (panel) by nutrient enrichment (color) combination. Error bars are mean ± 1 SD.

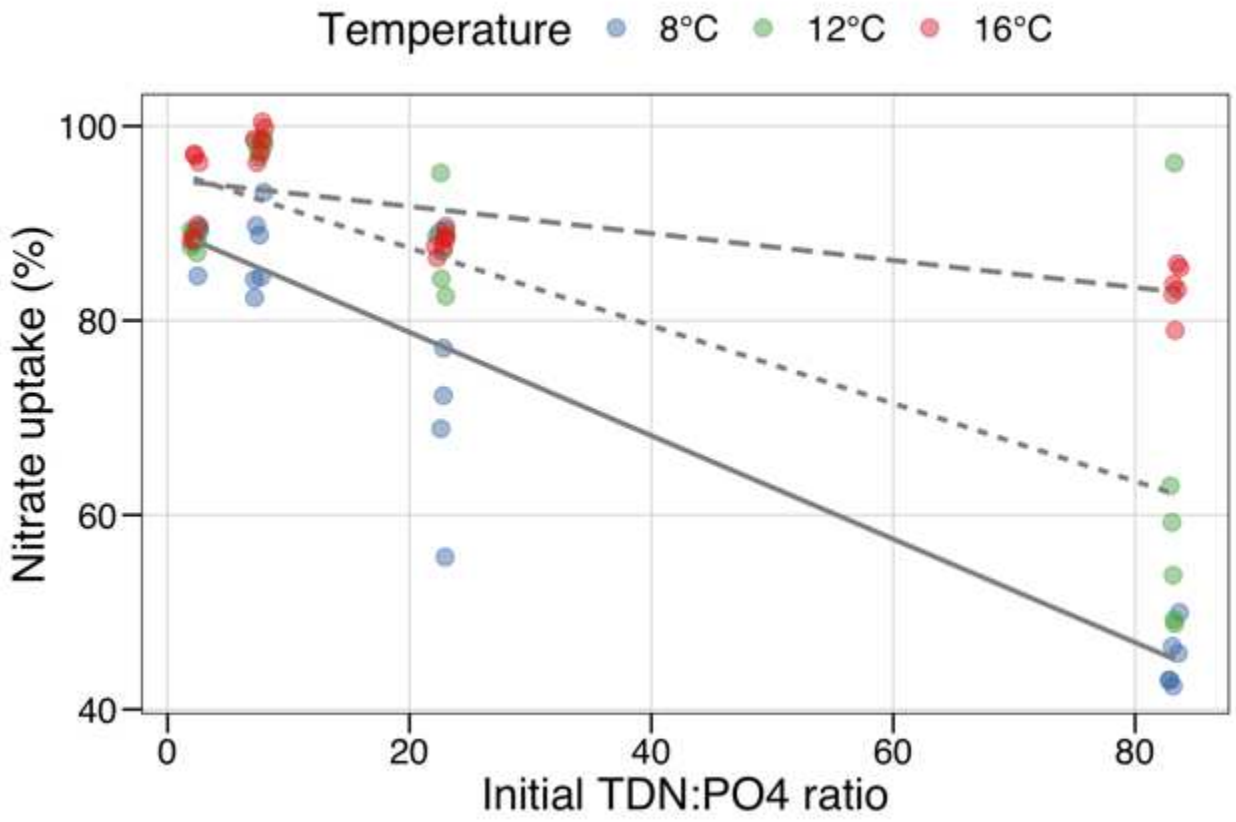

Figure 3.6. Percent nitrate assimilated versus initial TDN:PO4 ratio of treatment water with a separate linear regression for each temperature treatment. Points are jittered (small random quantities added to the x and/or y coordinates) to show individual response values. Slope coefficients were -0.53, -0.40, -0.14 for 8 ºC, 12 ºC, and 16 ºC, respectively. The slopes for 8 ºC and 12 ºC were not statistically different ($p = 0.1227$) but both were significantly steeper than the slope across all nutrient treatments at 16 ºC ($p < 0.001$).

3.3.2.2 Dissolved organic carbon exudates

In all of the treatments, there was a substantial amount of algal-derived DOC in the water at the end of the experiment. Final dissolved organic carbon (DOC) ranged between 1.4 and 4.4 mg C L^{-1} at the end of the incubations (2.1 and 6.6 times higher than initial conditions). Nutrient treatments by themselves did not influence final DOC concentrations, but overall, DOC concentrations were inversely related with temperature ($F_{2,58}$ =6.0023, p =0.0043; Figure 3.7A). There was a significant interaction between

temperature and nutrients on DOC ($F_{6,58}$ =4.2428, p=0.002). Dissolved organic carbon concentrations did not change with nutrient treatments at 8ºC but did at 12 ºC and 16 ºC (all pairwise comparisons p > 0.05; Figure 3.7B). At 12ºC, the P and N & P nutrient treatments had significantly less DOC than the Ctrl and N treatments. At 16ºC, the gap widened further, and the Ctrl and N treatments had approximately double the concentration of DOC compared to the P and N & P treatments (2.5 and 2.8 compared to 1.3 and 1.4, respectively).

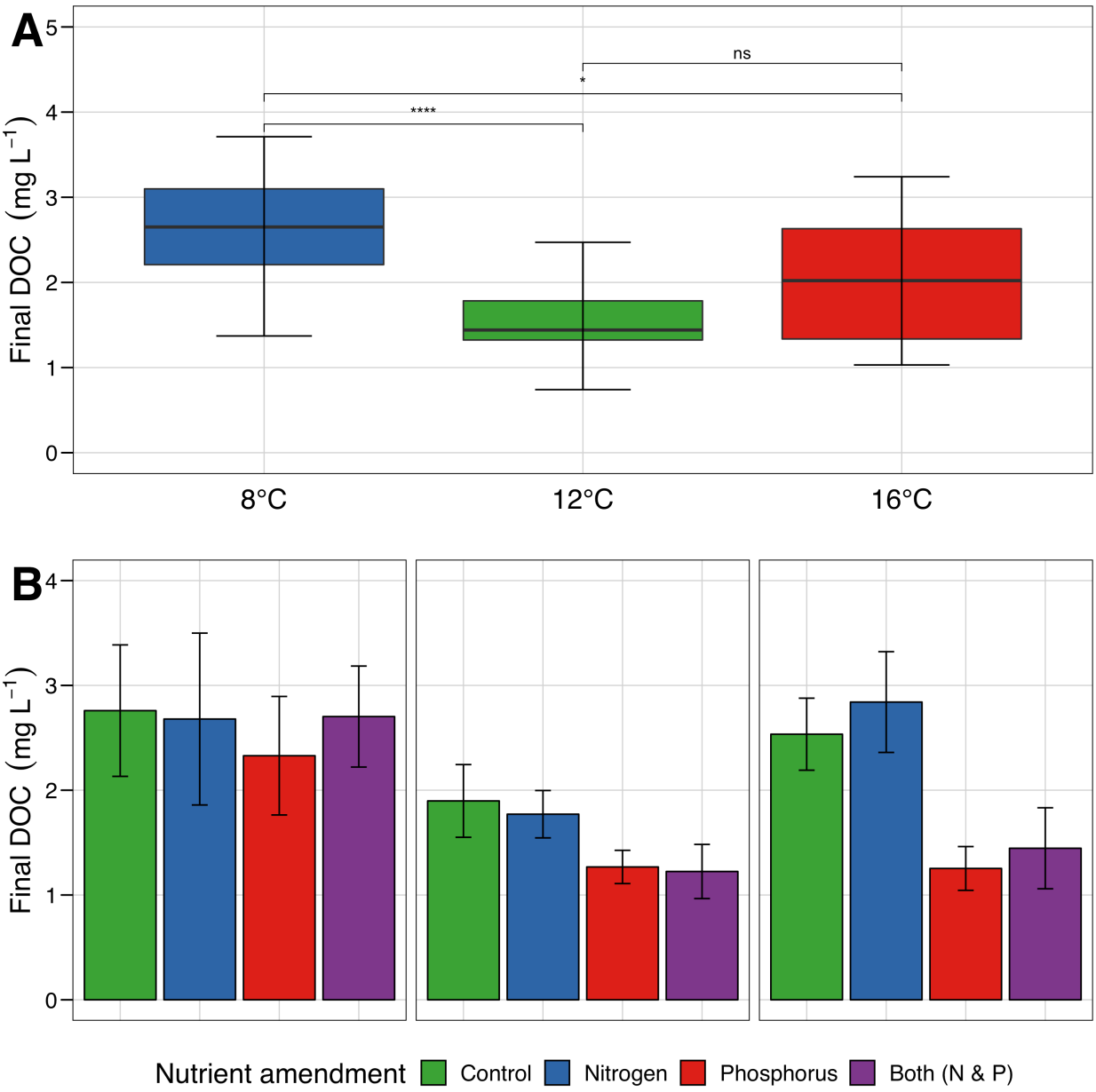

Figure 3.7. Final dissolved organic carbon (DOC) concentration (A) averaged across nutrient enrichments for each temperature treatment and (B) final DOC concentration across each temperature (panel) by nutrient enrichment (color) combination. Error bars are mean ± 1 SD. Statistical significance across pairwise comparisons across temperature treatments are denoted as: ns: $p > 0.05$, *: $p \leq 0.05$, **: $p \leq 0.01$, ***: $p \leq 0.001$, ****: $p \leq 0.0001$.

3.3.2.3 Metabolism

We ran short term (4 hour) light and dark incubations on each experimental treatment to estimate gross primary production (GPP), ecosystem respiration (ER), and net

ecosystem production (NEP; Figure 3.8A-C). Analysis of covariance on GPP revealed no significant effect of temperature or nutrient amendment alone, nor an interaction between the two (Table 3.2).

In contrast, ER rates increased significantly with temperature ($F_{2,60}$ =24.0709, p<0.0001) such that ER was significantly higher in the warmest treatment (-39.9 ± 5.46) than the 8 and 12 ºC treatments (-16.1 ± 6.93, -17.6 ± 9.56, respectively). Nutrient amendments alone did not stimulate ER ($F_{3,60}$ =1.7583, p=0.165), but the model identified an interaction between nutrients and temperature ($F_{6,60}$ =3.0315; p=0.012), indicating that the temperature effect was greater under certain nutrient conditions. The only significant pairwise comparison between nutrients, averaging across temperature treatment was between the Ctrl and N & P treatments at 12º C (p =0.0007). However, all pairwise comparisons by temperature within nutrient treatment groups were significantly different with the exception of between 8 ºC and 12 ºC in the N and P treatments (Figure 3.8B). The higher ER rates at 16 ºC yielded the lowest GPP:ER ratios with little variation across nutrient treatments (Figure 3.8D).

Net ecosystem production decreased as a function of temperature (Figure 3.8C). Temperature alone had the largest effect on NEP ($F_{2,60}$ =9.9869, p =0.0002), but the model also identified an interaction between temperature and nutrients ($F_{6,60}$ =2.8918, p=0.0155) and an effect of nutrients on NEP alone ($F_{3,60}$ =24.0709, p=0.0032). Averaged across all temperatures, the control had the highest NEP. At 8ºC, the control and P treatments had significantly higher NEP than N and N & P treatments. At 12 ºC, NEP was significantly lower than the control in all of the enriched treatments. And at 16ºC, the P treatment had the lowest NEP; NEP rates between the Ctrl, N and N & P

treatments were similar. NEP declined with increasing temperature in the Ctrl and P treatments, while there was no statistically significant difference between temperature treatments amended with N and N & P (Figure 3.8C).

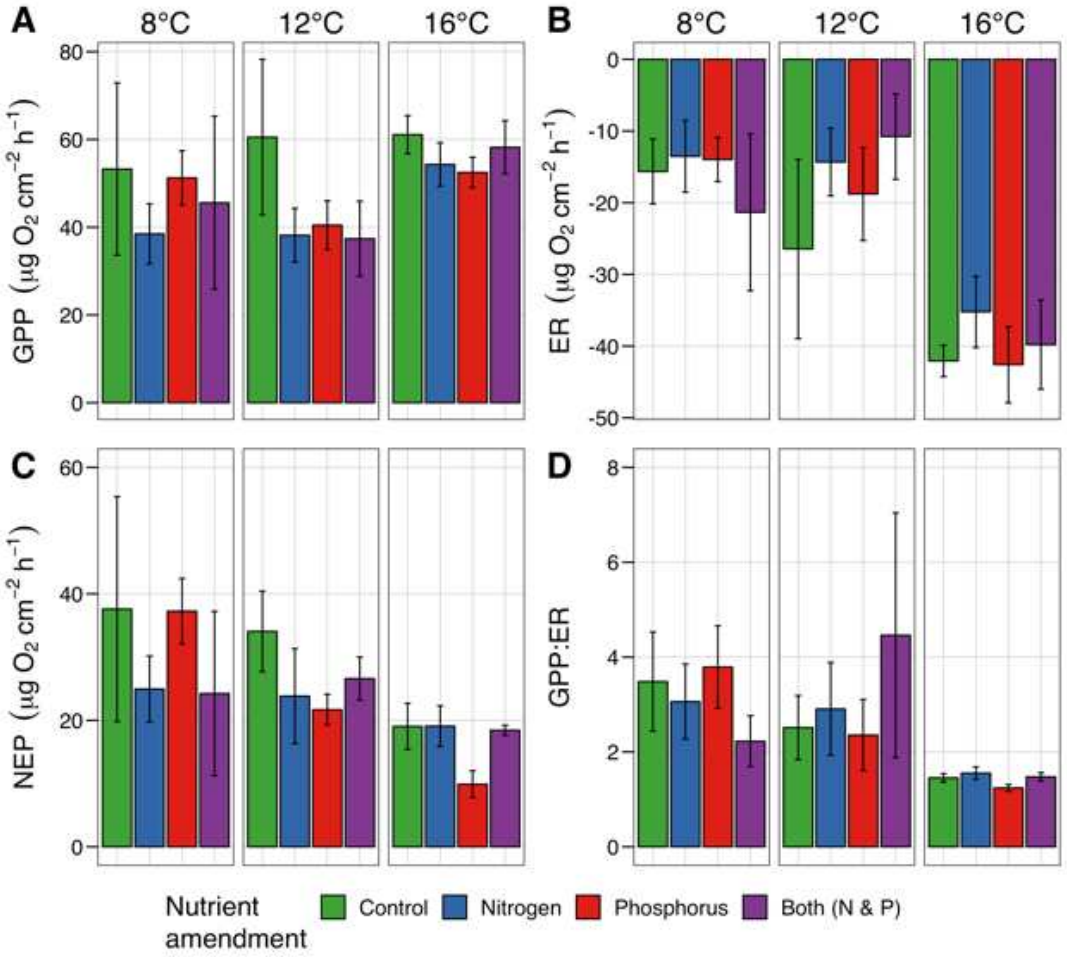

Figure 3.8. Metabolism assay results for (A) Gross Primary Production (B) Ecosystem Respiration, (C) Net Ecosystem Production, and (D) GPP:ER across each temperature (panel) by nutrient enrichment (color) combination. Error bars are mean ± 1 SD.

Table 3.2 Results of the analysis of variance (ANOVA), Kruskall-Wallis, and two-way analysis of covariance (ANCOVA) tests conducted for the NDS and incubation experiments. Response variables for NDS experiment include total algal biomass (as chlorophyll a), diatom biomass (as fucoxanthin), chlorophyte biomass (as chlorophyll b), and cyanobacteria biomass (as myxoxanthophyll). Measured responses in the incubation experiment include total dissolved nitrogen (TDN) uptake, TDN assimilated, dissolved organic carbon (DOC) exudation, gross primary production (GPP), ecosystem respiration (ER), net ecosystem production (NEP) and GPP:ER. Predictors with $p > 0.05$ appear in italics and $p \leq 0.05$ appear in bold.

Experiment	Response	Test	Predictors	F_{df}	p-value
NDS	Chlorophyll *a*	ANOVA	Nutrients	$F_{3,30} = 19.059$	**< 0.0001**
	Fucoxanthin	ANOVA	Nutrients	$F_{3,30} = 31.459$	**< 0.0001**
	Chlorophyll *b*	Kruskall-Wallis	Nutrients	$\chi^2_3 = 23.199$	**< 0.0001**
	Myxoxanthophyll	Kruskall-Wallis	Nutrients	$\chi^2_3 = 7.337$	**< 0.0001**
Incubation	TDN uptake	2-way ANCOVA	Temperature	$F_{2,59} = 2.0338$	*0.1401*
			Nutrients	$F_{3,59} = 300.7582$	**< 0.0001**
			Temp x Nutrients	$F_{6,59} = 44.1081$	**< 0.0001**
			Biomass change	$F_{1,59} = 0.0104$	*0.9190*
	% TDN assimilated	2-way ANCOVA	Temperature	$F_{2,59} = 11.0975$	**< 0.0001**
			Nutrient	$F_{3,59} = 65.8275$	**< 0.0001**
			Temp x Nutrients	$F_{6,59} = 19.9433$	**< 0.0001**
			Biomass change	$F_{1,59} = 0.3402$	*0.5620*
	DOC	2-way ANCOVA	Temperature	$F_{2,58} = 6.0023$	**0.0043**
			Nutrient	$F_{3,58} = 0.9823$	*0.4075*
			Temp x Nutrients	$F_{6,58} = 4.2428$	**0.0013**
			Biomass change	$F_{1,59} = 1.9669$	*0.1662*
	GPP	2-way ANCOVA	Temperature	$F_{2,60} = 1.0385$	*0.3605*
			Nutrient	$F_{3,60} = 2.1004$	*0.1100*
			Temp x Nutrients	$F_{6,60} = 1.5899$	*0.1665*
			Final biomass	$F_{1,59} = 0.8406$	*0.3630*
	ER	2-way ANCOVA	Temperature	$F_{2,60} = 23.8906$	**< 0.0001**
			Nutrient	$F_{3,60} = 1.4517$	*0.2371*
			Temp x Nutrients	$F_{6,60} = 2.8091$	**0.0181**
			Final biomass	$F_{1,59} = 0.5479$	*0.4621*

NEP	2-way ANCOVA	Temperature	$F_{2,60} = 9.9869$	**0.0002**
		Nutrient	$F_{3,60} = 5.1509$	**0.0032**
		Temp x Nutrients	$F_{6,60} = 2.8918$	**0.0155**
		Final biomass	$F_{1,59} = 0.4466$	*0.5066*
GPP:ER	2-way ANCOVA	Temperature	$F_{2,60} = 7.2154$	**0.0016**
		Nutrient	$F_{3,60} = 2.0418$	*0.1180*
		Temp x Nutrients	$F_{6,60} = 4.0689$	**0.0018**
		Final biomass	$F_{1,59} = 2.3117$	*0.1338*

3.4 Discussion

Sitting at the land-water interface, littoral zones are responsible for intercepting nutrients and are often indicators of eutrophication, particularly in shallow, oligotrophic systems (Wetzel, 1996). Periphyton, and the benthic phototrophs within them, can capture and store nutrients entering lakes from shores and upwelling groundwater. In alpine Sky Pond algal assemblages of periphyton changed in response to nutrient additions, and the combination of both nutrient addition and warming altered ecosystem processes and function. Total algal biomass was most responsive to the addition of both N and P in field NDS experiments, however, the responses varied by algal taxonomic group. Chlorophytes dominated when N additions were high (N, NP) and diatoms dominated when nitrogen concentrations were low (C, P) in the field experiment. Cyanobacteria comprised a minor proportion of the community overall, and were only responsive to the addition of both N and P. When experiments were conducted in the laboratory to study the responses to variations in temperature as well as nutrients on chlorophyte-dominated biofilms, warming had a strong, positive influence on N uptake rates and efficiency, ER, and NEP, but negligible influence on GPP. In spite of minor changes in total algal biomass, warmer temperatures and lower N:P ratios had the biggest influence on increasing N uptake rates and uptake efficiency.

3.4.1 Nutrient effects on algal assemblages and ecosystem processes

We expected to see a large response in benthic algal biomass in response to P additions in the field experiment, because inorganic NO_3^- is high in surface waters of Sky Pond from N deposition and a seasonal influx of N-rich glacier meltwaters from Taylor rock glacier. Abundant NO_3^- in lake waters has previously been shown to cause

P-limited phytoplankton (Elser, Andersen, et al. 2009; Baron et al. 2000; Nydick et al. 2003). Algal biomass increased with N&P additions, but P alone had no or a negative effect on total chlorophyll *a*. The analysis of major pigments indicative of chlorophytes (chlorophyll *b*), bacillariophytes (fucoxanthin), and cyanobacteria (myxoxanthophyll) provide additional context to explain more nuanced responses of contrasting algal taxonomic groups to nutrient enrichment.

Bacillariophytes comprised the largest proportion of the benthic autotroph community in control substrates and outcompeted benthic chlorophytes when additional P was added. In contrast, chlorophytes dominated in the N and N & P treatments. Chlorophytes tend to be higher in chl *a* per unit biomass as compared to bacillariophytes, which may be one explanation for why P-alone appeared to inhibit the growth of total algal biomass (as chl *a*) relative to the control. Chlorophytes like filamentous green algae are commonly found in N-enriched environments and increase with N enrichments in other oligotrophic lakes (Hogan et al., 2014; Lepori and Robin, 2014). In oligotrophic lakes in the Snowy Range, WY, USA, additions of both N and P increased densities of both planktonic and epilithic chlorophytes and cyanophytes, suggesting that nutrients can both stimulate production as well as change benthic community assemblages (Nydick et al., 2004). Benthic chlorophytes appear to outcompete benthic bacillariophytes in enriched conditions through differing nutrient-dependent growth and uptake optima (Litchman et al., 2007; Thomas et al., 2017). The response of cyanobacteria biomass to nutrients was low, likely because cyanobacteria make up a minor proportion of the algal community in Sky Pond.

In the absence of nutrient enrichment (controls) in the laboratory experiments, only 40-60% of the initial TDN pool was taken up in periphyton biomass. However, when both N and P were supplied, 70-85% was taken up, in spite of concentrations being 4x and 10x higher than the control, respectively. Nutrient uptake kinetics are highly plastic in algae and generally increase with increasing nutrient availability and higher P availability relative to N (Bonachela et al., 2011). While uptake of nutrients in some treatments, neither algal biomass nor GPP responded to nutrient enrichment. This could potentially be a result of slow growth rates, luxury uptake, high nutrient uptake capacity by benthic chlorophytes, or an artifact of the relatively short duration of the experiment (Dodds and Gudder, 1992; Gladyshev and Gubelit, 2019; Middleton and Frost, 2014). Our results mirror those from a whole-lake experiment in the Arctic, where the enrichment of N and P led to significant uptake of nutrients in benthic algae, with no increase in benthic GPP and no impact on phytoplankton biomass (Gettel, Giblin, and Howarth 2013).

Nitrogen uptake rates and efficiency increased as a function of temperature, but only when P was in low supply relative to N (high N:P). Our findings of greater N uptake at warmer temperatures are consistent with theory laid out by Cross et al. (2015), where nutrient use efficiency should increase with warmer temperatures. Nitrogen uptake appeared to be more efficient when N:P is low (Figure 3.6). In very high N treatments, the efficiency only approached that of N & P treatments when the temperature was high. In an experiment on planktonic chlorophytes, investigators found that the optimal N:P ratio changed with temperature, such that N demand was higher at higher temperatures owing to lower ribosome content at lower temperatures, which may partially explain this

phenomenon (Thrane et al., 2017). Our results suggest that at warmer temperatures, the initial N:P ratio is not as big of a factor in N uptake as it is at colder temperatures, when metabolic rates are likely temperature limited (Figure 3.6).

3.4.2 Metabolic functional responses to temperature increase

Our incubation results shed light on the relative importance of autotrophy versus heterotrophy in benthic periphyton in response to temperature and nutrient enrichment. Gross primary production was on average slightly greater at the warmest temperatures, the result was not statistically significant. In contrast, ER was highly responsive to temperature and NEP was lowest at the highest temperature treatments, with consistent GPP:ER across all possible nutrient enrichments at the warmest temperature. Both heterotrophic and autotrophic respiration rates (ER) increased more with warming than GPP or NEP (Martin et al., 2006; Yvon-Durocher et al., 2010). An increase in respiration from heterotrophic bacteria is supported by differential DOC concentrations at the end of the laboratory experiments. Although heterotrophic microbes were not measured directly, ER was highest in the warmest treatments where we also observed the lowest DOC concentrations, suggesting consumption of algal-derived DOC by heterotrophs in the periphyton matrix.

Significantly greater DOC concentrations were measured in the control and N amendments at the highest temperatures than in the P and NP treatments which may be explained by P-limitation generally resulting in greater exudation (Wyatt et al., 2014). Alternatively, nutrient additions may reduce extracellular carbon release (Durán et al., 2015). Algal carbon exudates are a major source of energy for heterotrophic bacteria in aquatic ecosystems and can be more readily consumed than recalcitrant C sources

from the terrestrial landscape (Baines and Pace, 1991; Haack and McFeters, 1982; Kaplan and Bott, 1989). Algal derived DOC can contribute substantially to the microbial loop in aquatic ecosystems, and can even enhance the breakdown of more recalcitrant OC (e.g., priming; Hotchkiss et al. 2014). Pathways of energy flow through the microbial loop may change as benthic primary producer communities, temperature and nutrient conditions interact to alter substrate quality and associated biogeochemical cycling in headwater mountain lakes. Future investigations would benefit from looking at additional heterotrophic functions such as extracellular enzyme activities to better elucidate autotrophic-heterotrophic linkages and implications for downstream lakes and streams with less labile organic carbon inputs.

3.4.3 Conclusions and implications for the food web, biogeochemical cycling

In mountain ecosystems, we can expect both warming temperature and changes in nutrient supply as a consequence of global change; understanding the interaction between the two stressors on benthic communities is imperative in predicting how headwater lakes and the downstream ecosystems they support will function as the climate continues to change. Nitrogen enrichment may lead to C:nutrient stoichiometry in the water column that alters the stoichiometry of primary producers (De Senerpont Domis et al., 2014; Lepori and Keck, 2012). Warming, too, may result in shifts in community structure to favor taxa with elevated C:nutrient and high nutrient use efficiencies, such as filamentous green algae (Cross et al., 2015). Although we did not analyze the C:nutrient ratio of the algae at the end of the experiment, field collected periphyton show that chlorophyte-dominated periphyton had much higher % C and % N than diatom-dominated periphyton in Sky Pond, illustrating both the nutritional value of

different periphyton types as well as their ability to retain nutrients (Figure 3.4). If high N ecosystems like these continue warming, littoral dominance of filamentous green algal generalists (e.g., *Oedogonium, Spirogyra, Cladophora*) and overall reductions in algal diversity may follow (Hickman, 1982). Large filamentous green algal blooms are known to simplify food webs, alter biogeochemical cycling, and decrease biodiversity (Turner et al., 1995; Vinebrooke et al., 2001). Especially in large mats, filamentous green algae are not a favored food source because they are difficult to harvest by many invertebrates and are a poorer food source (high C:P) (Allan and Castillo, 2007; Fulton, 1988). Thus, continued nutrient fertilization (e.g., N deposition in remote lakes) could benefit primary producers that are less palatable or nutritious for grazers. However, an increase in unpalatable benthic algae could decrease food chain efficiency and lead to trophic decoupling, when an increase in basal resources doesn't necessarily lead to an increase in higher trophic level production (Cashman et al., 2016; Müller-Navarra et al., 2000).

While the future of mountain lake function is far from certain, shifts in community structure have implications for biogeochemical function, particularly in N assimilation, carbon storage, and release of labile extracellular carbon. Chlorophytes like *Zygnema* and *Spirogyra*, which are now commonly observed in Sky Pond, may have higher temperature optima, high UV tolerance, and ability to survive desiccation with lake-level changes, all of which are traits that may favor their dominance in late summer as climate and particularly hydrological conditions change in the future (Holzinger et al., 2009; Holzinger and Karsten, 2013; Raven and Geider, 1988). The chlorophyte-dominated periphyton efficiently assimilated excess N and accumulated C through an

excess of primary production over respiration, even under warmer temperatures. The increase in at least seasonal storage of N and C has implications for downstream biogeochemical cycles and aquatic ecology.

4. UNDERSTANDING DRIVERS OF MOUNTAIN LAKE PHYTOPLANKTON ACROSS SPACE AND TIME

4.1 Introduction

Globally, lakes are warming as a result of increasing air temperatures and reduced cloud cover (O'Reilly et al., 2015). Changing lake thermal regimes are subsequently driving additional changes in biogeochemical, metabolic, and ecological functions in lake ecosystems (Gerten & Adrian, 2002; Kraemer et al., 2016; Michelutti et al., 2016). Indirect effects of warming, such as those caused by earlier ice-out dates, can also alter ecosystem dynamics by prolonging the growing season, with cascading effects on lake productivity and trophic status (Agbeti & Smol, 1995; Blenckner et al., 2002; George et al., 2004; Schindler et al., 1990). Warming and nutrients interact to alter productivity within lakes and will likely continue to do so in the future (Jeppesen et al., 2014; Meerhoff, 2012). Variation in adjacent land cover, lake morphometry, disturbance regimes, and connectivity to other water bodies may amplify or dampen an individual lake's response to regional climatic drivers (Kraemer et al., 2015; Leavitt, Fritz, Anderson, & Baker, 2009; Rose, Winslow, Read, & Hansen, 2016).

Mountain lakes are particularly vulnerable to these warming trends (Catalan et al., 2013; Pepin et al. 2015; Schmeller et al., 2018). Understanding the consequences of changing conditions on high-elevation lake ecology is critical for climate adaptation and biological conservation because these systems give rise to the major rivers of the world and support downstream communities (Huss et al., 2017; Klein et al., 2019). Mountain lakes integrate local, regional, and global changes and can serve as model

systems for studying how climate may impact spatiotemporal ecosystem dynamics and processes affecting lake systems everywhere (Adrian et al., 2009; Moser et al., 2019).

Much of our understanding about variation in lake processes has emerged from a legacy of research in the northern and midwestern United States and northern European lake districts, which have distinctly different climate and land use characteristics compared to mountain lakes. While this research has provided insight into the drivers of nutrient concentrations (Soranno et al., 2015; Wagner & Schliep, 2018), water clarity (Lottig et al., 2017), nutrient-productivity relationships (Filstrup et al., 2014; Wagner et al., 2011), and synchrony in responses across these landscapes (Magnuson et al., 2004), a thorough understanding of the patterns and drivers of ecological processes are lacking in mountain lakes. In Arctic lakes, climate change alone has altered primary producer assemblages and their relative contribution to ecosystem production through changes in ice cover and lake thermal structure (Griffiths, Michelutti, Sugar, Douglas, & Smol, 2017; Ruhland, Paterson, & Smol, 2008). Similar processes are likely at work in high elevation lakes but may be confounded by inputs of nutrient deposition, where both warming and enrichment are at work. The length of the ice-free season is increasing which has implications for lake thermal structure, solute concentrations, mixing regimes, and phytoplankton dynamics (Ficker, Luger, & Gassner, 2017; Michelutti et al., 2016; Peter & Sommaruga, 2017; Preston et al., 2016). Increases in mountain lake productivity and changes in algal diversity have also been attributed to nutrient inputs in mountain lakes, particularly in western North America (Brahney et al., 2014, 2015; Goldman, 1988; Wolfe, Baron, & Cornett, 2001; Wolfe, Van

Gorp, & Baron, 2003). These differences highlight the need for increased focus on mountain lakes.

Natural lakes are common in previously glaciated catchments; in the Southern Rocky Mountains there are an estimated 2,600 lakes above 2,700 meters above sea level (m.a.s.l.; Nelson, 1988). Given the recent changes in phytoplankton biomass observed in Southern Rocky Mountain lakes, we constructed predictive models to describe phytoplankton biomass (as chlorophyll *a*) dynamics across multiple spatial and temporal scales in the region. In particular, we asked: (1) What are the most important drivers of phytoplankton biomass across the Southern Rocky Mountains? (2) How do the drivers of phytoplankton biomass differ inter-annually and intra-seasonally?

We used boosted regression tree models (BRTs) to test the relative importance of a suite of variables we hypothesized as potentially important drivers or mediators of phytoplankton biomass. These variables included climate and land cover characteristics, lake morphometry, water chemistry, and perennial snow and ice cover. We then incorporated the most important variables from the BRTs into linear mixed models to account for the hierarchical structure of the data. We hypothesized that the impacts of summer climate on phytoplankton biomass would be mediated by site-specific characteristics such as land cover and lake morphometry. Given the role that snowpack plays in dictating the length of the growing season, we hypothesized that changes in annual snow-water equivalent (SWE) would explain variation in phytoplankton biomass at longer time scales. Within a season, we expected that the role of nutrients, particularly the relative availability of nitrogen (N) to phosphorus (P),

would explain the most variability in phytoplankton biomass, since the Southern Rocky Mountain region is subjected to high atmospheric N deposition.

4.2 Methods

We built three models with data collected from 28 high-elevation Southern Rocky Mountain lakes in Colorado, across a gradient of elevations, catchment types, land cover, and lake sizes. The first model, referred to as the Regional model, used a spatially diverse dataset to compare patterns across lakes with varying characteristics. To complement this broad regional survey, we built two additional models using data from two long-term watershed monitoring programs (Green Lakes Valley and the Loch Vale Watershed; Figure 4.1) to examine temporal drivers of inter-annual and intra-seasonal variability in lake productivity in spatially confined watersheds.

4.2.1 Study sites

4.2.1.1 Regional model

Between 2015 and 2016, we sampled 28 lakes located east of the continental divide on the Colorado Front Range (Figure 4.1). All lakes were sampled at least twice during the ice-free season (May-September) except one lake that was only sampled once (total n=147). Lake visits included individual measurements of water chemistry and chlorophyll *a* (hereafter chl *a*) collected at the deepest point in the lake. We collected samples at the surface (0.5 m below surface water-air interface) and the hypolimnion (below the thermocline or 0.5m above lake bottom in unstratified lakes). Lakes were located just below and above treeline between 2,987 and 3,550 m.a.s.l., and the majority were situated in catchments with less than 25% vegetation cover (Table 4.1).

The underlying geology was similar across the north-south gradient and characterized by weathering-resistant metamorphic granite and biotite gneiss bedrock (Garrity & Soller, 2009). The surface area of sampled lakes ranged from less than 1 to 16.3 ha (median of 4 ha); watershed size ranged from 20 to 1,306 ha (median of 202 ha); and maximum lake depth ranged from 1.8 to 42 m (median of 8 m). This subset of mountain lakes is characteristic of approximately 2,600 natural lakes in the SRM region, the majority of which are less than 7 ha in surface area and less than 10 m deep in watersheds 400 ha or smaller (Eilers et al., 1987). A full list of site variables is outlined in Table 1.

4.2.1.2 Long-term (Green Lakes Valley) model

Green Lakes Valley, located west of Boulder, Colorado, contains seven alpine lakes that have been monitored since the mid-1980s as part of the Niwot Ridge Long-Term Ecological Research Program. Two alpine lakes from GLV were included here: Green Lake 1 (GL1) and Green Lake 4 (GL4). Arikaree glacier and a rock glacier drain into GL4, which is second in a chain of lakes in the GLV. Green Lake 1 is a headwater, snow-fed lake that is hydrologically isolated from the glacially-fed stream (Figure 4.1). Lakes in the GLV dataset were sampled a minimum of five times between ice-off and September between 2008-2016 (excluding 2012, n=104) to assess inter-annual drivers of chl *a*.

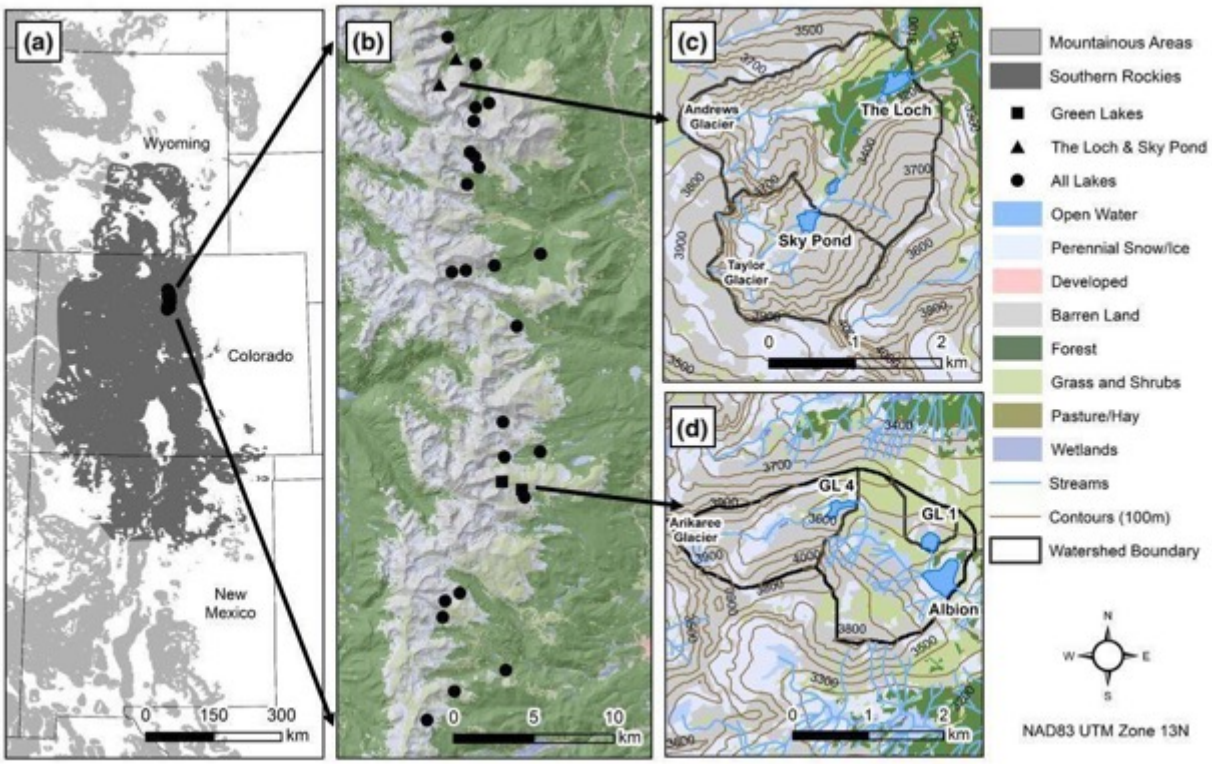

Figure 4.1 Locations of lakes included in this study: (a) the southern Rocky Mountain ecoregion; (b) all lakes sampled east of the Continental Divide in north-central Colorado as included in the Regional model; (c) the Loch Vale Watershed lakes (The Loch and Sky Pond; LVWS); and (d) the Green Lakes Valley lakes (GL1 and GL4; GLV).

4.2.1.3 Intra-seasonal (Loch Vale Watershed) model

The Loch Vale watershed, located in Rocky Mountain National Park, contains one subalpine and three alpine lakes. The two lakes included in this dataset, The Loch and Sky Pond, have been routinely monitored since 1983. Sky Pond is located above treeline and receives water from precipitation and glacial origin. The Loch is located just below treeline, and the two lakes are hydrologically connected via Icy Brook (Figure 4.1). The Loch and Sky Pond were sampled approximately weekly in 2015-2016 and monthly in 2017 (n=81) from the week of ice-off through mid-September to assess intra-seasonal chl *a* dynamics.

4.2.2 Data acquisition

We used three distinct datasets to produce our models. Datasets from all lakes from 2015-2016 were used to develop the Regional model. Due to the high number of samples from The Loch, Sky Pond, and Green Lakes 1 and 4, we randomly selected one sampling date per month for each site to prevent these four lakes from disproportionately influencing the Regional model results. The second dataset contained all data from Green Lakes 1 and 4 from 2008-2016 (Long Term model). The third dataset contained all data from The Loch and Sky Pond from 2015-2017 (Intra-Seasonal model). We classified predictor variables as environmental, climatic, or watershed (Table 4.1). With each field visit, water temperature was recorded and water samples at two depths were collected to analyze lake nutrient contents along with chl *a* concentrations. Climatic variables like precipitation, air temperature, and snowpack were measured at a range of spatio-temporal scales, and watershed variables were composed of time-invariant landscape characteristics. We initially attempted to incorporate spatial estimates of atmospheric N deposition in our models; however, these estimates combined data on N deposition and precipitation at different temporal and spatial scales, leading to high levels of uncertainty. Due to these difficulties, we did not include these estimates in the models.

Table 4.1 Summary information for predictor variables used in the Regional models (2015-2016). Summer statistics include minimum, maximum, mean, median, and standard deviation for each predictor variable. Randomly selected monthly observations from Loch Vale watershed and Green Lakes Valley lakes are included in the model and data summary presented below. Dashes indicate data were unavailable or summary statistics could not be computed on categorical variables. DIN:TP data were only available for Loch Vale lakes. Twenty-two land cover predictors were included in the original models but were dropped in the model selection procedure. Methods for land cover and summary of parameters can be found in Appendix B1.

Variable	Description [units]	Full dataset summary statistics				
		min.	max.	mean	med.	std. dev.
Response						
Chl *a*	Chlorophyll *a* [µg L^{-1}]	0.3	23.3	5.1	3.7	4.6
Indexing Variables						
DOY	Day of year	152	266	205	207	-
Measurement depth	Surface (0) or hypolimnion (1) measurement	0	1	-	-	-
Year	Year	-	-	-	-	-
Climate Variables						
Daily precip.	Precipitation on sample date [mm]	0.0	6.9	0.9	0.0	1.6
Weekly precip.	Cumulative precipitation for the week preceding sample date [mm]	0.0	27.0	7.1	5.8	6.3
Monthly precip.	Cumulative precipitation for the 30 days preceding sample date [mm]	8.9	114.9	37.5	31.7	20.1
Precip. % normal	Monthly precipitation as a percent of normal [%]	23%	122%	56%	42%	33%
Daily mean temp.	Mean air temperature sample date [ºC]	5.6	16.4	11.7	12.2	2.3
Monthly mean temp.	Mean air temperature for the 30 days preceding sample date [ºC]	2.4	14.5	10.9	10.9	2.0
Temp. % normal	Monthly average air temperature as a percent of normal [%]	86%	171%	123%	116%	21%
SWE % normal	Snow water equivalent as a percentage of normal maximum SWE [%]	95%	119%	106%	98%	9%
Max. SWE	Maximum observed SWE for the preceding winter [in]	4.5	21.8	14.9	18.0	7.1
Difference snow free	Difference between normal and actual snow free date [days]	-8	11	1.9	3.0	6.7
Environmental Variables						
DOC	Dissolved organic carbon [mg L^{-1}]	0.3	7.1	1.1	0.8	0.8
FISH	Fish absence (0) or presence (1)	0	1	-		-
NO3	Nitrate-N [mg L^{-1} N]	0.002	0.40	0.09	0.07	0.07
DIN:TDP	Total dissolved N to total dissolved P molar ratio	18.1	1287.4	167.4	121.5	153.5
DIN:TP	Total dissolved N to total P molar ratio	-	-	-		-
TDN	Total dissolved N [mg L^{-1}]	0.04	0.53	0.18	0.18	0.07

TDP	Total dissolved P [µg L^{-1}]	0.3	12.8	3.9	3.5	2.5
Water temp.	Water temperature of sample [ºC]	2.6	19.0	9.4	9.2	3.3
Max. lake depth	Maximum lake depth [m]	1.8	42.0	10.7	7.5	8.6
Watershed Variables (WS)						
Change snow ('92-'11)	Change in perennial snow & ice cover 1992 to 2011 [%]	-3.5%	0.0%	-1.1%	-0.9%	0.9%
Elevation	Elevation at lake outflow [m]	2987	3550	3310	3322	161
WS area	Watershed area [km^2]	0.2	13.1	3.1	2.2	3.1
Lake surface area	Lake surface area [m^2]	3209	163,801	54,691	41,311	39,661
Drainage ratio	Lake area as a percentage of watershed area [%]	0.5%	10.2%	3.1%	2.1%	2.7%

4.2.3 Environmental variables

Water samples for nutrient analysis were collected at the deepest point of each lake. Investigators retrieved surface samples as grab samples and hypolimnion samples were collected through pre-rinsed tubing connected to a hand-powered peristaltic pump. Samples were collected in acid-washed high-density polyethylene (HDPE) plastic bottles and triple-rinsed with sample water prior to filling the container for analysis of dissolved nutrients including nitrate (NO_3-N), total dissolved phosphorus (TDP), and total dissolved nitrogen (TDN). Samples to be analyzed for dissolved organic carbon (DOC) were collected in glass borosilicate bottles and filtered through glass fiber filters previously muffled at 900 °C for 6 hours. All samples were filtered within 24 hours of collection and frozen until analysis. Unfiltered aliquots for total phosphorus (TP) analysis were collected for Loch Vale sites only. Between 500 and 1,000 mL of water were filtered *in situ* for chl *a* content (0.7 µm), held on ice until returned to the laboratory, and then frozen until analysis. Water temperature and conductivity were measured *in situ* with a hand-held probe (Thermo Scientific Orion 3-Star). Maximum depth was measured with a handheld depth finder, and fish presence or absence data were based on investigator site-specific knowledge or through fish stocking records from Colorado Parks and Wildlife. We included sampling depth as a predictor in the models to account for differences in drivers between surface and hypolimnion samples.

With the exception of those collected at Loch Vale, all samples were analyzed at the Arikaree Environmental Laboratory (Boulder, CO) or at the University of Colorado, Boulder in accordance to standard procedures used in the Arikaree Environmental

Laboratory (https://instaar.colorado.edu/research/labs-groups/arikaree-environmental-lab/). Fluorescence spectroscopy was used to determine chl *a* concentrations (ISA Jobin Yvon-SPEX Fluormax-2 Spectrofluorometer); reactive nitrogen (NO_3^- and NH_4^+) and TDP concentrations were analyzed with spectrophotometric detection on a Lachat QuickChem 8500 System Flow Injection Analyzer (FIA) and Alpkem autoanalyzer, respectively (EPA Method 365.1). Loch Vale samples were analyzed according to standard procedures for the Loch Vale program at the EcoCore laboratory (Fort Collins, CO) (https://www2.nrel.colostate.edu/projects/lvws/data.html). Concentrations of chl *a* were analyzed using a benchtop fluorometer (Turner Designs Trilogy) using standardized extraction techniques (EPA method 445.0). Loch Vale reactive nitrogen (NO_3^- and NH_4^+) were analyzed on an Alpkem Flow Solution IV Automated wet chemistry system (O.I. Analytical, College Station, TX). Loch Vale samples are the only sites which have total phosphorus (TP) analyzed; sampled were sent to High Sierra Water Laboratory, Tahoe City, CA for analysis using persulfate digestion at (EPA method 365.1; O'Dell, 1993).

4.2.4 Climate variables

We used the *prism* package (Hart & Bell, 2015) in R version 3.5.0 (R Core Team, 2018) to obtain estimates of temperature and precipitation for each study site from the parameter-elevation regressions on independent slopes model (PRISM Climate Group 2018). For each sample date, we extracted the daily mean temperature and total precipitation from 4 km gridded PRISM data. We also calculated the mean daily temperature and total precipitation for the 7 days and the 30 days preceding the sampling date. To complement these data, we compared monthly temperature and

precipitation to climate normal data (1981-2010) for the calendar month closest to the sampling date. If the sampling date was the 1-14th day of the month, we used the preceding calendar month, and if it was the 15th-last day of the month, we used the same calendar month.

For each lake, we obtained snowfall data for the winter preceding sampling from the nearest snow telemetry (SNOTEL, U.S. Dept. of Agriculture) site which had data since at least 1980. We extracted several variables for each site-year: the maximum observed snow water equivalent comparisons of this maximum SWE to average historical SWE (1980-2010 data), and the difference between the observed spring snow free date and historical average snow free date. These variables provided an indication of the amount of snowfall from the preceding winter, and how the snowfall and length of snow cover compared to previous years.

4.2.5 Watershed variables

Watersheds for each lake were delineated from lake outlets with the USGS StreamStats online tool (USGS, 2017). We calculated and extracted several watershed predictors (WS) that we hypothesized might play a role in explaining lake-to-lake variation in chl *a*, including land cover vegetation type, wetland extent, rock glacier and perennial ice cover, and underlying geology. However, since most of these predictors were not included in the final models after model selection (see Statistical Analyses below), we have elaborated on the methods and summarized the predictors in the Supplementary Information (Appendix B1).

4.2.6 Statistical analyses

We completed a two-stage analysis to explore drivers of chl *a* patterns in the three datasets (Regional, Long-term, Intra-Seasonal). We first developed boosted regression tree models (BRTs) to identify the most important predictor variables and visualize their relationships with chl *a*. We then developed linear mixed effects models (LMMs) to account for the hierarchical structure in the datasets, incorporating important BRT predictors as fixed effects and variables such as lake identity and sampling event as random effects.

4.2.6.1 Boosted regression trees (BRTs)

We developed exploratory models for our three datasets using BRTs, a non-parametric machine learning technique commonly used to analyze complex datasets (Breiman, Friedman, Olshen, & Stone, 1984; Elith, Leathwick, & Hastie, 2008). Boosted regression trees improve upon the classic regression tree framework and have been used in a variety of aquatic ecology contexts including predicting cyanobacteria bloom occurrence (Bertani et al., 2017), macroinvertebrate biotic integrity (Waite & Van Metre, 2017), marine fish and coral diversity and abundance (Pittman, Costa, & Battista, 2009), and littoral fish abundance (Lewin, Mehner, Ritterbusch, & Brämick, 2014). A key feature of BRT is recursive partitioning, which splits the response variable into groups that are as homogenous as possible based on predictor variable values (Strobl et al. 2009). BRTs combine recursive partitioning with boosting, a method for combining hundreds to thousands of trees to improve model performance and predictive capacity (De'ath, 2007; Elith et al., 2008; Prasad, Iverson, & Liaw, 2006). Regression trees provide flexibility by allowing for nonlinear relationships between predictor and response

variables, and they are robust to missing predictor data and collinearity (De'ath & Fabricius, 2000). They can detect interactions among predictors and are often well-suited for hierarchically-structured predictor variables (De'ath & Fabricius, 2000). Regression trees address many of the problems encountered when analyzing ecological phenomena using traditional statistical techniques and can be a useful hypothesis generating approach for future analyses.

We implemented all BRT models in the *gbm* package (Ridgeway, 2006) of R version 3.5.0 (R Core Team, 2018). For all models, we used natural log-transformed chl *a* concentrations as the response variable. We removed the most highly correlated predictor variables based on Pearson's coefficients ($r \geq |0.8|$). We used the methods described by Bertani et al. (2017) to optimize the learning rate (contribution of each tree added to the model) and bag fraction (proportion of data randomly drawn at each step). We set the tree complexity (number of splits per tree) to 2, and controlled for over-fitting by ensuring the model used a small learning rate, which requires significant computation time but results in a final model with a larger number of trees (Friedman, 2001; Hastie et al., 2001; Elith et al., 2008). Optimization was based on minimizing the out-of-sample predictive error estimated through 10-fold cross validation. Once we selected the optimal values for learning rate and bag fraction, we used 10-fold cross validation (C.V.) again to determine the optimal number of trees for each model. We evaluated model performance using the C.V. R^2, which is a more conservative evaluation measure than the overall R^2. We assessed individual predictor importance using variable importance (V.I.) scores, which indicate the percentage of trees splits that can be attributed to a single predictor variable. We assessed the importance of

interactions between predictor variables using relative interaction strengths, which are calculated in the *gbm* package from the residual variances of linear models that use pairs of all the predictor variables to make predictions.

We first developed a Regional BRT model for the dataset that combined environmental, climate, and watershed predictors for all sample lakes (2015-2016 data), and this resulted in a low C.V. R^2 (0.29). We then developed three separate models for: (1) environmental, (2) climate, and (3) watershed predictors (Waite & Van Metre, 2017). For each of these models, we used a backward-selection procedure to iteratively remove variables of low importance starting with V.I. ≤ 1% and ending with V.I. ≤ 5% (Elith et al., 2008). We selected the models with the highest C.V. R^2 values as the top environmental, climate, and watershed models. Because the C.V. R^2 from the Regional environmental model was poor, we also created a second combined Regional model that included only climate and watershed variables.

We also developed separate BRTs for the Green Lakes Valley (Long-term model) and Loch Vale Watershed (Intra-seasonal model) datasets using only climate and environmental variables. We did not include watershed variables because only two, closely located lakes were included in each model. We completed a backward selection procedure on the climate and environmental variables in each model as described above to determine the combination of variables producing the highest C.V. R^2. We focused our model interpretations on variables with > 5% V.I. scores (De'ath & Fabricius, 2000; Elith et al., 2008) because they had the strongest influence on overall model fit.

4.2.6.2 Linear mixed-effects models (LMMs)

Building on the exploratory BRT analysis, we developed LMMs for each of the three datasets in the R package *lme4* (Bates et al. 2015). The fixed effects for each LMM included predictors with the five highest V.I. scores, as determined by the best BRTs. If any predictor interaction strengths were comparable in magnitude to the top predictor V.I. scores, these interactions were also included as fixed effects in the models. In the Regional model, we included "lake identity" and "sampling event" as random effects to account for correlations among observations that were collected in the same lake or on the same date. In the Long-term and Intra-seasonal models, we included "sampling date" as a random effect but did not include "lake identity" because each dataset contained only two lakes. We used the R package *MuMIN* (Barton, 2019) to calculate conditional R^2 values (R^2_c) for each model, which represent only the variability explained by fixed effects, and marginal R^2 values (R^2_m), which represent the variability explained by fixed and random effects in the model. We used the R Package *lmerTest* (Kuznetsova et al. 2017) to calculate p-values for each of the fixed effects.

4.3 Results

4.3.1 Regional models

Lake chl *a* concentrations were variable across sites in 2015-2016 and ranged from highly unproductive (0.3 µg L^{-1}) to mesotrophic (23.3 µg L^{-1}), with a median of 3.7 µg L^{-1} (Table 1, Figure 2, Appendix B3, Appendix B7). Nitrate (NO_3) concentrations ranged between 0.002 mg L^{-1} N to 0.4 mg L^{-1} N with a median of 0.07 mg L^{-1} N. Total dissolved phosphorus (TDP) ranged from below detection limit (< 2 µg L^{-1} P) to 12.8 µg

L^{-1} P with a median of 3.5 µg L^{-1} P. Overall, this period was much drier and warmer than the 30-year average; monthly precipitation ranged from 23% to 122% of the 30-year average with a median of 42% and monthly air temperature ranged between 86% and 171% of the 30-year average with a median of 116% (Appendix B11). Snowpack telemetry estimates for maximum SWE of the preceding winter indicate that 2015 and 2016 had average maximum snowpack in the context of the 30-year record and ranged from 95% to 114% of normal SWE (Appendix B10, Table 4.1).

The Regional BRT model performed poorly (C.V. R^2 = 0.29) when first fit with the full suite of watershed, climate, and environmental predictors across all sampled lakes. We subsequently examined environmental, climate, or watershed variables separately to determine which predictor variables best explained variation in chl *a* (Table 4.2). The model including only watershed variables had marginally better predictive capabilities (C.V. R^2 = 0.31) than the model with the full suite of variables; while the model including only environmental variables performed worst (C.V. R^2 = 0.15). Overall, the climate-only model was the best regional model with a training R^2 of 0.83 and C.V. R^2 of 0.38 (Figure 4.2; Figure 4.5). From the Regional climate model, influential predictor variables (V.I. > 5%) included weekly precipitation (V.I. = 25.1%), monthly mean air temperature (V.I. = 14.1%), daily mean air temperature (V.I. =13.9%), ordinal date of sample collection (V.I. = 10.6%), monthly air temperature as a percent of 30-year normals (V.I. =10.5%), monthly precipitation as a percent of 30-year normals (V.I. = 8.6%), daily precipitation (V.I. = 8.1%), and maximum SWE of the previous winter (V.I. = 5.1%). When we combined the top performing variables from the environmental and watershed models into the climate model, we did not find any marked improvement to our predictions.

Results of these models are presented in the Supplementary Information (Appendix B7) and focus the rest of our discussion on the Regional climate model as the best performing.

One interaction was identified between monthly mean air temperature and measurement depth (interaction strength = 9.15), whereby warmer air temperatures tended to stimulate chl *a* in the hypolimnion (sampling depth = 1) compared to surface (sampling depth = 0) (Appendix B8). Although 2015 and 2016 were average snow years, summer air temperatures were well above normal at all sites (Appendix B10, B11), with high phytoplankton abundances during all but the hottest days and months. High chl *a* was generally associated with the driest weeks and meteorological drought, where monthly precipitation was observed as <50% of normal summer precipitation on the majority of sampling occasions. However, there were a few exceptions to this finding where increased chl *a* was seen at higher precipitation values in a subset of observations (15%, n = 26) during a single week that was particularly wetter than normal.

We then combined the variables with highest V.I. (> 5% V.I.) from the Climate + Watershed (WS) regional models and found that the combined Regional Climate + WS model performed slightly worse than the Regional Climate-only model (C.V. R^2= 0.37; Table 4.2, Appendix B7). The combined Regional Climate + WS model identified eight key explanatory variables (V.I. > 5%); there was overlap with top predictors in the climate-only model, but lake area as a percentage of watershed area (drainage ratio; V.I. = 10.3%), maximum lake depth (V.I. = 7.9%), change in perennial snow and ice cover between 1992 and 2011 (V.I. = 6.3%), and 2011 perennial snow and ice cover

(V.I. = 5.0%) also emerged as important predictors. Once again, when we added environmental predictors ≥ 5% V.I., such as nutrient chemistry and water temperature, into the climate + WS model, the C.V. R^2 consistently decreased but the training R^2 increased (Appendix B5).

The regional LMM included the top five variables from the Regional Climate model as fixed effects, along with sampling event and lake identity as random effects. It had a very low R^2_c of 0.024 and moderate R^2_m of 0.451 (Table 4.3). None of the fixed effects were significant predictors in the model (all $p > 0.05$). Sampling event explained more variation in chl *a* than did lake identity as a random effect.

Table 4.2. Top predictors from the Regional Climate and Regional Climate + WS models, produced from a backward-selection process, whereby variables of low importance were removed until cross-validation (C.V.) R^2 values were maximized. See Table 1 for a complete list of variables initially included in each model and Appendix B1 for WS predictor variable description. Variable importance (V.I.) indicates the percentage of trees in which the specified predictor variable created the best response variable split.

Climate + WS variables C.V. R^2 = 0.37	**V.I.** (%)	**Climate variables** C.V. R^2 = 0.38	**V.I.** (%)	**WS variables** C.V. R^2 = 0.31	**V.I.** (%)	**Envt variables** C.V. R^2 = 0.15	**V.I.** (%)
Weekly precip.	13.4	Weekly precip.	25.1	DOY	22.8	DIN:TDP	22.7
Drainage ratio	10.3	Monthly mean temp.	14.1	Max. lake depth	12.6	TDP	19.2
Daily mean temp.	10.2	Daily mean temp.	13.8	Drainage ratio	8.5	NO3	17.2
Monthly mean temp.	9.9	DOY	10.5	Elevation	7.9	Lake temp.	15.7
Max. lake depth	7.9	Temp. % normal	10.5	Change in snow cover (’92-’11)	6.5	TDN	8.0
Precip. % normal	7.0	Precip. % normal	8.6	Shrub cover (2011)	5.7	DOC	6.9
DOY	7.0	Daily precip.	8.1	Lake SA	5.3	DOY	6.7
Change in snow cover (’92-’11)	6.3	Max. SWE	5.1	Snow cover (2011)	5.0	Measurement depth	3.7
Temp. % normal	5.5	Measurement depth	4.2	Summer radiation	4.8		
Snow cover (2011)	5.0			Biotite-gneiss (%)	4.6		
Elevation	4.9			East mean	3.8		
Daily precip.	4.4			Measurement depth	3.5		
East mean	4.1			Rock glacier area	3.3		
Measurement depth	3.8			Change in water cover (’92-’11)	3.0		
				Longitude	2.7		

Table 4.3. Results of linear mixed effects models for each of the three datasets, which included the most important boosted regression tree variables as fixed effects. The Regional Climate model included sampling event and lake identity as random effects, and the Long-term and Intra-seasonal models included sampling date as a random effect. R^2_m refers to the marginal R^2 value incorporating variance explained by fixed effects only. R^2_c refers to the conditional R^2 value incorporating variance explained by fixed and random effects. P-values <0.05 are denoted as "*".

Model	Predictor	Est.	SE	df	t-val	p-val	R^2_m	R^2_c
Regional Climate							0.02	0.451
	Intercept	-0.076	1.344	44.52	-0.05	0.955		
	Weekly precip.	0.001	0.014	36.83	0.08	0.935		
	Monthly mean temp.	0.022	0.063	37.21	0.35	0.725		
	Mean temp. % normal	-0.052	0.498	46.45	-0.10	0.917		
	DOY	0.005	0.005	46.42	1.01	0.317		
Long-Term							0.76	0.903
	Intercept	1.398	0.213	46.20	6.55	<0.001*		
	NO3	-7.595	4.967	50.32	-1.52	0.133		
	Max. SWE	-0.430	0.050	42.54	-8.67	<0.001*		
	Water temp.	-0.115	0.099	73.83	-1.15	0.252		
	DIN:TDP	0.000	0.000	70.25	0.35	0.725		
	Daily precip.	0.015	0.038	39.08	0.38	0.703		
	Year	-0.087	0.104	51.34	-0.84	0.405		
	NO3* Year	6.141	2.057	49.50	2.98	0.004*		
	NO3 * Max. SWE	6.580	0.908	52.40	7.24	<0.001*		
Intra-Seasonal							0.51	0.718
	Intercept	-0.186	1.225	56.50	-0.15	0.880		
	DOY	0.011	0.003	43.60	3.24	0.002*		
	Monthly precip.	0.000	0.003	31.09	-0.00	0.993		
	Weekly mean temp.	0.068	0.045	43.62	1.49	0.142		
	Water temp.	-0.104	0.031	66.38	-3.38	0.001*		
	DIN:TP	-0.013	0.005	68.47	-2.50	0.015*		

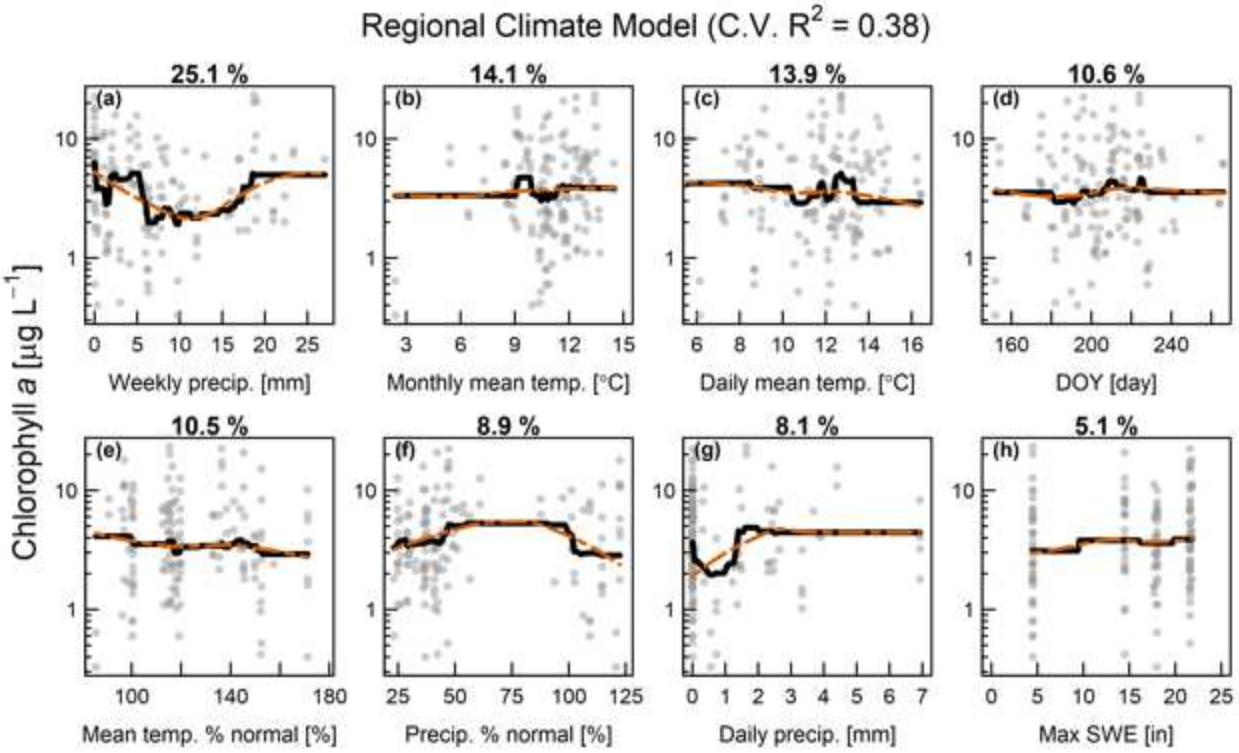

Figure 4.2. Partial dependency plots of the predictor variables (V.I. > 5%) in the best Regional BRT model including only climate predictors (variable importance ≥ 5%) with the relative contribution of each variable printed at the top of each panel. The y-axis fitted function (black line) represents the effect of the selected variable on chl *a* when all other predictor variables are held at their mean values. The red dashed line is a loess curve fit to this relationship. Grey dots represent individual observations. Refer to Table 1 for predictor variable explanations.

4.3.2 Long-term model

The Green Lakes Valley dataset (2008-2016) spanned a much larger range in chl *a* concentrations than the regional dataset, from 0.01 µg L^{-1} to 19.9 µg L^{-1} with a median value of 2.1 µg L^{-1} (Appendix B2, B6). These data also spanned a much larger range of maximum SWE values compared to the Regional and Loch Vale datasets, which had similar maximum SWE in all years, close to the 30-year SNOTEL normals (Appendix B10, B11). Chlorophyll *a* was not statistically different between GL1 and GL4 across all years (Wilcoxon rank sum test p = 0.73). Nitrate concentrations were significantly higher

in glacier-fed GL4 than snow-fed GL1 (t = -3.8906, df = 70.734, p-value < 0.01) but were within the range observed in the regional dataset. Monthly precipitation ranged from 30% to 148% of the 30-year average with a median of 113% (Appendix B11). All of the extremely dry summer conditions (< 50% of normal) occurred in 2015 and 2016. Monthly air temperature ranged between 92% and 152% of the 30-year average with a median of 106% of normal (Appendix B10).

We used the Long-term dataset to explore drivers of inter-annual variability in lake chl *a* from 2008-2016. We found that over the 9-year period, water column NO_3 (V.I. = 25.6%) and maximum observed SWE of the preceding winter (V.I. = 19.5%) had the biggest influence on chl *a* (Table 4.4, Figure 4.3). Year sampled (V.I. = 16.8%), water temperature (V.I.= 8.0%), and DIN:TDP (V.I. = 7.9%) also had relatively high influence on chl *a* values. The GLV model had a training R^2 of 0.96 and C.V. R^2 of 0.75 (Figure 5).

The Long-term model uncovered two strong interaction terms (Appendix B9). We found that the strongest interaction occurred between NO_3 and year, with moderate to high NO_3 levels leading to the highest chl *a* values in more recent years (2015-2016). There is also a strong interaction between maximum SWE and NO_3, leading to the highest predicted chl *a* concentrations at lower maximum SWE values and intermediate NO_3 values (between approximately 0.10-0.15 mg L^{-1} N).

The Long-term LMM including the top five variables from the Long-term BRT model as fixed effects, along with sampling date as a random effect, had a strong R^2_c of 0.76 and R^2_m of 0.90 (Table 4.3). Maximum SWE had a significant negative relationship

with chl *a* ($p<0.001$). Additionally, NO_3 and year had a significant positive interaction on chl *a* ($p=0.004$), and NO_3 and Max. SWE had a significant positive interaction on chl *a* ($p<0.001$).

Table 4.4. Final Long-term (Green Lakes Valley dataset) and Intra-Seasonal (Loch Vale Watershed dataset) models produced from a backward-selection process, whereby variables of low importance were removed until cross-validation (C.V.) R^2 values were maximized. Variable importance (V.I.) indicates the percentage of trees in which the specified predictor variable created the best response variable split.

Long-term model (GLV) variables C.V. $R^2 = 0.75$	**V.I.** (%)	**Intra-Seasonal model (LVWS) variables** C.V. $R^2 = 0.64$	**V.I.** (%)
NO3	26.5	DIN:TP	25.4
Max. SWE	19.5	Water temp.	18.6
Year	16.8	DOY	14.8
Water temp.	8.0	Monthly precip.	9.4
DIN:TDP	7.9	Mean weekly temp.	6.9
Daily precip.	3.5	Precip. % normal	6.2
TDP	3.3	DIN:TDP	5.6
DOC	2.7	Weekly precip.	5.2
DOY	2.3	NO3	4.6
Mean monthly temp.	2.0	Temp. % normal	3.0

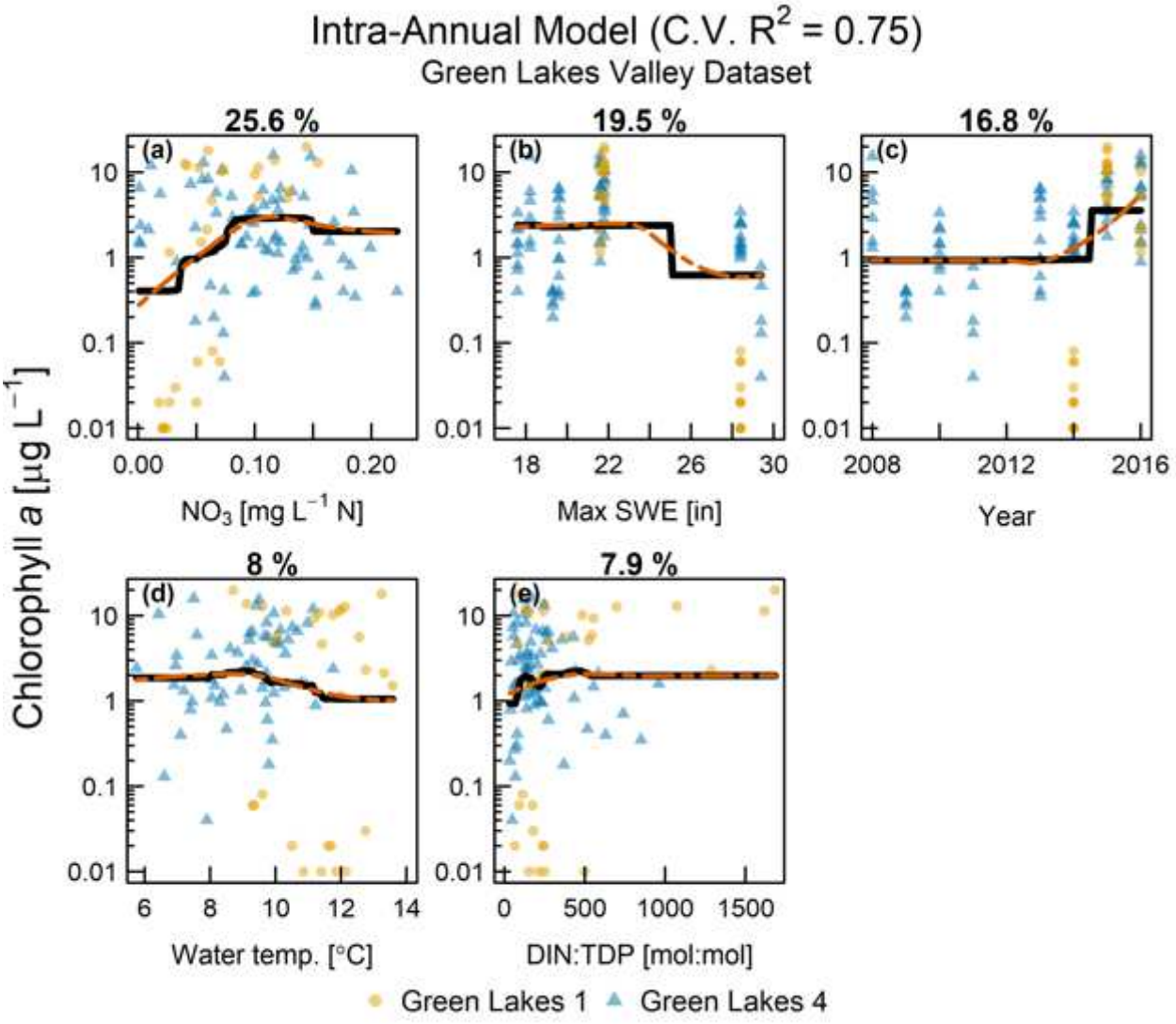

Figure 4.3. Partial dependency plots for the best Long-term (Green Lakes Valley) model for all variables (V.I. ≥ 5%) with the relative contribution of each variable printed at the top of each panel. The y-axis fitted function (black line) represents the effect of the selected variable on chl *a* with all other predictors held at their means. The red dashed line is a loess curve fit to this relationship. Yellow dots and blue triangles represent individual observations for GL1 and GL4 (respectively). Refer to Table 1 for predictor variable explanations.

4.3.3 Intra-Seasonal model

Within the years sampled (2015-2017), chl *a* in the Intra-seasonal dataset ranged between 0.3 and 11.3 µg L^{-1} (Appendix B2, B6). The overall mean chl *a* concentration of

Sky Pond was greater than that of The Loch (Wilcoxon rank sum test $p < 0.0001$) and was on average twice as high in Sky Pond (5.4 μg L^{-1}) as in The Loch (2.3 μg L^{-1}). Total dissolved phosphorus was similar to observations from the regional dataset and ranged from 0.64 to 14.4 μg L^{-1} P. Nitrate concentrations also fell within the range of observed values across the region (0.08 to 0.35 mg L^{-1} N). Total phosphorus ranged from 6 to 21 μg L^{-1} with a median of 10 μg L^{-1}. Summer monthly precipitation ranged from 24% to 184% of the 30-year average, but the median of 38% indicates these summers were drier than normal (Appendix B2, Appendix B10). Summer monthly air temperature ranged between 86% and 150% of the 30-year average with a median of 115% (Appendix B2, Appendix B11). In contrast to summer precipitation, SNOTEL estimates for maximum SWE of the preceding winter-spring indicate that all three years in the dataset were near or above the 30-year averages and ranged from 95% to 125% of normal SWE (Appendix B11).

The highest chl *a* concentrations were observed late in the open-water season several weeks after ice-off. Many of the highest chl *a* observations were in dry summer months with < 50 mm of rain in the month preceding sample collection and when monthly precipitation fell below the 30-year PRISM normals. Results from the Intra-seasonal model indicate several drivers of variation in chl *a* with better predictive capabilities than the regional models (C.V. $R^2 = 0.64$, training $R^2 = 0.93$; Table 4.4, Figure 4.4, Figure 4.6). Dissolved inorganic N to total P molar ratios (V.I. = 25.4%) and water temperature (V.I. = 18.6%) were the most important variables, followed by DOY (V.I. = 14.8%), monthly precipitation (V.I. = 9.4%), weekly mean temperature (V.I. = 6.9%), monthly precipitation as a percentage of 30-year normal values (V.I. = 6.3%),

dissolved inorganic N to dissolved P molar ratios (V.I. = 5.6%), and weekly precipitation (V.I. = 5.3%).

The Intra-seasonal LMM including the top five variables from the Intra-seasonal BRT model as fixed effects, along with sampling date as a random effect, had a moderate R^2_c of 0.52 and strong R^2_m of 0.72. The molar ratio of DIN to TP and water temp. had significant negative relationships with chl *a* (p=0.001 and p=0.015, Table 4.3). Additionally, DOY had a significant positive relationship with chl *a* (p=0.004, Table 4.3).

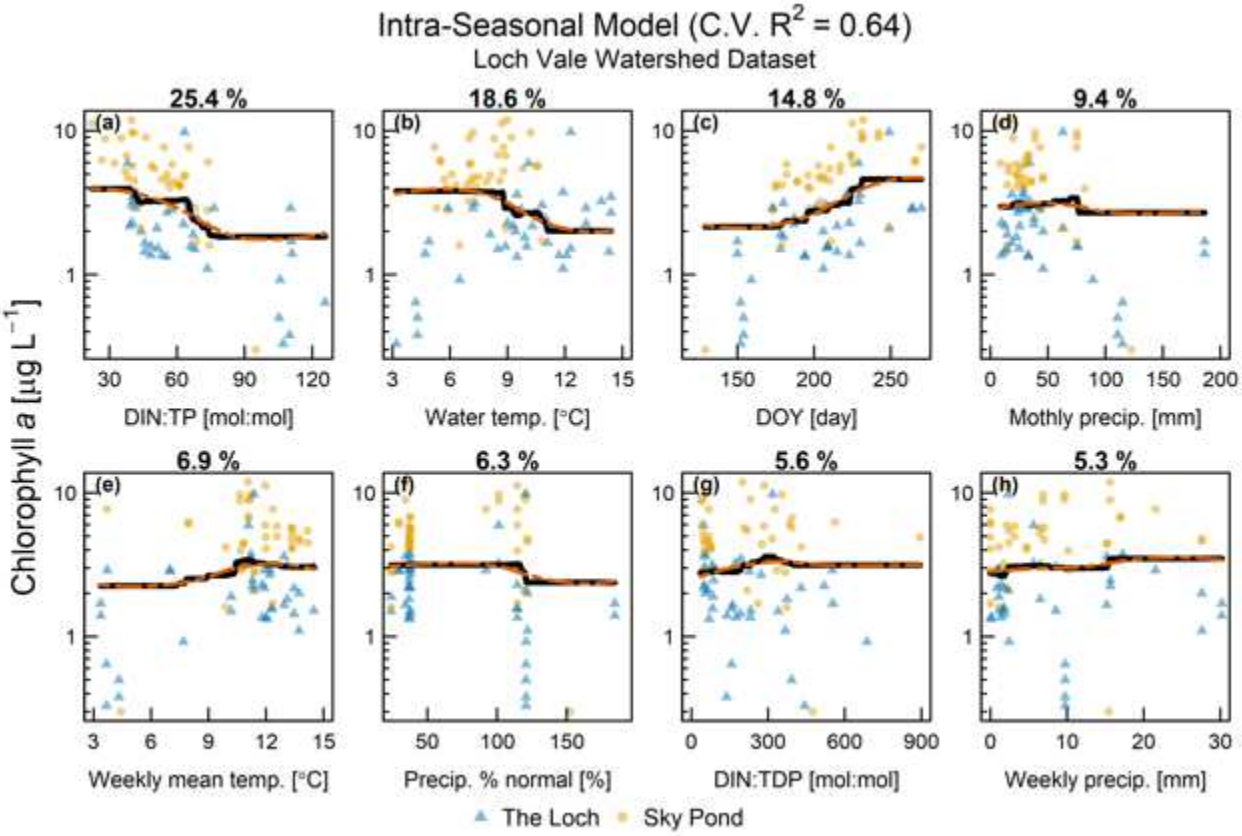

Figure 4.4. Partial dependency plots for the best Intra-seasonal (Loch Vale watershed) model for all variables (V.I. ≥ 5%). The relative contribution of each variable is printed at the top of the panel. The y-axis fitted function (black line) represents the effect of the

selected variable on chl *a*, holding all other predictors at their means. The red dashed line is a loess curve fit to this relationship. Blue triangles and yellow dots represent individual observations for The Loch and Sky Pond (respectively).

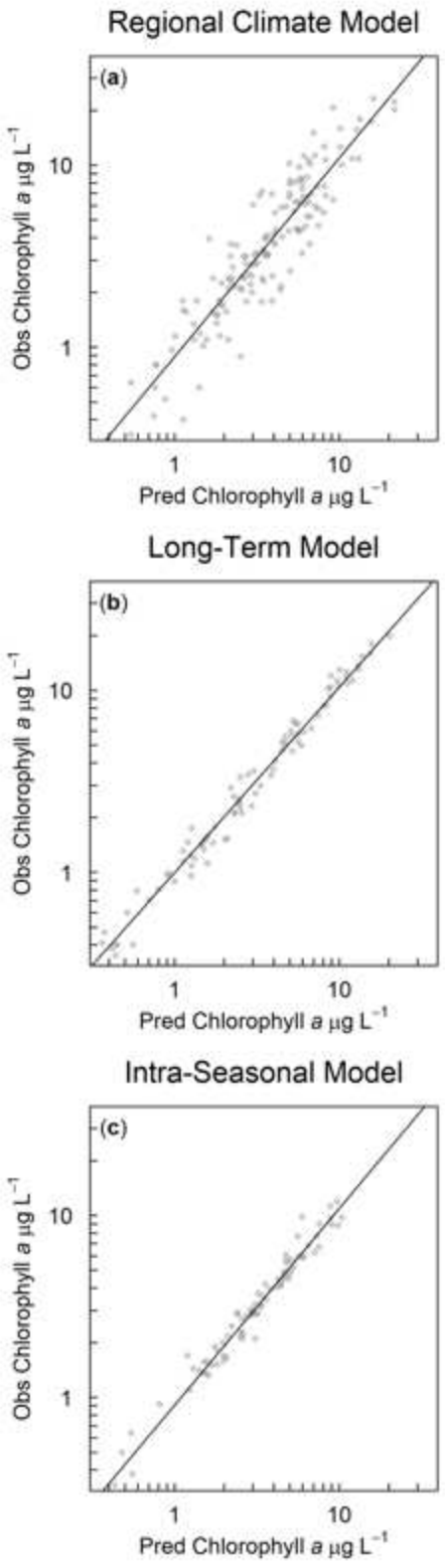

Figure 4.5. Chlorophyll *a* observed versus predicted values for the best Regional (Climate) (a), Long-term (b), and Intra-seasonal (c) models, with fitted regression lines described by the training R^2 values. Regional Climate model training R^2 = 0.83 and C.V. R^2= 0.38, Long-term model training R^2 = 0.96 and C.V. R^2 = 0.75, Intra-seasonal model training R^2 = 0.93 and C.V. R^2= 0.64.

4.4 Discussion

In this paper, we aimed to identify the most important drivers of phytoplankton (chl *a*) in the Southern Rocky Mountains, and to better understand their variation across space and time. We first used boosted regression trees (BRTs) to explore a dataset of 28 high alpine lakes in Colorado, focusing on two watersheds to investigate long-term (Green Lakes Valley) and intra-seasonal (Loch Vale Watershed) patterns in drivers of phytoplankton biomass. We then used linear mixed effects models (LMMs) to account for the hierarchical structure of our data, investigating the relationship between chl *a* and the top performing BRT predictor variables.

We found that Southern Rocky Mountain lakes are sensitive to regional variability in both winter and summer climate, but the processes governing lake-to-lake variability are site- and time-specific. Summer air temperature and precipitation emerged as the most important drivers of chl *a*, but these relationships were often non-linear and highly heterogeneous at the regional scale. Our results are consistent with other studies that illustrate how local and regional drivers can interact to influence lake ecology and water quality (Rose et. al., 2017, Vogt et al., 2017). Like lower elevation North American lakes, Southern Rocky Mountain lakes are sensitive to climatic variation, but regional (lake-to-lake) heterogeneity leads to large variation in responses, making it difficult to infer causal mechanisms (McCullough et al., 2019).

By investigating phytoplankton dynamics in two watershed-scale case studies, we were better able to consider how variation in climate alters nutrient availability, hydrology, and other limnological processes that influence chl *a* at inter-annual and

intra-seasonal timescales. At longer timescales, water column nitrate and snowpack maxima exert dominant control on lake phytoplankton in these mountainous systems. Within a single season, water temperature and the relative ratio of DIN:TP explained most of the variability in phytoplankton dynamics. Overall, our results highlight the difficulty of trying to infer broad-scale spatial patterns in conjunction with temporal dynamics (Lottig et al., 2017), but also illustrate the importance of incorporating both winter and summer climatic conditions into our understanding of mountain lake ecological dynamics (Collins et al., 2019).

4.4.1 The role of snowpack

In the Long-term model, we found that SWE and NO_3^- explained patterns in phytoplankton biomass (Figure 4.3B). In other systems characterized by large seasonal snowpack, such as the Sierra Nevada mountains of California, spring SWE explains interannual variability in both phytoplankton biomass and lake temperature (Sadro, Melack, Sickman, & Skeen, 2018; Sadro, Sickman, Melack, & Skeen, 2018). Snowpack regulates nutrients and water temperatures through a few different mechanisms, many of which were described in a previous study of the Green Lakes Valley (Preston et al., 2016). These authors found higher spring snowfall was associated with shorter ice-free periods and higher flushing rates, which consequently led to lower phytoplankton biomass. In both the Long-term and Intra-seasonal models, nutrients and water temperature were influential in explaining variation in chl *a*. Within a season, chl *a* increased with decreasing DIN:TP later in the season later in the summer during baseflow conditions, when the dilution effect of snowmelt subsided (Figure 4A,C). Our results provide additional support for the links between snowpack, nutrient

concentrations, and water temperature, as we observed lower chl *a* with higher maximum SWE across our eight-year study period (2008 – 2016; Figure 4.3B). However, some of the highest chl *a* concentrations we observed occurred in years with average snowpack but anomalously warm and dry summers with earlier snow-free dates (Appendix B10, B11). This indicates that the role of summer meteorological conditions on lake temperature, chemistry, and phytoplankton dynamics may become more relevant as the climate continues to change and may override the influence of snowmelt conditions on phytoplankton dynamics.

The interplay between timing of snowmelt and water chemistry is partially dependent on glaciers and rock glaciers, which are present in both the Long-term and Intra-seasonal datasets, but not in all watersheds in our regional dataset (Appendix B1). Glacial inputs alter the biogeochemistry and phytoplankton ecology of headwater lakes (Saros et al., 2010; Slemmons et al., 2013) and variation in SWE can increases the importance of glacial meltwater on lake chemistry (Preston et al., 2016). Glaciers and rock glaciers in Green Lakes Valley and Loch Vale Watershed are important sources of nitrate and other mineral weather products to headwater aquatic ecosystems (Baron, Schmidt, & Hartman, 2009; Fegel, Baron, Fountain, Johnson, & Hall, 2016; Williams, Knauf, Cory, Caine, & Liu, 2007). Glacially-fed GL4 has significantly higher nitrate concentrations than GL1, a snowmelt-only fed lake (t-test $p < 0.0001$) and this contrast resulted in lake nitrate concentrations significantly decreasing with increasing snowpack (i.e. dilution) in non-glacial GL1 (Pearson's $r = -0.59$, $p = 0.0005$) but not in glacial GL4 (Pearson's $r = -0.1$, $p = 0.4$). This suggests that glacier meltwater is a relevant watershed filter that moderates the effect of snowpack changes on lake water chemistry

and subsequent productivity. Particularly during dry and warmer than average summers like 2015 and 2016, small cryospheric features like glaciers may be an important nutrient subsidy fueling phytoplankton growth in headwater lakes, in addition to providing a steady supply of cold water. However, even in mountain watersheds without glaciers, low snow years also result in increased water column nitrate when because the dilution effect of snowmelt is less influential (Park et al., 2004; Parker, Vinebrooke, & Schindler, 2008; Sadro et al., 2018b).

4.4.2 The role of summer climate

Several mechanisms could explain why 2015 and 2016 resulted in anomalously high chl *a* observations in the Long-term dataset. These summers were warmer and drier than average, which may have increased the amount of lake evaporation (and watershed evapotranspiration) relative to inflow, which concentrates nutrients in the water column (Lewis et al., 2015; Markensten, 2006; Webster et al., 1996) and reduces water residence times (Schindler et al., 1996). Summer precipitation represents a relatively minor fraction of total annual precipitation in these mountain systems, with summer precipitation typically arriving in the form of intense convective thunderstorms (Baron & Denning, 1993). These storms could influence phytoplankton biomass by flushing phytoplankton downstream, dampening primary production through reductions in solar radiation, or disrupting stratification through wind-driven mixing (Perga, Bouffard, Bruel, Rodriguez, & Guénand, 2018; Sadro & Melack, 2012).

However, we found more complicated relationships between summer climate and chl *a* in the Regional model, and the lake to lake variation was considerable. Both the

driest and wettest weeks led to the highest chl *a* concentrations. These same convective thunderstorms may encourage horizontal and vertical mixing, potentially supporting phytoplankton growth by recirculating nutrients (Kasprzak et al., 2017; Rusak et al., 2018). Alternatively, high precipitation weeks may lead to increased allochthonous inputs which could decrease water transparency. This would reduce photosynthetic activity lower in the water columns while also providing UV-B protection to phytoplankton, thereby stimulating growth near the surface in these high-elevation lakes (>3000 m.a.s.l; Parker et al., 2008; Sommaruga & Psenner 1997).

Others have shown that summer precipitation and air temperature typically result in similar responses among lakes in a region (Soranno et al., 1999; Webster, Soranno, Baines, & Kratz, 2000). Similarly, in the Regional Climate model, we found daily and monthly air temperature were also important predictors of phytoplankton biomass. Air temperature influences lake temperature and nutrient dynamics either directly via sensible heat flux or indirectly by modifying stratification dynamics (Michelluti et al., 2016). In some shallow, unstratified lakes in our study, these warm air temperatures alone may have increased water temperatures and in turn stimulated primary production by increasing metabolic rates (Kraemer et al., 2016). However, in the deeper lakes, extended periods of warm air temperatures can create a large temperature difference between surface and bottom layers and lead to increased intensity and duration of stratification. Stratification can promote the formation of a deep chlorophyll maxima near the hypolimnion, where nutrient concentrations may be higher (Saros et al., 2005). However, it is relevant to note that after accounting for the random effects of sampling event and lake identity, none of the BRT predictors were significant in the Regional

LMMs (Table 4.3). This underscores the utility of BRTs as exploratory tools for small, noisy datasets where other statistical methods may be insufficient, particularly because BRTs can capture nonlinear relationships between predictors and the response variable, as well as test multi-order interactions among predictor variables.

4.4.3 The importance of watershed context

While our models do not demonstrate mechanistically how phytoplankton respond to deviations in climate at the regional scale, summer precipitation and air temperature are known to influence lakes indirectly by interacting with local watershed characteristics and hydrology to regulate nutrient concentrations that ultimately govern phytoplankton dynamics (Figure 4.6; Kosten et al., 2009; Oliver et al., 2017; Wagner et al., 2011). We originally hypothesized that land cover and lake morphometry would have a larger influence in explaining lake-to-lake variability by modifying the sensitivity of chl *a* to climatic variables (Thompson et al., 2005). The combined Regional Climate + WS model (Appendix B7) suggests that the size of the lake relative to the watershed, lake depth, and both loss of and present-day perennial snow and ice cover may be important in explaining variation in lake-to-lake algal responses to climate change. Generally, chl *a* was positively correlated with the drainage ratio and lake depth. Although lakes in larger watersheds are typically associated with higher nutrient loads (Soranno et al., 1999), water residence time is an approximate inverse function of drainage ratio (watershed area:lake area), which could explain why headwater lakes generally had higher phytoplankton biomass across the Southern Rocky Mountains (Kling, Kipphut, Miller, & O'Brien, 2000).

The modest C.V. R^2 of the Regional BRT and poor performance of Regional LMM indicates we are likely missing variables that could predict landscape variation in chl *a* such as full fluorescence profiles, light levels, acidity, and biological community structure. Variation in watershed and lake morphometry can also drive large differences in algal community structure (Heil et al., 2007; Muylaert et al., 2009), algal traits (Litchman & Klausmeier, 2008), and food web structure (Post, Pace, & Hairston, 2000), but we did not explicitly account for these ecological processes in the models. Point estimates of phytoplankton biomass and the land cover predictors are static measures that may not be able to fully integrate spatio-temporal interactions, a limitation that has been pointed out in other macroscale studies of lakes (Lottig et al. 2017).

The importance of landscape position and lake morphometry in explaining inter-lake variability in chl *a* was most apparent in the Loch Vale watershed, where the lakes vary substantially in surface area, depth, and land cover (Appendix B2; Slemmons, Saros, & Simon, 2013; Vadeboncoeur, Peterson, Zanden, & Kaliff, 2008). Sky Pond chl *a* was less directly affected by variation in precipitation compared to The Loch (Figure 4.4D), due to the mediating influence of cold, glacial meltwater on headwater lakes (Baron & Caine, 2000). Similar contrasts were observed in Green Lakes Valley whereby glacially-fed GL4 was consistently colder than snow-fed GL1, despite both alpine lakes being at similar elevations above treeline (Figure 4.3D). Lake morphometry, water residence time, and distance from cryospheric features are watershed filters that may explain some of the differences observed between Sky Pond (alpine) and The Loch (subalpine) by affecting and responses to warming (Butcher et al., 2015; Lerman et al., 1995; Milner et al., 2009).

4.4.4 Conceptualizing cross-scale drivers of mountain lake productivity

The combined results from the Regional, Long-term, and Intra-seasonal models allowed us to examine how processes at multiple spatial and temporal scales influence high alpine lake productivity. We drew on these results to propose a conceptual framework linking the drivers that directly and indirectly influence the chemical and thermal limnological properties that give rise to variation in phytoplankton biomass (Figure 4.6). This framework builds upon the growing understanding of dominant processes that govern phytoplankton dynamics in mountain lakes (Baron et al., 2009; Parker et al., 2008b; Preston et al., 2016; Sadro et al., 2012; Sadro et al., 2018a; Sommaruga-Wograth et al., 1997). In years with average SWE and summers characterized by below-average precipitation and warmer than average air temperatures, weekly precipitation and mean monthly air temperatures were the most important predictors of chl *a*. Snow-water equivalent influences water residence time, with high SWE years typically having high flushing and lower nutrient concentrations resulting in lower phytoplankton biomass (Preston et al., 2016a; Sadro et al., 2018b). In contrast, dry and warm summer periods enhance evapotranspiration and evaporation, which concentrates nutrients, resulting in higher phytoplankton biomass. Episodic heavy precipitation may also deliver nutrients, colored dissolved organic matter, or particles that can also enhance productivity. Lake and watershed filters, such as lake depth, catchment position, and presence of perennial ice and snow can mediate lake temperatures and nutrients, thereby influencing lake-specific phytoplankton responses.

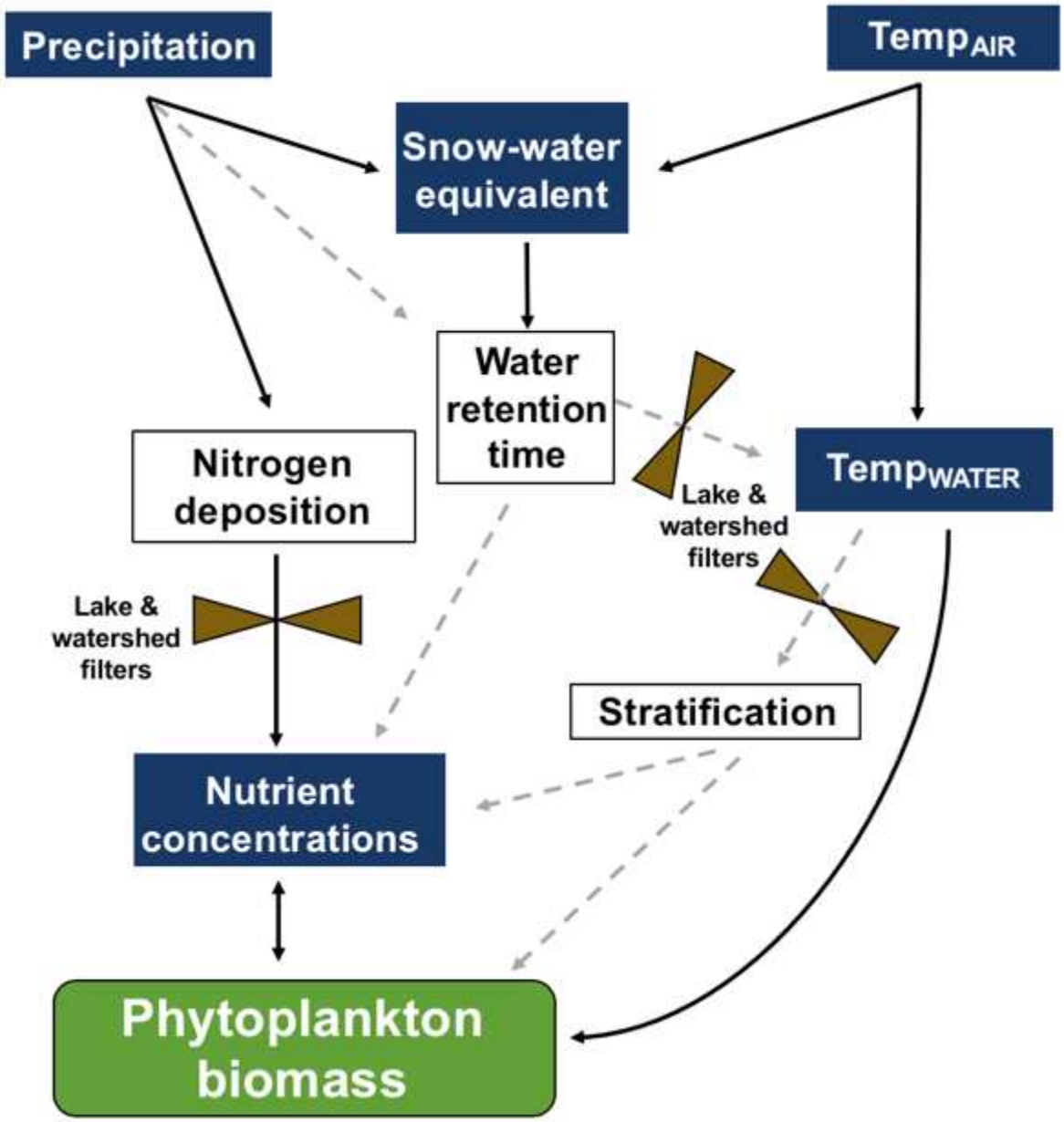

Figure 4.6. Conceptual framework depicting pathways of physical and chemical drivers of phytoplankton biomass (as chl *a*) in mountain lakes. Blue boxes represent model-identified variables significantly influencing lake dynamics and predicting patterns in phytoplankton dynamics. White boxes represent processes not directly measured in our study that are known to influence drivers that influence phytoplankton. Black arrows depict direct relationships; dashed arrows depict indirect relationships. Control valves depict lake- or watershed-specific filters that modify the influence of specific predictors. Precipitation and air temperature ($Temp_{AIR}$) are considered at daily, weekly, and monthly timescales as well as deviations from normal, with direct and indirect effects on water temperature ($Temp_{WATER}$). Snow water equivalent influences water retention time

(e.g., flushing) and nutrient concentrations at interannual timescales. Nitrogen deposition loads influence nutrient concentrations across the southern Rocky Mountain region, but lake specific concentrations are mediated by lake and watershed filters (land cover, lake morphometry and depth, glaciers), landscape position, and nutrient uptake.

This study and others highlight the importance of considering both winter and summer climate in anticipating future changes to mountain and non-mountain lake ecosystems (Collins et al., 2019). While the role of variable snowpack is increasingly recognized as a driver of biogeochemical and ecological dynamics in these systems, we identified processes that may give rise to increased phytoplankton biomass as the climate continues to change. Summers in the Southern Rocky Mountains have been consistently getting warmer and drier and are changing faster than winter climatic conditions (Fassnacht, Venable, McGrath, & Patterson, 2018). Because of this, summer drought and warmer than average temperatures may start to overpower the influence of snowmelt to alter lake thermal and chemical properties that are important drivers of lake productivity. Like the Arctic, many mountainous regions across the globe are experiencing amplified rates of warming, adding urgency to understand how warming associated climatic shifts may be impacting alpine aquatic ecosystems (Pepin et al. 2015; Palazzi et al. 2019).

We anticipate that continued warming of air and water temperatures in combination with earlier snowpack melting and continued trends toward longer ice-free seasons may lead to increased productivity in high-elevation lakes (Christianson, Johnson, Hooten, & Roberts, 2019; Clow, 2010; Mote, Hamlet, Clark, & Lettenmaier, 2005; Preston et al., 2016; Stewart, 2009). As the surrounding terrestrial landscape responds to these changes loading of materials into lakes as the climate continues to

change may also play a role in altered ecology and biogeochemical cycling (Dong et al. 2019). More thoroughly assessing the role of watershed factors in mediating or amplifying lake responses will help us quantify which lakes are more resistant or resilient to environmental change. Anticipating future lake productivity will also require better accounting of both N and P deposition because there is a legacy of N deposition that has led to widespread P-limitation of phytoplankton in the Southern Rocky Mountains (Elser et al., 2009a, 2009b), and dust deposition of P is on the rise regionally (Clow, Williams, & Schuster, 2016). Continued and expanded distribution of monitoring stations are needed to improve the quality and resolution of these data. Nutrient inputs from atmospheric deposition and the cryosphere, coupled with a changing climate could have complex implications for lake biogeochemical cycling and primary production. This study provides valuable insights toward next steps for hypothesis testing and research in this area. We must continue to work towards understanding drivers of lake productivity to aid managers in preparing for an uncertain future in headwaters around the world.

REFERENCES

Adrian, R., Reilly, C. M. O., Zagarese, H., Baines, S. B., Hessen, D. O., Keller, W., Winder, M. (2009). Lakes as sentinels of climate change. *Limnology and Oceanography*, 54(6), 2283–2297.

Agbeti, M. D., Smol, J. P. (1995). Winter limnology: a comparison of physical, chemical and biological characteristics in two temperate lakes during ice cover. *Hydrobiologia*, 304(3), 221–234.

Allan, J.D., Castillo, M.M. (2007). Chapter 6: Primary Producers, in: Stream Ecology: Structure and Function of Running Waters. Springer Science & Business Media.

Appleby, P. G., Oldfield, F. (1978). The calculation of lead-210 dates assuming a constant rate of supply of unsupported 210Pb to the sediment. *Catena*, 5(1), 1–8.

Arthur, M. A., Denning, A. S., Harris, M. A., Mast, M. A., McKnight, D. M., McLaughlin, P., Baron, J. S. (1992). Vegetation. In Biogeochemistry of a Subalpine Ecosystem: Loch Vale Watershed. Springer Science & Business Media. p76-93.

Axler, R.P., Reuter, J.E. (1996). Nitrate uptake by phytoplankton and periphyton: Whole-lake enrichments and mesocosm-15N experiments in an oligotrophic lake. *Limnology and Oceanography* 41, 659–671.

Baines, S.B., Pace, M.L. (1991). The production of dissolved organic matter by phytoplankton and its importance to bacteria: patterns across marine and freshwater systems. *Limnology and Oceanography* 36, 1078–1090.

Barnes, R. T., Williams, M. W., Parman, J. N., Hill, K., Caine, N. (2014). Thawing glacial and permafrost features contribute to nitrogen export from Green Lakes Valley, Colorado Front Range, USA. *Biogeochemistry*, 117(2–3), 413–430.

Baron, J. S. (1992). Surface Waters. Baron, J. S., editor, Biogeochemistry of a Subalpine Ecosystem: Loch Vale Watershed. Springer Science & Business Media. p142–187

Baron, J. S., & Caine, N. (2000). Temporal coherence of two alpine lake basins of the Colorado Front Range, U.S.A. *Freshwater Biology*, 463–476.

Baron, J. S., & Denning, A. S. (1993). The influence of mountain meteorology on precipitation chemistry at low and high elevations of the Colorado Front Range, USA. *Atmospheric Environment*, 27(15), 2337–2349.

Baron, J. S., Del Grosso, S. J., Ojima, D. S., Theobald, D. M., Parton, W. J. (2004). Nitrogen emissions along the Colorado Front Range: response to population growth, land and water use change, and agriculture. Ecosystem Interactions and Land Use Change. DeFries, R. S., Asner, G. P., and Houghton, R. A., editors.

Geophysical Monography Series, American Geophysical Union. Vol 153, p117-127.

Baron, J. S., Hall, E. K., Nolan, B. T., Finlay, J. C., Bernhardt, E. S., Harrison, J. A., Boyer, E. W. (2012). The interactive effects of excess reactive nitrogen and climate change on aquatic ecosystems and water resources of the United States. *Biogeochemistry*, 114(1–3), 71–92.

Baron, J. S., McKnight, D., Denning, A. S. (1991). Sources of dissolved and particulate organic material in Loch Vale Watershed, Rocky Mountain National Park, Colorado, USA. *Biogeochemistry*, 15(1), 89–110.

Baron, J. S., Rueth, H. M., Wolfe, A. M., Nydick, K. R., Allstott, E. J., Minear, J. T., Moraska, B. 2000. Ecosystem Responses to Nitrogen Deposition in the Colorado Front Range. *Ecosystems*, 3(4), 352–368.

Baron, J. S., Schmidt, T. M., Hartman, M. D. (2009). Climate-induced changes in high elevation stream nitrate dynamics. *Global Change Biology*, 15(7), 1777–1789.

Baron, J.S. and Campbell, D.H. (1997). Nitrogen fluxes in a high elevation Colorado Rocky Mountain basin. *Hydrological Processes*, 11(7), 783-799.

Baron, J.S., Rueth, H.M., Wolfe, A.M., Nydick, K.R., Allstott, E.J., Minear, J.T., Moraska, B. (2000). Ecosystem Responses to Nitrogen Deposition in the Colorado Front Range. *Ecosystems* 3, 352–368. https://doi.org/10.1007/s100210000032

Baron, Jill S. (2006). Hindcasting nitrogen deposition to determine an ecological critical load. *Ecological Applications* 16 (3): 433–39.

Baron, Jill S., Heather M. Rueth, Alexander M. Wolfe, Koren R. Nydick, Eric J. Allstott, J. Toby Minear, and Brenda Moraska. (2000). Ecosystem Responses to Nitrogen Deposition in the Colorado Front Range. *Ecosystems* 3 (4): 352–68.

Baron, Jill S., Travis M. Schmidt, and Melannie D. Hartman. (2009). Climate-Induced Changes in High Elevation Stream Nitrate Dynamics. *Global Change Biology* 15 (7): 1777–89.

Barton, K. (2019). MuMIn: Multi-Model Inference. R package version 1.43.6. https://CRAN.R-project.org/package=MuMIn

Bates, D., Maechler, M., Bolker, B., Walker, S. (2015). Fitting linear mixed-effects models using lme4. *Journal of Statistical Software*, 67(1), 1-48.

Beck, W.S., Markman, D.W., Oleksy, I.A., Lafferty, M.H., Poff, N.L. (2019). Seasonal shifts in the importance of bottom–up and top–down factors on stream periphyton community structure. *Oikos* 128, 680–691.

Beck, W.S., Rugenski, A.T., Poff, N.L. (2017). Influence of experimental, environmental, and geographic factors on nutrient-diffusing substrate experiments in running waters. *Freshwater Biology* 62, 1667–1680. https://doi.org/10.1111/fwb.12989

Bellinger, Edward G., and David C. Sigee. (2015). Freshwater Algae: Identification and Use as Bioindicators. John Wiley & Sons.

Berglund, Bjorn E. (2011). How Mankind Has Shaped European Nature. *Vegetation History and Archaeobotany* 20: 79–81.

Bergström, A. K., Jansson, M. (2006). Atmospheric nitrogen deposition has caused nitrogen enrichment and eutrophication of lakes in the northern hemisphere. *Global Change Biology*, 12(4), 635-643.

Bertani, I., Steger, C. E., Obenour, D. R., Fahnenstiel, G. L., Bridgeman, T. B., Johengen, T. H., Scavia, D. (2017). Tracking cyanobacteria blooms: Do different monitoring approaches tell the same story? *Science of the Total Environment,* 575, 294–308.

Birks, H. J. B., Lotter, A. F., Juggins, S., Smol, J. P. (2012). Data Handling and Numerical Techniques. Last, William M., Smol, John P., editors. Tracking Environmental Change Using Lake Sediments - Volume 5. Springer Netherlands.

Birks, Hilary H., H.J.B. Birks, Peter Emil Kaland, and Dagfinn Moe. (1988). The Cultural Landscape: Past, Present and Future. Cambridge University Press.

Blenckner, T., Omstedt, A., & Rummukainen, M. (2002). A Swedish case study of contemporary and possible future consequences of climate change on lake function. *Aquatic Sciences*, 64(2), 171–184.

Bloemberg, T. G., Gerretzen, J., Wouters, H. J. P., Gloerich, J., van Dael, M., Wessels, H. J. C. T., Wehrens, R. (2010). Improved Parametric Time Warping for Proteomics. *Chemometrics and Intelligent Laboratory Systems,* 104(1), 65–74.

Blumenshine, A. S. C., Vadeboncoeur, Y., Lodge, D. M., Cottingham, K. L. (1997). Benthic-Pelagic Links: Responses of Benthos to Water-Column Nutrient Enrichment. *Journal of the North American Benthological Society*, 16(3), 466–479.

Bonachela, J.A., Raghib, M., Levin, S.A. (2011). Dynamic model of flexible phytoplankton nutrient uptake. *Proceedings of the National Academy of Sciences* 108, 20633–20638.

Bonilla, S., Villeneuve, V., Vincent, W.F. (2005). Benthic and planktonic algal communities in a high arctic lake: Pigment structure and contrasting responses to nutrient enrichment. *Journal of Phycology* 41, 1120–1130.

Bradshaw, Emily G., Peter Rasmussen, and Bent Vad Odgaard (2005). Mid- to late-Holocene land-use change and lake development at Dallund So, Denmark: synthesis of multiproxy data, linking land and lake. *The Holocene* 15 (8): 1152–1162.

Brahney, J. A., Ballantyne, A. P., Kociolek, P., Spaulding, S. A., Otu, M., Porwoll, T., Neff, J. C. (2014). Dust mediated transfer of phosphorus to alpine lake ecosystems of the Wind River Range, Wyoming, USA. *Biogeochemistry*, 120(1–3), 259–278.

Brahney, J., A. P. Ballantyne, C. Sievers, and J. C. Neff. (2013). Increasing Ca2+ deposition in the Western US: The Role of Mineral Aerosols. *Aeolian Research*, 10, 77-87.

Brahney, J., A.P. Ballantyne, P. Kociolek, P.R. Leavitt, G.L. Farmer, and J.C. Neff. (2015). Ecological Changes in Two Contrasting Lakes Associated with Human Activity and Dust Transport in Western Wyoming. *Limnology and Oceanography* 60 (2): 678–95.

Brahney, J., Ballantyne, a. P., Kociolek, P., Spaulding, S. A., Otu, M., Porwoll, T., & Neff, J. C. (2014). Dust mediated transfer of phosphorus to alpine lake ecosystems of the Wind River Range, Wyoming, USA. *Biogeochemistry*, 120(1–3), 259–278.

Brahney, J., N. Mahowald, D. S. Ward, A.P. Ballantyne, and J.C. Neff. (2015). Is Atmospheric Phosphorus Pollution Altering Global Alpine Lake Stoichiometry? Global *Biogeochemical Cycles* 29: 263–84.

Breiman, L., Friedman, J. H., Olshen, R. A., & Stone, C. J. (1984). Classification and Regression Trees, The Wadsworth statistics probability series, 19, 368.

Brighenti, S., Tolotti, M., Bruno, M.C., Wharton, G., Pusch, M.T., Bertoldi, W. (2019). Ecosystem shifts in Alpine streams under glacier retreat and rock glacier thaw: A review. *Science of the Total Environment* 675, 542-559.

Bunting, L., Leavitt, P. R., Gibson, C. E., McGee, E. J., Hall, V. A. (2007). Degradation of water quality in Lough Neagh, Northern Ireland, by diffuse nitrogen flux from a phosphorus-rich catchment. *Limnology and Oceanography*, 52(1), 354–369.

Bunting, L., Leavitt, P. R., Simpson, G. L., Wissel, B., Laird, K. R., Cumming, B. F., Engstrom, D. R. (2016). Increased variability and sudden ecosystem state change in Lake Winnipeg, Canada, caused by 20th century agriculture. *Limnology and Oceanography,* 61(6), 2090 2107.

Butcher, J. B., Nover, D., Johnson, T. E., & Clark, C. M. (2015). Sensitivity of lake thermal and mixing dynamics to climate change. *Climatic Change*, 129(1), 295–305.

Cantonati, Marco, and Rex L. Lowe (2014). Lake Benthic Algae: Toward an Understanding of Their Ecology. *Freshwater Science* 33(2): 475–86.

Cashman, M.J., Pilotto, F., Harvey, G.L., Wharton, G., Pusch, M.T. (2016). Combined stable-isotope and fatty-acid analyses demonstrate that large wood increases the autochthonous trophic base of a macroinvertebrate assemblage. *Freshwater Biology* 61, 549–564.

Castañeda, I. S., Werne, J. P., Johnson, T. C. (2009). Influence of climate change on algal community structure and primary productivity of Lake Malawi (East Africa) from the Last Glacial Maximum to present. *Limnology and Oceanography*, 54(6part2), 2431 2447.

Catalan, J., Pla-Rabes, S., Wolfe, A. P., Smol, J. P., Ruhland, K. M., Anderson, N. J., Renberg, I. (2013). Global change revealed by palaeolimnological records from remote lakes: A review. *Journal of Paleolimnology*, 49(3), 513–535.

Catalan, Jordi, Lluís Camarero, Marisol Felip, Sergi Pla, Marc Ventura, Teresa Buchaca, Frederic Bartumeus, et al. (2006). High Mountain Lakes: Extreme Habitats and Witnesses of Environmental Changes. *Limnetica* 25(1–2): 551–584.

Cattaneo, Antonella, Ginette Methot, Bernadette Pinel-Alloul, and Theophile Niyonsenga. (1995). Epiphyte Size and Taxonomy as Biological Indicators of

Ecological and Toxicological Factors in Lake Saint-Francois (Quebec). *Environmental Pollution* 87: 357–372.

Christianson, K. R., Johnson, B. M., Hooten, M. B., Roberts, J. J. (2019). Estimating lake-climate responses from sparse data: An application to high elevation lakes. *Limnology and Oceanography,* 64(3), 1371-1385.

Clow, D. W. (2010). Changes in the timing of snowmelt and streamflow in Colorado: A response to recent warming. *Journal of Climate*, 23(9), 2293–2306.

Clow, D. W., Schrott, L., Webb, R., Campbell, D. H., Torizzo, A., Dornblaser, M. (2003). Ground water occurrence and contributions to streamflow in an alpine catchment, Colorado Front Range. *Groundwater*, 41(7), 937-950.

Clow, D. W., Williams, M. W., & Schuster, P. F. (2016). Increasing aeolian dust deposition to snowpacks in the Rocky Mountains inferred from snowpack, wet deposition, and aerosol chemistry. *Atmospheric Environment*, 146, 183–194.

Clow, David W., Sarah M. Stackpoole, Kristine L. Verdin, David E. Butman, Zhiliang Zhu, David P. Krabbenhoft, and Robert G. Striegl. (2015). Organic Carbon Burial in Lakes and Reservoirs of the Conterminous United States. *Environmental Science & Technology* 49 (13): 7614–22.

Collins, S. M., Yuan, S., Tan, P. N., Oliver, S. K., & Lapierre, J. F. (2019). Winter Precipitation and Summer Temperature Predict Lake Water Quality at Macroscales Water Resources Research. *Water Resources Research*, 55, 2708–2721.

Colombaroli, Daniele, Madlena Beckmann, Willem O. Van Der Knaap, Philippe Curdy, and Willy Tinner. (2013). Changes in Biodiversity and Vegetation Composition in the Central Swiss Alps during the Transition from Pristine Forest to First Farming. *Diversity and Distributions* 19: 157–170.

Cross, W.F., Hood, J.M., Benstead, J.P., Huryn, A.D., Nelson, D. (2015). Interactions between temperature and nutrients across levels of ecological organization. *Global Change Biology* 21, 1025–1040.

De Senerpont Domis, L.N., Van de Waal, D.B., Helmsing, N.R., Donk, E.V., Mooij, W.M. (2014). Community stoichiometry in a changing world: combined effects of warming and eutrophication on phytoplankton dynamics. *Ecology* 95, 1485–1495.

De'ath, G. (2007). Boosted regression trees for ecological modeling and prediction. *Ecology*, 88(1), 243–251.

De'ath, G., & Fabricius, K. E. (2000). Classification and Regression Trees : A Powerful Yet Simple Technique for Ecological Data Analysis. *Ecology*, 81(11), 3178–3192.

Delcourt, Paul A., Hazel R. Delcourt, Cecil R. Ison, William E. Sharp, and Kristen J. Gremillion (1998). Prehistoric Human Use of Fire, the Eastern Agricultural Complex, and Appalachian Oak-Chestnut Forests: Paleoecology of Cliff Palace Pond, Kentucky. *American Antiquity* 63 (2): 263–278.

DeNicola, D. (1996). Periphyton response to temperature at different ecological levels. Stevenson, R.J., Bothwell M. L., Lowe R. L., editors. Algal Ecology. Academic Press. p150–183.

Dodds, W.K., Gudder, D.A. (1992). The ecology of Cladophora. *Journal of Phycology* 28, 415–427.

Dong, Zheng, Charles T. Driscoll, John L. Campbell, Afshin Pourmokhtarian, Anne M.K. Stoner, and Katharine Hayhoe. (2019). Projections of water, carbon, and nitrogen dynamics under future climate change in an alpine tundra ecosystem in the Southern Rocky Mountains using a biogeochemical model." *Science of the Total Environment* 650: 1451–1464.

Dubois, N., Saulnier-Talbot, É., Mills, K., Gell, P., Battarbee, R., Bennion, H., Valero-Garcés, B. (2018). First human impacts and responses of aquatic systems: A review of paleolimnological records from around the world*. The Anthropocene Review*, 5(1), 28 68.

Durán, C., Medina-Sánchez, J.M., Herrera, G., Carrillo, P. (2015). Changes in the phytoplankton-bacteria coupling triggered by joint action of UVR, nutrients, and warming in Mediterranean high-mountain lakes. *Limnology and Oceanography*, 61(2), 413-429.

Eilers, J. M., Kanciruk, P., McCord, R. A., Overton, W. S., Hook, L., Blick, D. J., … Landers, D. H. (1987). Western Lake Survey. Phase I. Characteristics of Lakes in the Western United States. Volume II. Data Copendium for Selected Physical and Chemical Variables. Washington, DC: U.S. Environmental Protection Agency.

Elith, J., Leathwick, J. R., & Hastie, T. (2008). A working guide to boosted regression trees. *Journal of Animal Ecology*, 77(4), 802–813.

Elser, J. J., Andersen, T., Baron, J. S., Bergström, A.-K., Jansson, M., Kyle, M., Hessen, D. O. (2009)a. Shifts in lake N:P stoichiometry and nutrient limitation driven by atmospheric nitrogen deposition. *Science*, 326(5954), 835–837.

Elser, J. J., Kyle, M., Steuer, L., Nydick, K. R., & Baron, J. S. (2009)b. Nutrient availability and phytoplankton nutrient limitation across a gradient of atmospheric nitrogen deposition. *Ecology*, 90(11), 3062–3073.

Enders, S. K., Pagani, M., Pantoja, S., Baron, J. S., Wolfe, A. P., Pedentchouk, N., Nuñez, L. (2008). Compound-specific stable isotopes of organic compounds from

lake sediments track recent environmental changes in an alpine ecosystem, Rocky Mountain National Park, Colorado. *Limnology and Oceanography*, 53(4), 1468–1478.

ESRI. (2018). ArcGIS Desktop: Release 10.5. Redlands, CA: Environmental Systems Research Institute.

Fassnacht, S. R., Venable, N. B. H., McGrath, D., & Patterson, G. G. (2018). Sub-seasonal snowpack trends in the Rocky Mountain National Park Area, Colorado, USA. *Water*, 10(5), 1–20.

Fegel, T. S., Baron, J. S., Fountain, A. G., Johnson, G. F., & Hall, E. K. (2016). The differing biogeochemical and microbial signatures of glaciers and rock glaciers. *Journal of Geophysical Research: Biogeosciences*, 919–932. http://doi.org/10.1002/2015JG003236.Received

Fegel, T.S., Boot, C.M., Broeckling, C.D., Baron, J.S., Hall, E.K. (2019). Assessing the chemistry and bioavailability of dissolved organic matter from glaciers and rock glaciers. *Journal of Geophysical Research Biogeosciences.* https://doi.org/10.1029/2018JG004874

Ficker, H., Luger, M., & Gassner, H. (2017). From dimictic to monomictic: empirical evidence of thermal regime transitions in three deep alpine lakes in Austria induced by climate change. *Freshwater Biology*, 62(8), 1335–1345.

Filstrup, C. T., Wagner, T., Soranno, P. a., Stanley, E. H., Stow, C. a., Webster, K. E., & Downing, J.A. (2014). Regional variability among nonlinear chlorophyll-phosphorus relationships in lakes. *Limnology and Oceanography*, 59(5), 1691–1703.

Florian, C. R., Miller, G. H., Fogel, M. L., Wolfe, A. P., Vinebrooke, R. D., Geirsdottir, A. (2015). Algal pigments in Arctic lake sediments record biogeochemical changes due to Holocene climate variability and anthropogenic global change. *Journal of Paleolimnology,* 54(1), 53–69.

Frey, K. E., McClelland, J. W. (2008). Impacts of permafrost degradation on Arctic river biogeochemistry. *Hydrological Processes*, 23(1), 169–182.

Frossard, V., Verneaux, V., Millet, L., Jenny, J.P., Arnaud, F., Magny, M., Perga, M.E., (2014). Reconstructing long-term changes (150 years) in the carbon cycle of a clear-water lake based on the stable carbon isotope composition ($\delta^{13}C$) of chironomid and cladoceran subfossil remains. *Freshwater Biology* 59, 789–802.

Fu, W., Magnúsdóttir, M., Brynjólfson, S., Palsson, B.Ø., Paglia, G. (2012). UPLC-UV-MS E analysis for quantification and identification of major carotenoid and chlorophyll species in algae*. Analytical and bioanalytical chemistry,* 404, 3145–3154.

Fulton, R.S. (1988). Grazing on filamentous algae by herbivorous zooplankton. *Freshwater Biology* 20, 263–271.

George, D. G., Maberly, S. C., & Hewitt, D. P. (2004). The influence of the North Atlantic Oscillation on the physical, chemical and biological characteristics of four lakes in the English Lake District. *Freshwater Biology*, 49(6), 760–774.

Gerten, D., & Adrian, R. (2002). Effects of climate warming, North Atlantic Oscillation, and El Niño-Southern Oscillation on thermal conditions and plankton dynamics in Northern Hemispheric lakes. *The Scientific World Journal*, 2, 586–606.

Gettel, G.M., Giblin, A.E., Howarth, R.W. (2013). Controls of benthic nitrogen fixation and primary production from nutrient enrichment of oligotrophic, arctic lakes. *Ecosystems* 16, 1550–1564.

Giorgino, T. (2009). Computing and Visualizing Dynamic Time Warping Alignments in R: The dtw Package. *Journal of Statistical Software*, Articles, 31(7), 1–24.

Gladyshev, M.I., Gubelit, Y.I. (2019). Green Tides: New Consequences of the Eutrophication of Natural Waters Green Tides: New Consequences of the Eutrophication of Natural Waters. *Contemporary Problems in Ecology* 12, 109–125.

Glew, J. R. (1991). Miniature gravity corer for recovering short sediment cores. *Journal of Paleolimnology,* 5(3), 285–287.

Goldman, C. R. (1988). Primary productivity, nutrients, and transparency during the early onset of eutrophication in ultra-oligotrophic Lake Tahoe, California-Nevada. *Limnology and Oceanography*, 33(6), 1321–1333.

González-Sampériz, Penélope, Josu Aranbarri, Ana Pérez-sanz, Graciela Gil-romera, Ana Moreno, María Leunda, Miguel Sevilla-callejo, et al. (2017). Environmental and Climate Change in the Southern Central Pyrenees since the Last Glacial Maximum: A View from the Lake Records. *Catena* 149: 668–688.

Grêt-Eegamey, Adrienne, Sibyl Hanna Brunner, and Felix Kienast. (2012). Mountain Ecosystem Services: Who Cares? *Mountain Research and Development* 32 (SI): 23–34.

Griffiths, K., Michelutti, N., Sugar, M., Douglas, M. S. V., & Smol, J. P. (2017). Ice-cover is the principal driver of ecological change in High Arctic lakes and ponds. *Plos One*, 12(3), e0172989.

Haack, T.K., McFeters, G.A. (1982). Microbial dynamics of an epilithic mat community in a high alpine stream. *Applied Environmental Microbiology*. 43, 702–707.

Hagerthey, S.E., Kerfoot, W.C. (1998). The biomass and nutrient ratios of epibenthic algae in a Groundwater flow influences seepage lake north temperate. *Limnology and Oceanography* 43, 1227–1242.

Hampton, S.E., Fradkin, S., Leavitt, P.R., Rosenberger, E.E. (2011). Disproportionate importance of nearshore habitat for the food web of a deep oligotrophic lake. *Marine and Freshwater Research* 62, 350–358.

Hart, E. M., & Bell, K. (2015). prism: Download data from the Oregon prism project. R package version 0.0.6. http://doi.org/10.5281/zenodo.33663

Hastie, T., Tibshirani, R. (1987). Generalized Additive Models, Cubic Splines and Personalized Likelihood. University of Toronto, Department of Statistics.

Hawes, I. (1988). The Seasonal Dynamics of Maritime Antarctic Lake Spirogyra in a Shallow. *Polar Biology* 8, 429–437.

Heil, C. A., Revilla, M., Glibert, P. M., & Murasko, S. (2007). Nutrient quality drives differential phytoplankton community composition on the southwest Florida shelf. *Limnology and Oceanography*, 52(3), 1067–1078.

Hickman, M. (1982). The removal of a heated water discharge from a lake and the effect upon an epiphytic algal community. *Hydrobiologia* 87, 21–32.

Hilfinger, Martin F., Henry T. Mullins, Adam Burnett, and Matthew E. Kirby. (2001). A 2500 Year Sediment Record from Fayetteville Green Lake, New York: Evidence for Anthropogenic Impacts and Historic Isotope Shift. *Journal of Paleolimnology* 26: 293–305.

Hogan, E.J., McGowan, S., Anderson, N.J. (2014). Nutrient limitation of periphyton growth in arctic lakes in south-west Greenland. *Polar Biology* 37, 1331–1342.

Holtgrieve, G. W., Schindler, D. E., Hobbs, W. O., Leavitt, P. R., Ward, E. J., Bunting, L., Wolfe, A. P. (2011). A coherent signature of anthropogenic nitrogen deposition to remote watersheds of the Northern Hemisphere. *Science*, 334(6062), 1545–1548.

Holzinger, A., Karsten, U. (2013). Desiccation stress and tolerance in green algae: consequences for ultrastructure, physiological and molecular mechanisms. *Frontiers in Plant Science* 4, 1–18.

Holzinger, A., Roleda, M. Y., Lütz, C. (2009). The vegetative Arctic freshwater green alga Zygnema is insensitive to experimental UV exposure. *Micron*, 40(8), 831-838.

Homer, C. G., Dewitz, J. A., Yang, L., Jin, S., Danielson, P., Xian, G., Megown, K. (2015). Completion of the 2011 National Land Cover Database for the conterminous United States - representing a decade of land cover change

information. *Photogrammetric Engineering and Remote Sensing*. http://doi.org/10.14358/PERS.81.5.345

Hotchkiss, E.R., Hall, R.O., Baker, M.A., Rosi-Marshall, E.J., Tank, J.L. (2014). Modeling priming effects on microbial consumption of dissolved organic carbon in rivers. *Journal of Geophysical Research: Biogeosciences* 119, 982–995.

Huss, M., Bookhagen, B., Huggle, C., Jacobsen, D., Bradley, R. S., Clague, J. J., Winder, M. (2017). Toward mountains without permanent snow and ice. *Earth's Future,* 5(May), 1–18.

Ives, J.D., Fahey, B.D. (1971). Permafrost Occurrence in the Front Range, Colorado Rocky Mountains, U.S.A. *Journal of Glaciology,* 10, 105–111.

Jeppesen, E., Meerhoff, M., Davidson, T. a., Trolle, D., Søndergaard, M., Lauridsen, T. L., Nielsen, A. (2014). Climate change impacts on lakes: an integrated ecological perspective based on a multi-faceted approach, with special focus on shallow lakes. *Journal of Limnology,* 73(s1), 88–111.

Kann, J., Falter, C.M. (1989). Periphyton as indicators of enrichment in Lake Pend Oreille, Idaho*. Lake and Reservoir Management* 5, 39–48.

Kaplan, L.A., Bott, T.L. (1989). Diel fluctuations in bacterial activity on streambed substrata during vernal algal blooms: effects of temperature, water chemistry, and habitat. *Limnology and Oceanography* 34, 718–733.

Kasprzak, P., Shatwell, T., Gessner, M. O., Gonsiorczyk, T., Kirillin, G., Selmeczy, G., & Engelhardt, C. (2017). Extreme weather event triggers cascade towards extreme turbidity in a clear-water lake. *Ecosystems*, 20(8), 1407-1420.

Kendrick, M. R., Huryn, A. D., Bowden, W. B., Deegan, L. A., Findlay, R. H., Hershey, A. E., Schuett, E. (2018). Linking permafrost thaw to shifting biogeochemistry and food web resources in an Arctic river. *Global Change Biology*, 24(12), 5738-5750.

Kendrick, M.R., Huryn, A.D., Bowden, W.B., Deegan, L.A., Findlay, R.H., Hershey, A.E., Peterson, B.J., Benes, J., Schuett, E. (2018). Linking permafrost thaw to shifting biogeochemistry and food web resources in an arctic river. *Global Change Biology* 24(12), 5738-5750.

Klein, J.A., Tucker, C.M., Nolin, A.W., Hopping, K.A., Reid, R.S., Steger, C., Grêt-Regamey, A., Lavorel, S., Müller, B., Yeh, E.T. and Boone, R.B. (2019). Catalyzing transformations to sustainability in the world's mountains*. Earth's Future,* 7(5), 547-557.

Kling, G. W., Kipphut, G. W., Miller, M., & O'Brien, W. J. (2000). Integration of lakes and streams in a landscape perspective: the importance of material processing on spatial patterns and temporal coherence. *Freshwater Biology*, 43, 477–497.

Kosten, S., Huszar, V. L. M., Mazzeo, N., Scheffer, M., Sternberg, L. D. S. L., & Jeppesen, E. (2009). Lake and watershed characteristics rather than climate in shallow lakes influence nutrient limitation. *Ecological Applications*, 19(7), 1791–1804.

Köster, Dörte, Reinhard Pienitz, Brent B. Wolfe, Sylvia Barry, R.M. Andrew, and Sushil S. Dixit. (2007). Paleolimnological assessment of human-induced impacts on Walden Pond (Massachusetts, USA) using diatoms and stable isotopes. *Aquatic Ecosystem Health & Management 8* (2): 117–131.

Kraemer, B. M., Anneville, O., Chandra, S., Dix, M., Kuusisto, E., Livingstone, D. M., McIntyre, P. B. (2015). Morphometry and average temperature affect lake stratification responses to climate change. *Geophysical Research Letters*, 42(12), 4981-4988.

Kraemer, B. M., Chandra, S., Dix, M., Kuusisto, E., Livingstone, D. M., Schladow, G., McIntyre, P. B. (2016). Global patterns in aquatic ecosystem responses to warming based on activation energies. *Global Change Biology,* 23(5), 1881-1890.

Kravtsova, Lyubov S., Lyudmila A. Izhboldina, Igor V. Khanaev, Galina V. Pomazkina, Elena V. Rodionova, Valentina M. Domysheva, Mariya V. Sakirko, et al. (2014). Nearshore benthic blooms of filamentous green algae in Lake Baikal. *Journal of Great Lakes Research* 40 (2): 441–448.

Kuznetsova, A., Brockhoff, P.B., Christensen, R.H.B. (2017). *lmerTest* package: Tests in linear mixed effects models*. Journal of Statistical Software*, 82(13), 1-26.

Ladyzhenskaya, O. A. (1985). The Method of Finite Differences. The Boundary Value Problems of Mathematical Physics. Springer, New York, NY. p212–307.

Lambert, D, Antonella C., and Richard C. (2008). Periphyton as an Early Indicator of Perturbation in Recreational Lakes*. Canadian Journal of Fisheries and Aquatic Sciences* 265: 258–265.

Lange, K., Townsend, C.R., Matthaei, C.D. (2016). A trait-based framework for stream algal communities. *Ecology and Evolution* 6, 23–36.

Leavitt, P. R., Fritz, S. C., Anderson, N. J., Baker, P. A., Blenckner, T., Bunting, L., Werne, J. (2009). Paleolimnological evidence of the effects on lakes of energy and mass transfer from climate and humans. *Limnology and Oceanography*, 54(6part2), 2330–2348.

Leavitt, P. R., Hodgson, D. A. (2001). Sedimentary Pigments. Smol, J.P., Birks, H. J., Last, W. M. editors. Tracking Environmental Change Using Lake Sediments Vol. 3. Springer Netherlands. p295–325.

Leavitt, P. R., Schindler, D. E., Paul, A. J., Hardie, A. K., Schindler, D. W. (1994). Fossil pigment records of phytoplankton in trout-stocked alpine lakes. *Canadian Journal of Fisheries and Aquatic Sciences,* 51(11), 2411–2423.

Leavitt, P., Fritz, S., Anderson, N., & Baker, P. (2009). Paleolimnological evidence of the effects on lakes of energy and mass transfer from climate to humans. *Limnology and Oceanography,* 54, 2330–2348.

Leavitt, P.R., Findlay, D.L. (1994). Comparison of fossil pigments with 20 years of phytoplankton data from eutrophic Lake 227, Experimental Lakes Area, Ontario. *Canadian Journal of Fisheries and Aquatic Science*, 51, 2286-2299.

Leavitt, P.R., Hodgson, D.A., (2002). Sedimentary Pigments, in: Tracking Environmental Change Using Lake Sediments. Springer, pp. 295–325.

Leopold, M., Lewis, G., Dethier, D., Caine, N., Williams, M.W. (2015). Cryosphere: ice on Niwot Ridge and in the Green Lakes Valley, Colorado Front Range*. Plant Ecology & Diversity* 8(5-6), 1–14.

Lepori, F., Keck, F. (2012). Effects of atmospheric nitrogen deposition on remote freshwater ecosystems. *AMBIO* 41, 235–46.

Lepori, F., Robin, J. (2014). Nitrogen limitation of the phytobenthos in Alpine lakes: results from nutrient-diffusing substrata. *Freshwater Biology* 59, 1633–1645.

Lerman, A., Imboden, D. M., Gat, J., & Chou, L. (1995). Physics and chemistry of lakes. Springer-Verlag Berlin.

Lewin, W. C., Mehner, T., Ritterbusch, D., & Brämick, U. (2014). The influence of anthropogenic shoreline changes on the littoral abundance of fish species in German lowland lakes varying in depth as determined by boosted regression trees. *Hydrobiologia*, 724(1), 293–306.

Lewis, T. L., Lindberg, M. S., Schmutz, J. A., Heglund, P. J., Rover, J., Koch, J. C., & Bertram, M. R. (2015). Pronounced chemical response of Subarctic lakes to climate-driven losses in surface area. *Global Change Biology*, 21(3), 1140–1152.

Litchman, E., & Klausmeier, C. A. (2008). Trait-based community ecology of phytoplankton. *Annual Review of Ecology, Evolution, and Systematics*, 39, 615–639.

Litchman, E., Klausmeier, C. A., Schofield, O. M., Falkowski, P. G. (2007). The role of functional traits and trade-offs in structuring phytoplankton communities: Scaling from cellular to ecosystem level. *Ecology Letters*, 10(12), 1170–1181.

Loewen, C. J. G., Strecker, A. L., Larson, G. L., Vogel, A., Fischer, J. M., Vinebrooke, R. D. (2018). Macroecological drivers of zooplankton communities across the mountains of western North America. *Ecography*, 1–13.

Lottig, N. R., Tan, P.-N., Wagner, T., Cheruvelil, K. S., Soranno, P. A., Stanley, E. H., Yuan, S. (2017). Macroscale patterns of synchrony identify complex relationships among spatial and temporal ecosystem drivers. *Ecosphere*, 8(12), e02024.

Lougheed, V.L., Hernandez, C., Andresen, C.G., Miller, N.A., Alexander, V., Prentki, R. (2015). Contrasting responses of phytoplankton and benthic algae to recent nutrient enrichment in Arctic tundra ponds. *Freshwater Biology* 60, 2169–2186.

Magnuson, J. J., Benson, B. J., & Kratz, T. K. (2004). Patterns of coherent dynamics within and between lake districts at local to intercontinental scales*. Boreal Environment Research,* 9(5), 359–369.

Markensten, H. (2006). Climate effects on early phytoplankton biomass over three decades modified by the morphometry in connected lake basins. *Hydrobiologia*.

Martin, E.S., Harris, R.P., Irigoien, X. (2006). Scaling the metabolic balance of the oceans. *Proceedings of the National Academy of Sciences* 103, 8739–8744.

Mast, M. A., Clow, D. W., Baron, J. S., Wetherbee, G. A. (2014). Links between N Deposition and Nitrate Export from a High- Elevation Watershed in the Colorado Front Range. *Environmental Science & Technology*, 48(24), 14258-14265.

Mast, M.A. (1992). Geochemical characteristics, in: Baron, J.S. (Ed.), Biogeochemistry of a Subalpine Ecosystem: Loch Vale Watershed, Ecological Studies Series. Spring, pp. 93–107.

McCabe, G., Clark, M. P. (2005). Trends and Variability in Snowmelt Runoff in the Western United States. *Journal of Hydrometeorology*, 6(4), 476–482.

McClain, M.E., Boyer, E.W., Dent, C.L., Gergel, S.E., Grimm, N.B., Groffman, P.M., Hart, S.C., Harvey, J.W., Johnston, C.A., Mayorga, E., McDowell, W.H., Pinay, G. (2003). Biogeochemical hot spots and hot moments at the interface of terrestrial and aquatic ecosystems. *Ecosystems* 6, 301–312.

McCullough, I. M., Cheruvelil, K. S., Collins, S. M., & Soranno, P. A. (2019). Geographic patterns of the climate sensitivity of lakes. *Ecological Applications*, 29(2), e01836.

McGuire, C. R., Nufio, C. R., Bowers, M. D., Guralnick, R. P. (2012). Elevation-dependent temperature trends in the Rocky Mountain Front Range: changes over a 56- and 20-year record. *PloS one*, 7(9), e44370

McKnight, D. M., Smith, R. L., Bradbury, J. P., Baron, J. S., Spaulding, S. (1990). Phytoplankton dynamics in three Rocky Mountain lakes, Colorado, U.S.A. *Arctic and Alpine Research,* 22(3), 264.

Meerhoff, M. (2012). Environmental Warming in Shallow Lakes. Advances in Ecological Research: Global Change in Multispecies Systems, Pt 1, 46(1), 259–349.

Meyers, P. A., Ishiwatari, R. (1993). Lacustrine organic geochemistry- an overview of indicators of organic matter sources and diagensis in lake sediments. O*rganic Geochemistry*, 20(7), 867–900.

Michelutti, N., Labaj, A. L., Grooms, C., & Smol, J. P. (2016). Equatorial mountain lakes show extended periods of thermal stratification with recent climate change. *Journal of Limnology,* 75(2), 403–408.

Middleton, C.M., Frost, P.C. (2014). Stoichiometric and growth responses of a freshwater filamentous green alga to varying nutrient supplies: slow and steady wins the race. *Freshwater Biology* 59, 2225–2234.

Milner, A. M., Brown, L. E., & Hannah, D. M. (2009). Hydroecological response of river systems to shrinking glaciers. *Hydrological Processes*, 23(1), 62–77.

Milner, Alexander M., Kieran Khamis, Tom J. Battin, John E. Brittain, Nicholas E. Barrand, Leopold Füreder, Sophie Cauvy-Fraunié, et al. (2017). Glacier Shrinkage Driving Global Changes in Downstream Systems. *Proceedings of the National Academy of Sciences,* 114(37), 9770-9778.

Morris, D. P., Lewis Jr, W. M. (1988). Phytoplankton nutrient limitation in Colorado mountain lakes. *Freshwater Biology*, 20(3), 315-327.

Morris, K. 2018. (2016) Data Summary of Wet Nitrogen Deposition at Rocky Mountain National Park. Natural Resource Report NPS/NRSS/ARD/NRR No. 2018/1610. National Park Service, Fort Collins, CO.

Moser, K.A., J.S. Baron, J. Brahney, I.A. Oleksy, J.E. Saros, E.J. Hundey, S.A. Sadro, et al. (2019). Mountain Lakes: Eyes on Global Environmental Change. *Global and Planetary Change* 178: 77–95.

Moss, B., McKee, D., Atkinson, D., Collings, S., Eaton, J., Gill, A., Harvey, I., Hatton, K., Heyes, T., Wilson, D. (2003). How important is climate? Effects of warming, nutrient addition and fish on phytoplankton in shallow lake microcosms. *Journal of applied Ecology* 40, 782–792.

Mote, P. W., Hamlet, A. F., Clark, M. P., & Lettenmaier, D. P. (2005). Declining mountain snowpack in western North America. *Bulletin of the American Meteorological Society*, 1, 39–49.

Mueller, Derek R., Patrick Van Hove, Dermot Antoniades, Martin O. Jeffries, and Warwick F. Vincent. (2009). High Arctic lakes as sentinel ecosystems: Cascading regime shifts in climate, ice cover, and mixing. *Limnology and Oceanography* 54 (6): 2371–85.

Müller-Navarra, D.C., Brett, M.T., Liston, A.M., Goldman, C.R. (2000). A highly unsaturated fatty acid predicts carbon transfer between primary producers and consumers. *Nature* 403, 74–77.

Muylaert, K., Sabbe, K., & Vyverman, W. (2009). Changes in phytoplankton diversity and community composition along the salinity gradient of the Schelde estuary (Belgium/The Netherlands). *Estuarine, Coastal and Shelf Science 82(2), 335-340.*

Naranjo, R.C., Niswonger, R.G., Smith, D., Rosenberry, D., Chandra, S. (2019). Linkages between Hydrology and Seasonal Variations of Nutrients and Periphyton in a Large Oligotrophic Subalpine Lake. *Journal of Hydrology* 568 (November 2018): 877–890.

National Climate Assessment (2018). Fourth National Climate Assessment. https://nca2018.globalchange.gov/

Neff, J. C., Ballantyne, A. P., Farmer, G. L., Mahowald, N. M., Conroy, J. L., Landry, C. C., Reynolds, R. L. (2008). Increasing aeolian dust deposition in the western United States linked to human activity. *Nature Geoscience,* 1(3), 189–195.

Nelson, C.E., Bennett, D.M., Cardinale, B.J. (2013). Consistency and sensitivity of stream periphyton community structural and functional responses to nutrient enrichment. *Ecological Applications* 23, 159–173.

Nelson, W. G. (1988). High lake research and management in Colorado. *Colorado Division of Wildlife, Special Report* 64.

Nydick, K. R., Lafrancois, B. M., Baron, J. S. (2004). NO3 uptake in shallow, oligotrophic, mountain lakes: the influence of elevated NO3 concentrations. *Journal of North American Benthological Society*, 23(3), 397–415.

Nydick, K. R., Moraska Lafrancois, B., Baron, J. S., Johnson, B. M. (2003). Lake-specific responses to elevated atmospheric nitrogen deposition in the Colorado Rocky Mountains, U.S.A. *Hydrobiologia*, 510(1–3), 103–114.

Nydick, K.R., Lafrancois, B.M., Baron, J.S., Johnson, B.M. (2004). Nitrogen regulation of algal biomass, productivity, and composition in shallow mountain lakes, Snowy

Range, Wyoming, USA. *Canadian Journal of Fisheries and Aquatic Sciences* 61, 1256–1268. https://doi.org/10.1139/f04-085

O'Dell, J. W. (1993). Method 365.1, Revision 2.0: Determination of Phosphorus by Semi-Automated Colorimetry. In U.S. Environmental Protection Agency, Washington, DC.

O'Reilly, C. M., Sharma, S., Derek K. Gray, Hampton, S. E., Read, J. S., Rowley, R. J., Zhang, G. (2015). Rapid and highly variable warming of lake surface waters around the globe. *Geophysical Research Letters*, 42(10), 1–9.

Oleksy, I., Baron, J., Leavitt, P., Spaulding, S., in review. Multiple stressors interact to force mountain lakes into unprecedented ecological state. *Ecosystems*.

Oliver, S. K., Collins, S. M., Soranno, P. A., Wagner, T., Stanley, E. H., Jones, J. R., … Lottig, N. R. (2017). Unexpected stasis in a changing world: Lake nutrient and chlorophyll trends since 1990. *Global Change Biology*, 23(12), 5455-5467.

Ollinger, S.V., Aber, J.D., Lovett, G.M., Millham, S.E., Lathrop, R.G., Ellis, J.M.. (1993). A spatial model of atmospheric deposition for the Northeastern US. *Ecological Applications* 3 (3): 459–472.

Palazzi, Elisa, Luca Mortarini, Silvia Terzago, and Jost Von Hardenberg (2019). Elevation-dependent warming in global climate model simulations at high spatial resolution. *Climate Dynamics* 52: 2685–2702.

Park, S., Brett, M. T., Müller-Solger, A., & & Goldman, C. R. (2004). Climatic forcing and primary productivity in a subalpine lake : Interannual variability as a natural experiment. *Limnology and Oceanography,* 49(2), 614–619.

Parker, B. R., Vinebrooke, R. D., & Schindler, D. W. (2008). Recent climate extremes alter alpine lake ecosystems. *Proceedings of the National Academy of Sciences,* 105(35), 12927-12931.

Pepin, N., Bradley, R. S., Diaz, H. F., Baraer, M., Caceres, E. B., Forsythe, N., Yang, D. Q. (2015). Elevation-dependent warming in mountain regions of the world. *Nature Climate Change*, 5(5), 424–430.

Perga, M. E., Bouffard, D., Bruel, R., Rodriguez, L., & Guénand, Y. (2018). Storm impacts on alpine lakes : Antecedent weather conditions matter more than the event intensity*. Global Change Biology*, 24, 5004–5016.

Périllon, C., Pöschke, F., Lewandowski, J., Hupfer, M., Hilt, S. (2017). Stimulation of epiphyton growth by lacustrine groundwater discharge to an oligo-mesotrophic hardwater lake. *Freshwater Science* 36(3), 555-570.

Petchey, O.L., Belgrano, A., Petchey, O.L., Belgrano, A. (2010). Body-size distributions and size-spectra: universal indicators of ecological status 434–437.

Peter, H., & Sommaruga, R. (2017). Alpine glacier-fed turbid lakes are discontinuous cold polymictic rather than dimictic. *Inland Waters,* 7(1), 45–54.

Pite, D. P., Lane, K. A., Hermann, A. K., Spaulding, S. A., Finney, B. P. (2009). Historical abundance and morphology of Didymosphenia species in Naknek Lake, Alaska. *Acta Botanica Croatica,* 68(2), 183–197.

Pittman, S. J., Costa, B. M., & Battista, T. A. (2009). Using lidar bathymetry and boosted regression trees to predict the diversity and abundance of fish and corals. *Journal of Coastal Research,* 27–38.

Post, D. M., Pace, M. L., & Hairston, N. G. (2000). Ecosystem size determines food-chain length in lakes. *Nature* 405(6790), 1047.

Prasad, A. M., Iverson, L. R., & Liaw, A. (2006). Newer classification and regression tree techniques: bagging and random forests for ecological prediction. *Ecosystems*, 9(2), 181–199.

Preston, D. L., Caine, N., McKnight, D. M., Williams, M. W., Hell, K., Miller, M. P., Johnson, P. T. J. (2016). Climate regulates alpine lake ice cover phenology and aquatic ecosystem structure. *Geophysical Research Letters*, 43(10), 5353–5360.

Price, J. R., Moore, J., Kerans, D. (2017). Monazite chemical weathering, rare earth element behavior, and paleoglaciohydrology since the last glacial maximum for the Loch Vale watershed, Colorado, USA. *Quaternary Research*, 1–17.

PRISM Climate Group. (2018). Oregon State University. Retrieved from http://prism.oregonstate.edu

Program, N. A. D. (2018). National Atmospheric Deposition Program (NRSP-3) (NADP Progr).

R Core Team (2018). R: A language and environment for statistical computing. R Foundation for Statistical Computing, Vienna, Austria. URL https://www.R-project.org/.

Raven, J. A., Geider, R. J. (1988). Temperature and algal growth. *New Phytologist*, 110(4), 441–461.

Redfield, A. C. (1958). The biological control of chemical factors in the environment. *American Scientist,* 46(3), 230-221.

Reisinger, A.J., Tank, J.L., Dee, M.M. (2016). Regional and seasonal variation in nutrient limitation of river biofilms. *Freshwater Science* 35(2), 474-489.

Reyes, F. R., Lougheed, V. L. (2015). Rapid Nutrient Release from Permafrost Thaw in Arctic Aquatic Ecosystems. *Arctic, Antarctic, and Alpine Research,* 47(1), 35–48.

Ridgeway, G. (2006). Generalized Boosted Models: A guide to the gbm package.

Roberts, J. J., Fausch, K. D., Schmidt, T. S., Walters, D. M. (2017). Thermal regimes of Rocky Mountain lakes warm with climate change. *PLoS ONE*, 12(7), 1–17.

Rose, K. C., Greb, S. R., Diebel, M., & Turner, M. G. (2016). Annual precipitation regulates spatial and temporal drivers of lake water clarity. *Ecological Applications*, 27(2), 632–643.

Rose, K. C., Winslow, L. A., Read, J. S., & Hansen, G. J. A. (2016). Climate-induced warming of lakes can be either amplified or suppressed by trends in water clarity. *Limnology and Oceanography Letters*, 1(1), 44–53.

Rosenberger, E.E., Hampton, S.E., Fradkin, S.C., Kennedy, B.P. (2008). Effects of shoreline development on the nearshore environment in large deep oligotrophic lakes. *Freshwater Biology* 53, 1673–1691.

Rosenlund, B., Stevens, D. (1990). Fisheries and aquatic management: Rocky Mountain National Park 1988–1989. Colorado Fish and Wildlife Assistance Office, US Fish and Wildlife Service, 730 Simms, Suite 292, Golden, Colorado 80401 USA.

Ruhland, K., Paterson, A. M., & Smol, J. P. (2008). Hemispheric-scale patterns of climate-related shifts in planktonic diatoms from North American and European lakes. *Global Change Biology,* 14(11), 2740–2754.

Rusak, J. A., Tanentzap, A. J., Klug, J. L., Rose, K. C., Hendricks, S. P., Jennings, E., Zhu, G. (2018). Wind and trophic status explain within and among-lake variability of algal biomass. *Limnology and Oceanography Letters*, 3(6), 409-418.

Sadro, S., & Melack, J. M. (2012). The effect of an extreme rain event on the biogeochemistry and ecosystem metabolism of an the effect of an extreme rain event on the biogeochemistry and ecosystem metabolism of an oligotrophic high-elevation lake. *Arctic, Antarctic, and Alpine Research*, 44(2), 222–231.

Sadro, S., Melack, J. M., Sickman, J. O., & Skeen, K. (2018). Climate warming response of mountain lakes affected by variations in snow. *Limnology and Oceanography Letters*, 4(1), 9-17.

Sadro, S., Melack, J.M., MacIntyre, S. (2011). Spatial and temporal variability in the ecosystem metabolism of a high-elevation lake: integrating benthic and pelagic habitats. *Ecosystems* 14, 1123–1140.

Sadro, S., Nelson, C. E., & Melack, J. M. (2012). The inluence of landscape position and catchment characteristics on aquatic biogeochemistry in high-elevation lake-chains. *Ecosystems*, 15(3), 363–386.

Sadro, S., Sickman, J. O., Melack, J. M., & Skeen, K. (2018). Effects of climate variability on snowmelt and implications for organic matter in a high-elevation lake. *Water Resources Research*, 54(7), 4563-4578.

Saros, J. E., Clow, D. W., Blett, T., Wolfe, A. P. (2011). Critical nitrogen deposition loads in high-elevation lakes of the western U.S. inferred from paleolimnological records. *Water, Air, & Soil Pollution*, 216(1–4), 193–202.

Saros, J. E., Interlandi, S. J., Doyle, S., Michel, T. J., & Williamson, C. E. (2005). Are the deep chlorophyll maxima in alpine lakes primarily induced by nutrient availability, not UV avoidance*? Arctic, Antarctic, and Alpine Research*, 37(4), 557-563.

Saros, J. E., Interlandi, S. J., Wolfe, A. P., Daniel, R., & Engstrom, D. R. (2003). Recent Changes in the Diatom Community Structure of Lakes in the Beartooth Mountain Range, U.S.A. *Arctic, Antarctic, and Alpine Research,* 35(1), 18–23.

Saros, J. E., Michel, T. J., Interlandi, S. J., Wolfe, A. P. (2005). Resource requirements of *Asterionella formosa* and *Fragilaria crotonensis* in oligotrophic alpine lakes: implications for recent phytoplankton community reorganizations. *Canadian Journal of Fisheries and Aquatic Sciences*, 62(7), 1681–1689.

Saros, J. E., Rose, K. C., Clow, D. W., Stephens, V. C., Nurse, A. B., Arnett, H. A., … Wolfe, A. P. (2010). Melting alpine glaciers enrich high-elevation lakes with reactive nitrogen. *Environmental Science and Technology,* 44, 4891–4896.

Savage, C., Elmgren, R. (2004). Macroalgal (*Fucus vesiculosus*) $\delta^{15}N$ values trace decrease in sewage influence. *Ecological Applications*, 14(2), 517-526.

Scheffer, M., Carpenter, S., Foley, J. A., Folke, C., Walker, B. (2001). Catastrophic shifts in ecosystems. *Nature*, 413(6856), 591-596.

Schindler, D. E., Kitchell, J. F., He, X., Carpenter, S. R., Hodgson, J. R., Cottingham, K. L. (1993). Food Web Structure and Phosphorus Cycling in Lakes. *Transactions of the American Fisheries Society,* 122(5), 756–772.

Schindler, D. W., Bayley, S. E., Parker, B. R., Beaty, K. G., Cruikshank, D. R., Fee, E. J., Stainton, M. P. (1996). The effects of climatic warming on the properties of boreal lakes and streams at the Experimental Lakes Area, northwestern Ontario. *Limnology and Oceanography* (5), 1004–1017.

Schindler, D. W., Beaty, K. G., Fee, E. J., Cruikshank, D. R., DeBruyn, E. R., Findlay, D. L., Turner, M. A. (1990). Effects of climatic warming on lakes of the central boreal forest. *Science*, 250(4983), 967–970.

Schmeller, D. S., Loyau, A., Bao, K., Brack, W., Chatzinotas, A., Vleeschouwer, F. De, Vredenburg, V. T. (2018). People, pollution and pathogens – Global change impacts in mountain freshwater ecosystems. *Science of The Total Environment*, 623, 756–763.

Schmeller, Dirk S, Adeline Loyau, Kunshan Bao, Werner Brack, Antonis Chatzinotas, Francois De Vleeschouwer, Jan Friesen, et al. (2018). People, Pollution and Pathogens – Global Change Impacts in Mountain Freshwater Ecosystems. *Science of The Total Environment* 623: 756–763.

Schneider, S.C., Cara, M., Eriksen, T.E., Budzakoska Goreska, B., Imeri, A., Kupe, L., Lokoska, T., Patceva, S., Trajanovska, S., Trajanovski, S., Talevska, M., Veljanoska Sarafiloska, E. (2014). Eutrophication impacts littoral biota in Lake Ohrid while water phosphorus concentrations are low. *Limnologica* 44, 90–97.

Sharma, Sapna, Kevin Blagrave, John J. Magnuson, Catherine M O Reilly, Samantha Oliver, Ryan D. Batt, Madeline R. Magee, et al. (2019). Widespread Loss of Lake Ice around the Northern Hemisphere in a Warming World. *Nature Climate Change* 9: 227–231.

Simpson, G. L. (2018). Modelling palaeoecological time series using generalised additive models. *Frontiers in Ecology and Evolution*, 10, 1–21.

Simpson, G., Anderson, N. (2009). Deciphering the effect of climate change and separating the influence of confounding factors in sediment core records using additive models. *Limnology and Oceanography*, 54(6part2), 2529-2541.

Slemmons, K. E. H., Rodgers, M. L., Stone, J. R., Saros, J. E. (2017). Nitrogen subsidies in glacial meltwaters have altered planktonic diatom communities in lakes of the US Rocky Mountains for at least a century. *Hydrobiologia*, 800(1), 129–144.

Slemmons, K. E. H., Saros, J. E., & Simon, K. (2013). The influence of glacial meltwater on alpine aquatic ecosystems: a review. *Environmental Science. Processes & Impacts*, 15(10), 1794–806.

Smol, John P., Alexander P. Wolfe, H. John B. Birks, Marianne S.V. Douglas, Vivienne J Jones, Atte Korhola, Sanna Sorvari, et al. (2005). Climate-driven regime shifts in the biological communities of Arctic lakes. *Proceedings of the National Academy of Sciences* 102 (12): 4397–4402.

Smol, John P., and Brian F. Cumming. (2000). Tracking Long-Term Changes in Climate Using Algal Indicators in Lake Sediments. *Journal of Phycology* 36: 986–1011.

Sommaruga-Wograth, S., Koinig, K. A., Schmidt, R., Sommaruga, R., Tessadri, R., & Psenner, R. (1997). Temperature effects on the acidity of remote alpine lakes. *Nature*, 387(May), 64–67.

Sommaruga, R., & Psenner, R. (1997). Ultraviolet radiation in a high mountain lake of the Austrian Alps: air and underwater measurements. Photochemistry and *Photobiology*, 65(6), 957-963.

Soranno, P. A., Cheruvelil, K. S., Wagner, T., Webster, K. E., & Bremigan, M. T. (2015). Effects of land use on lake nutrients: the importance of scale, hydrologic connectivity, and region. *PloS One,* 10(8), e0135454.

Soranno, P. A., Cheruvelil, K. S., Webster, K. E., Bremigan, M. T., Wagner, T., & Stow, C. A. (2010). Using landscape limnology to classify freshwater ecosystems for multi-ecosystem management and conservation. *BioScience*, 60(6), 440–454.

Soranno, P. A., Webster, K. E., Riera, J. L., Kratz, T. K., Baron, J. S., Bukaveckas, P. A., Leavitt, P. R. (1999). Spatial variation among lakes within landscapes: ecological organization along lake chains. *Ecosystems*, 2, 395–410.

Soranno, P. A., Cheruvelil, K. S., Bissell, E. G., Bremigan, M. T., Downing, J. A., Fergus, C. E., Stow, C. A. (2014). Cross-scale interactions: quantifying multi-scaled cause–effect relationships in macrosystems. *Frontiers in Ecology and the Environment,* 12(1), 65-73.

Spaulding, S. A. (2018). Diatoms of North America. Retrieved from https://diatoms.org/

Spaulding, S. A., Harris, M. A., McKnight, D. M., Rosenlund, B. D. (1992). Aquatic Biota. Baron, J.S. editor. Biogeochemistry of a Subalpine Ecosystem: Loch Vale Watershed. Springer Science & Business Media. p187–217.

Spaulding, S. A., Otu, M. K., Wolfe, A. P., Baron, J. S. (2015). Paleolimnological records of nitrogen deposition in shallow, high-elevation lakes of Grand Teton National Park, Wyoming, U.S.A. *Arctic, Antarctic, and Alpine Research*, 47(4), 703–717.

Steffen, W., Broadgate, W., Deutsch, L., Gaffney, O., Ludwig, C. (2015). The trajectory of the anthropocene: The great acceleration. *Anthropocene Review,* 2(1), 81–98.

Steffen, W., Crutzen, P. J., McNeill, J. R. (2007). The Anthropocene: Are Humans Now Overwhelming the Great Forces of Nature. *AMBIO: A Journal of the Human Environment*, 36(8), 614–621.

Steffen, W., Richardson, K., Rockström, J., Cornell, S.E., Fetzer, I., Bennett, E.M., Biggs, R., Carpenter, S.R., De Vries, W., De Wit, C.A. (2015). Planetary boundaries: Guiding human development on a changing planet. *Science* 347, 1259855.

Steinman, A.D., Lamberti, G.A., Leavitt, P.R., Uzarski, D.G. (2017). Biomass and pigments of benthic algae, in: Methods in Stream Ecology, Volume 1. Elsevier, pp. 223–241.

Stewart, I. T. (2009). Changes in snowpack and snowmelt runoff for key mountain regions. *Hydrological Processes: An International Journal,* 23(1), 78–94.

Stoddard, J.L., Van Sickle, J., Herlihy, A.T., Brahney, J., Paulsen, S., Peck, D.V., Mitchell, R. and Pollard, A.I. (2016). Continental-scale increase in lake and stream phosphorus: Are oligotrophic systems disappearing in the United States? *Environmental Science & Technology*, 50(7), 3409-3415.

Strobl, C., Malley, J., & Tutz, G. (2009). An introduction to recursive partitioning: rationale, application, and characteristics of classification and regression trees, bagging, and random forests*. Psychological Methods*, 14(4), 323.

Survey, U. S. G. (2016). The StreamStats program. Retrieved December 19, 2017, from http://streamstats.usgs.gov

Tank, J.L., Reisinger, A.J., Rosi, E.J. (2017). Nutrient limitation and uptake, in: Methods in Stream Ecology. Elsevier, pp. 147–171.

Taranu, Z.E., Gregory-Eaves, I., Leavitt, P.R., Bunting, L., Buchaca, T., Catalan, J., Domaizon, I., Guilizzoni, P., Lami, A., McGowan, S. and Moorhouse, H. (2015). Acceleration of cyanobacterial dominance in north temperate-subarctic lakes during the Anthropocene. *Ecology Letters*, 18(4), 375-384.

Team, R. C. (2018). R: A Language and Environment for Statistical Computing, R Foundation for Statistical Computing. ISBN 3-900051-07-0: URL http://www. R-project. org.

Thomas, M.K., Aranguren-Gassis, M., Kremer, C.T., Gould, M.R., Anderson, K., Klausmeier, C.A., Litchman, E. (2017). Temperature–nutrient interactions exacerbate sensitivity to warming in phytoplankton. *Global Change Biology* 23, 3269–3280.

Thompson, P. L., St. Jacques, M.-C., Vinebrooke, R. D. (2008). Impacts of climate warming and nitrogen deposition on alpine plankton in lake and pond habitats: an in vitro experiment. *Arctic, Antarctic, and Alpine Research*, 40(1), 192–198.

Thompson, R., Kamenik, C., & Schmidt, R. (2005). Ultra-sensitive Alpine lakes and climate change. *Journal of Limnology*, 64(2), 139–152. http://doi.org/10.4081/jlimnol.2005.139

Thompson, Roy, Christian Kamenik, Roland Schmidt. (2005). Ultra-Sensitive Alpine Lakes and Climate Change. *Journal of Limnology* 64 (2): 139–152.

Thrane, J.E., Hessen, D.O., Andersen, T. (2017). Plasticity in algal stoichiometry: Experimental evidence of a temperature-induced shift in optimal supply N:P ratio. *Limnology and Oceanography* 62, 1346–1354.

Tranvik, Lars J., John A. Downing, James B. Cotner, Steven A. Loiselle, Robert G Striegl, Thomas J. Ballatore, Peter Dillon (2009). Lakes and Reservoirs as Regulators of Carbon Cycling and Climate. *Limnology and Oceanography* 54 (1): 2298–2314.

Trochine, C., Guerrieri, M., Liboriussen, L., Meerhoff, M., Lauridsen, T. L., Søndergaard, M., Jeppesen, E. (2011). Filamentous green algae inhibit phytoplankton with enhanced effects when lakes get warmer. *Freshwater Biology*, 56(3), 541–553.

Turner, M.A., Townsend, B.E., Robinson, G.G.C., Hann, B.J., Amaral, J.A. (1995). Ecological effects of blooms of filamentous green algae in the littoral zone of an acid lake. *Canadian Journal of Fisheries and Aquatic Sciences* 52, 2264–2275.

Turner, M. A., Schindler, D. W., Findlay, D. L., Jackson, M. B., & Robinson, G. G. (1995). Disruption of littoral algal associations by experimental lake acidification. *Canadian Journal of Fisheries and Aquatic Science*s, 52(10), 2238-2250.

U.S. Geological Survey (2016). The StreamStats program. Retrieved December 19, 2017, from http://streamstats.usgs.gov

Vadeboncoeur, Y., Lodge, D. M., Carpenter, S. R. (2001). Whole-lake fertilization effects on distribution of primary production between benthic and pelagic habitats. *Ecology*, 82(4), 1065–1077.

Vadeboncoeur, Y., Peterson, G., Zanden, M. J. Vander, & Kaliff, J. (2008). Benthic algal production across lake size gradients: interactions among morphometry, nutrients, and light. *Ecology*, 89(9), 2542–2552.

Vadeboncoeur, Y., Steinman, A.D. (2002). Periphyton function in lake ecosystems. *The Scientific World Journal* 2, 1449–1468.

Vadeboncoeur, Y., Vander Zanden, M.J., Lodge, D.M. (2002). Putting the lake back together: eeintegrating benthic pathways into lake food web models. *BioScience* 52, 44.

Vale, T.R. (1998). The Myth of the Humanized Landscape: An Example from Yosemite National Park. *Natural Areas Journal*. 18: 231.

Vale, T.R. (2002). The Pre-European Landscape of the United States: Pristine or Humanized? Washington, DC: Island Press.

Vinebrooke, R.D., Turner, M.A., Kidd, K.A., Hann, B.J., Schindler, D.W. (2001). Truncated food web effects of omnivorous minnows in a recovering acidified lake. *Journal of the North American Benthological Society* 20, 629–642.

Vitousek, P. M., Mooney, H. A., Lubchenco, J., & Melillo, J. M. (1997). Human domination of Earth's ecosystems. *Science*, 277(5325), 494-499.

Vogt, R. J., Sharma, S., & Leavitt, P. R. (2017). Direct and interactive effects of climate, meteorology, river hydrology, and lake characteristics on water quality in productive lakes of the Canadian Prairies. *Canadian Journal of Fisheries and Aquatic Sciences*, 75(1), 47-59.

Wagner, T., & Schliep, E. M. (2018). Combining nutrient, productivity, and landscape-based regressions improves predictions of lake nutrients and provides insight into nutrient coupling at macroscales. *Limnology and Oceanography*, 63(6), 2372-2383.

Wagner, T., Soranno, P. A., Webster, K. E., & Cheruvelil, K. S. (2011). Landscape drivers of regional variation in the relationship between total phosphorus and chlorophyll in lakes. *Freshwater Biology,* 56(9), 1811-1824.

Waite, I. R., & Van Metre, P. C. (2017). Multistressor predictive models of invertebrate condition in the Corn Belt, USA. *Freshwater Science*, 36(4), 901-914.

Webster, K. E., Kratz, T. K., Bowser, C. J., Magnuson, J. J., & Rose, W. J. (1996). The influence of landscape position on lake chemical responses to drought in northern Wisconsin. *Limnology and Oceanography,* 41(5), 977–984.

Webster, K. E., Soranno, P. A., Baines, S. B., & Kratz, T. K. (2000). Structuring features of lake districts: landscape controls on lake chemical responses to drought. *Freshwater Biology,* 43, 499–515.

Wehrens, R., Bloemberg, T. G., Eilers, P. H. C. (2015). Fast parametric warping of peak lists. *Bioinformatics*, 31(18), 3063-3065.

Wetzel, R.G. (1996). Benthic algae and nutrient cycling in lentic freshwater ecosystems, in: Algal Ecology. Elsevier, pp. 641–667.

Williams, M. W., Knauf, M., Cory, R., Caine, N., & Liu, F. (2007). Nitrate content and potential microbial signature of rock glacier outflow, Colorado Front Range*. Earth Surface Processes and Landforms.* http://doi.org/10.1002/esp.1455

Williams, M.W., Baron, J.S. (1996). Nitrogen saturation in the Rocky Mountains. *Environmental Science & Technology* 30 (2): 640–46.

Winder, M., Reuter, J.E., Schladow, S.G. (2009). Lake warming favors small-sized planktonic diatom species*. Proceedings. Biological sciences / The Royal Society* 276, 427–35. https://doi.org/10.1098/rspb.2008.1200

Wohl, E., Lininger, K. B., & Baron, J. (2017). Land before water: The relative temporal sequence of human alteration of freshwater ecosystems in the conterminous United States. *Anthropocene*, 18, 27-46.

Wolfe, A. P., Baron, J. S., Cornett, R. J. (2001). Anthropogenic nitrogen deposition induces rapid ecological changes in alpine lakes of the Colorado Front Range (USA). *Journal of Paleolimnology*, 3, 1–7.

Wolfe, A. P., Hobbs, W. O., Birks, H. H., Briner, J. P., Holmgren, U., Ingólfsson, Ó., Vinebrooke, R. D. (2013). Stratigraphic expressions of the Holocene – Anthropocene transition revealed in sediments from remote lakes. *Earth-Science Reviews*, 116, 17–34.

Wolfe, A.P., Van Gorp, A.C., Baron, J.S. (2003). Recent ecological and biogeochemical changes in alpine lakes of Rocky Mountain National Park (Colorado, USA): a response to anthropogenic nitrogen deposition. *Geobiology*, 1, 153–168.

Wood, S.N. (2004). Stable and efficient multiple smoothing parameter estimation for generalized additive models. *Journal of the American Statistical Association*, 99(467), 673–686.

Wood, S.N. (2017). Generalized Additive Models, 2nd edition. New York: Chapman and Hall/CRC.

Wurtsbaugh, W.A., Gross, H.P., Budy, P., Luecke, C. (2001). Effects of epilimnetic versus metalimnetic fertilization on the phytoplankton and periphyton of a mountain lake with a deep chlorophyll maxima. *Canadian Journal of Fisheries and Aquatic Sciences* 58, 2156–2166.

Wyatt, K.H., Tellez, E., Woodke, R.L., Bidner, R.J., Ian, R., Davison, I.R. (2014). Effects of nutrient limitation on the release and use of dissolved organic carbon from benthic algae in Lake Michigan. *Freshwater Science* 33, 557–567.

Yvon-Durocher, G., Jones, J.I., Trimmer, M., Woodward, G., Montoya, J.M. (2010). Warming alters the metabolic balance of ecosystems. *Philosophical transactions of the Royal Society of London. Series B, Biological Sciences* 365, 2117–2126.

Zaharescu, Dragos G., Carmen I. Burghelea, Peter S. Hooda, Richard N. Lester, and Antonio Palanca-Soler (2016). Small lakes in big landscape: multi-scale drivers of littoral ecosystem in alpine lakes. *Science of the Total Environment* 551, 496-505.

Appendix A: Supplementary information for Chapter 2

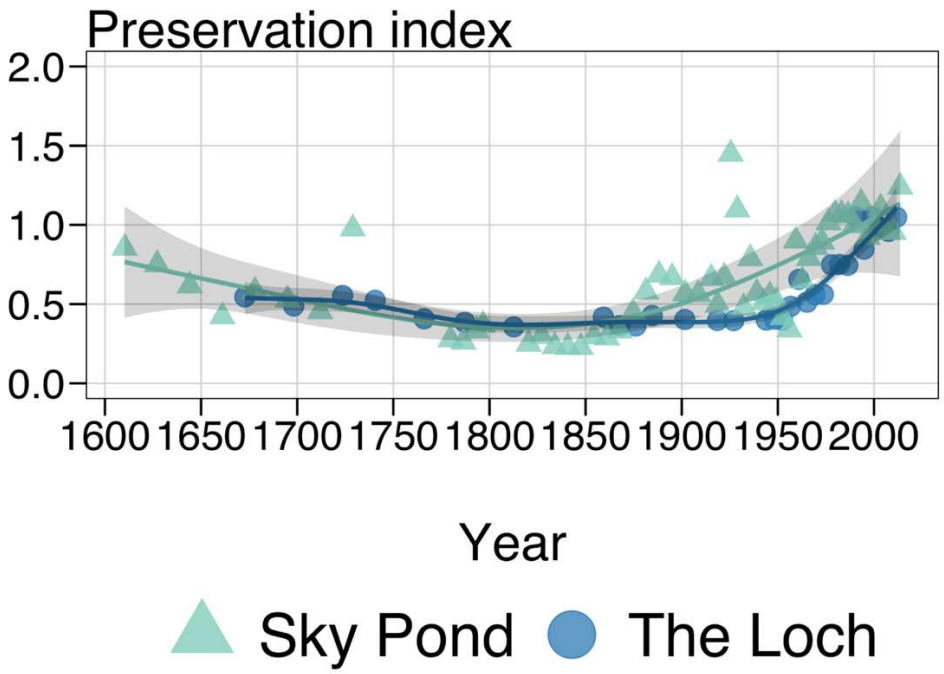

A1. Change in preservation. Preservation index, or the ratio of labile chlorophyll *a* to stable pheophytin *a*, was used as a proxy of changes in the preservation down-core. Both compounds were present at high concentrations throughout the period of interest (ca. 1800 CE to present). The pigment preservation index was stable until ca. 1970 suggesting no marked change until surface deposits and is consistent with the relatively stable concentrations of β-carotene in recently deposited sediments. There was no significant rate of change detected for the preservation index in Sky Pond sediments (see A2, below).

A2. GAMS significant rate of change. We calculated the first derivative of the fitted trend using the method of finite differences to assess the timing of significant rate of change in our response variables (Ladyzhenskaya, 1985). Here we accounted for uncertainty around the estimate with the simultaneous confidence interval on the derivative, calculated using simulation from the posterior distribution of the model coefficients (Simpson, 2018). The onset of a period of significant change was identified as the time point when the confidence intervals on the first derivative did not include zero. Since aging The Loch sediments was problematic (see Methods section "core collection and chronology"), we did not assess rates of change in pigments and geochemical proxies in The Loch sediments.

	Sky Pond
proxy	**approximate year range**
% C	N.S.
% N	N.S.
$\delta^{13}C$	ca. 1946-2001
C:N	N.S.
pheophytin *a*	ca. 1942-2001
pheophytin *b*	ca. 1932-1962
β-carotene	N.S.
lutein-zeaxanthin	ca. 1924-1956
echinenone	N.S.
alloxanthin	N.S.
canthaxanthin	ca. 1940-1975
diatoxanthin	ca. 1860-1877
preservation index	N.S.

Appendix B: Supplementary information for Chapter 4

B1. We calculated and extracted several watershed predictors that we hypothesized might play a role in explaining lake-to-lake variation in chlorophyll *a.* Most of these variables did not make it into the final regional, Loch Vale, or Green Lake Valley models, but are reported below. Land cover and recent land cover change for each watershed polygon were estimated using National Land Cover Database (NLCD) data 30 m resolution rasters (Homer et al., 2015). Land cover change from 1992 to 2011 was calculated for forest, wetland, water, and perennial snow and ice by extracting and comparing percent coverage for each year using ArcMap 10.5 Spatial Analyst tools. Additional surficial geology data were extracted from the USGS Geologic Map of North America (Garrity & Soller, 2009). Watershed specific information on rock glacier coverage from the Portland State University Rock Glacier Inventory was added to the land cover database (Johnson, 2018). Slope, aspect, and solar radiation for each watershed were calculated from the USGS National Elevation Dataset ⅓ arc-second (≈ 10 m) resolution raster and extracted using ArcMap 10.5 Spatial Analyst tools (ESRI, 2018; Nussear et al., 2009). Eastness is derived from degree aspect using the equation: eastness = sin((degree aspect * π)/180); northness is derived from degree aspect using the equation: northness = cos((degree aspect * π)/180). Solar radiation was calculated in watt hours per square meter (WH m^{-2}) at a daily time step, then aggregated to monthly, using unique centroid latitudes for each watershed. A generally clear sky with a transmissivity of 0.5 and diffuse proportion of 0.3 was assumed, with 32 unique horizon calculations considered each hour. Each watershed polygon was buffered by 50 m to include the influences of all immediately surrounding topography in the high and rugged alpine terrain of the study area.

Garrity, C. P., & Soller, D. R. (2009). Database of the Geologic Map of North America- Adapted from the Map by JC Reed, Jr. et. al., (2005). *U.S. Geologic Survey*. Retrieved from https://pubs.usgs.gov/ds/424/

Homer, C. G., Dewitz, J. A., Yang, L., Jin, S., Danielson, P., Xian, G., Megown, K. (2015). Completion of the 2011 National Land Cover Database for the conterminous United States-Representing a decade of land cover change information. *Photogrammetric Engineering and Remote Sensing*. http://doi.org/10.14358/PERS.81.5.345

Johnson, G. F. (2018). *Rock Glaciers of the Contiguous United States: Spatial Distribution, Cryospheric Context, and Riparian Vegetation*.

Nussear, K. E., Esque, T. C., Inman, R. D., Gass, L., Thomas, K. A., Wallace, C. S. A.,

Webb, R. H. (2009). Modeling Habitat of the Desert Tortoise (Gopherus agassizii) in the Mojave and Parts of the Sonoran Deserts of California, Nevada, Utah, and Arizona. Open-File Report. Retrieved from http://pubs.er.usgs.gov/publication/ofr20091102

Full dataset summary statistics

Watershed variables	Description [units]	min.	max.	mean	med.	std. dev.
Barren (2011)	Barren land cover [%]	0.0%	96%	45%	41%	21%
Forest (2011)	Forest land cover [%]	0%	92%	8%	1%	15%
Shrub (2011)	Shrub land cover [%]	0%	50%	14%	11%	12%
Snow (2011)	Perennial snow and ice land cover [%]	0%	77%	31%	32%	18%
Wetland (2011)	Wetland land cover [%]	0.0%	1.2%	0.2%	0.0%	0.3%
Change shrub ('92-'11)	Change in shrub land cover 1999 to 2011 [%]	-1.9%	1.7%	0.2%	0.0%	0.5%
Change forest ('92-'11)	Change in forest land cover from 1992 to 2011 [%]	0.0%	0.2%	0.0%	0.0%	0.1%
Change snow ('92-'11)	Change in perennial snow & ice land cover 1992 to 2011 [%]	-3.5%	0.0%	-1.1%	-0.9%	0.9%
Change water ('92-'11)	Change in water land cover 1992 to 2011 [%]	-0.1%	1.9%	0.1%	0.0%	0.3%
Change wetland ('92-'11)	Change in wetland land cover 1992 to 2011 [%]	0.0%	0.0%	0.0%	0.0%	0.0%
Biotite-gneiss	Biotite-gneiss underlying geology [%]	0%	100%	51%	56%	36%
Granite	Granite underlying geology [%]	0%	100%	32%	17%	34%
East mean	East-ness of watershed [sin(aspect)]	-0.078	0.138	0.023	0.015	0.038
North mean	North-ness of watershed [cos(aspect)]	-0.049	0.118	0.012	0.012	0.0
Elevation	Elevation at lake outflow [m]	2987	3550	3310	3322	161
Elevation range	Elevation range of watershed [m]	116.0	1317.1	614.7	620.7	228.2
WS area	Watershed area [km^2]	0.2	13.1	3.1	2.2	3.1
Lake SA	Lake surface area [m^2]	3209	163,801	54,691	41,311	39,661
Drainage ratio	Lake area as a percentage of watershed area [%]	0.5%	10.2%	3.1%	2.1%	2.7%
Summer radiation	Total monthly solar radiation [W m^{-2}]	171,494	227,293	202,013	207,416	15,035
Rock glacier area	Rock glacier area [km^2]	0.00	0.56	0.07	0.03	0.09
Rock glacier %	Percent of catchment occupied by rock glaciers [%]	0.0%	19.0%	2.9%	1.5%	3.8%
Longitude	Longitude [decimal degrees]	-105.7	-105.59	-	-	-

B2. Summary of all predictor variables used to model chl *a* in the Loch Vale and Green Lakes Valley datasets. Means and standard deviation for watershed variables are not presented because model only included two lakes.

		Loch Vale dataset				Green Lakes Valley Dataset			
Variable	**Description [units]**	**min**	**max**	**mean**	**sd**	**min**	**max**	**mean**	**sd**
Response									
Chl *a*	Chlorophyll a [µg L^{-1}]	0.3	11.3	3.7	3.1	0.01	19.9	5.0	5.0
Indexing Variables									
DOY	Ordinal date	152	232	204.3	26.9	189	238	213.6	13.1
Measurement depth	Surface (0) or hypolimnion (1) measurement	0	1	-	-	0	1	-	-
Year	Year	2015	2017	-	-	2009	2016	-	-
Climate Variables (Climate)									
Daily precip.	Precipitation on sample date [mm]	0.0	4.9	0.5	1.1	0	16.1	2.3	4.2
Weekly precip.	Cumulative precipitation for the week preceding sample date [mm]	0	17.0	6.4	5.3	0	57.2	16.3	15.5
Monthly precip.	Cumulative precipitation for the 30 days preceding sample date [mm]	8.8	114.9	42.9	35.5	-	-	-	-
Precip. % normal	Monthly precipitation as a percent of normal [%]	24%	184%	76%	40%	30%	148%	97%	38%
Daily mean temp.	Mean air temperature sample date [ºC]	5.6	14.2	11.0	2.7	3.7	13.2	9.7	2.3
Weekly mean temp.	Mean air temperature for the week preceding sample date [ºC]	3.7	14.5	11.2	3.2	-	-	-	-
Monthly mean temp.	Mean air temperature for the 30 days preceding sample date [ºC]	2.4	13.1	10.5	3.5	8.1	11.8	9.8	0.8
Mean temp. % normal	Monthly average air temperature as a percent of normal [%]	86%	150%	118%	20%	92%	152%	107%	12%
SWE % normal	Snow water equivalent (SWE) as a percentage of normal maximum SWE [%]	95%	125%	103%	13%	93%	155%	119%	20%
Max. SWE	Maximum observed snow-water-equivalent for the preceding winter [in]	17.7	18.0	17.9	0.1	19.6	28.4	23.2	3.3
Difference snow free date	Difference between normal and actual snow free date [days]	-2	-1	-1.4	0.5	-6	6	-1.3	4.8

Environmental Variables (Envt)									
DOC	Dissolved organic carbon [mg L^{-1}]	0.3	2.8	0.9	0.9	0.4	2.5	0.9	0.4
FISH	Fish absence (0) or presence (1)	1	1			0	1		
Max. lake depth	Maximum lake depth [m]	5	7.2	5.8	1.1	7	13.1	10.6	3.0
NO3	Nitrate-N [mg L^{-1} N]	0.08	0.35	0.2	0.1	0.0	0.2	0.1	0.1
DIN:TDP	Total dissolved N to total dissolved P molar ratio	44.2	686.4	228.8	160	53.6	1685.1	328.2	345
DIN:TP	Total dissolved N to total P molar ratio	22.3	125.7	57.7	27.2	-	-	-	-
TDN	Total dissolved N [mg L^{-1}]	0.1	0.5	0.2	0.1	0.0	0.4	0.2	0.1
TDP	Total dissolved phosphorus [µg L^{-1}]	0.64	14.4	5.1	3.8	0.3	4.8	1.9	1.1
TP	Total phosphorus [µg L^{-1}]	6	21	10.4	2.6				
Lake temp.	Water temperature of sample [ºC]	3.2	13.9	9.1	2.7	5.8	13.3	10.0	1.6
Watershed Variables (WS)									
Barren cover (2011)	Barren land cover [%]	70%	81%	-	-	31.7%	60.4%	-	-
Forest cover (2011)	Forest land cover [%]	0%	8%	-	-	0.0%	0.0%	-	-
Shrub cover (2011)	Shrub land cover [%]	1.4%	6.4%	-	-	7%	50%	-	-
Snow cover (2011)	Perennial snow and ice land cover [%]	14%	15%	-	-	12%	32%	-	-
Wetland cover (2011)	Wetland land cover [%]	0.0%	0.2%	-	-	0.0%	0.3%	-	-
Change shrub (’92-’11)	Change in forest land cover from 1992 to 2011 [%]	0.0%	0.2%	-	-	0%	0%	-	-
Change forest (’92-’11)	Change in shrub land cover 1999 to 2011 [%]	-0.07%	0.00%	-	-	0.0%	0.2%	-	-
Change snow (’92-’11)	Change in perennial snow & ice land cover 1992 to 2011 [%]	-0.9%	-0.6%	-	-	-2.5%	-1.8%	-	-
Change water (’92-’11)	Change in water land cover 1992 to 2011 [%]	0	0	-	-	0.00%	0.16%	-	-
Change wetland (’92-’11)	Change in wetland land cover 1992 to 2011 [%]	0.0%	0.0%	-	-	0%	0%	-	-
Biotite-gneiss	Biotite-gneiss underlying geology [%]	85%	93%	-	-	56%	70%	-	-
Granite	Granite underlying geology [%]	7%	15%	-	-	15%	30%	-	-

East mean	East-ness of watershed	0.016	0.024	-	-	0.008	0.073	-	-
Elevation	Elevation at lake outflow [m]	3048	3322	-	-	3425	3561	-	-
Elevation range	Elevation range of watershed [m]	696.8	902.5	-	-	280.7	520.7	-	-
WS area	Watershed area [km^2]	2.2	6.8	-	-	0.4	2.2	-	-
Lake SA	Lake surface area [m^2]	41126	52731.4	-	-	40016.7	41311.8	-	-
Drainage ratio	Lake area as a percentage of watershed area [%]	0.8%	1.9%	-	-	1.9%	9.8%	-	-
Summer radiation	Total monthly solar radiation [W m^{-2}]	171494	180812	-	-	205694	227294	-	-
Rock glacier area	Rock glacier area [km^2]	0.15	0.19	-	-	0.000	0.035	-	-
Rock glacier %	Percent of catchment occupied by rock glaciers [%]	3%	7%	-	-	0.0%	1.6%	-	-

B3. Summary of lake morphometry, watershed (WS) area, and chlorophyll *a*, conductivity, and secchi depth for lakes included in the regional dataset. Water clarity and chemical parameters are reported as the mean of n sampling trips. Missing values are indicated with a dash.

Lake Name	Longitude	Latitude	Elevation (m)	Max. Depth (m)	Lake as % WS area	Lake area (ha)	WS area (km^2)	Water temp. (ºC)	Chl *a* (µg L^{-1})	Secchi depth (m)	Cond. (µS cm^{-1})	n
Albion	40.0468	-105.6036	3345	15.0	2.4	13.1	5.4	11.6	11.7	3.9	24.2	4
Black	40.2653	-105.6413	3236	31.0	0.6	3.2	5.4	10.0	4.6	5.8	-	2
Blue	40.0889	-105.6198	3449	42.0	3.5	9.2	2.7	6.9	2.4	4.6	5.0	3
Blue 2	40.2679	-105.6316	3408	9.1	4.7	1.0	0.2	17.0	5.2	2.3	-	2
Cony	40.1729	-105.6580	3508	19.2	5.6	5.3	0.9	7.9	1.9	5.0	-	2
Diamond	39.9927	-105.6504	3340	7.0	4.0	5.8	1.4	12.1	2.4	5.3	18.0	3
Finch	40.1834	-105.5930	3021	3.2	10.3	2.4	0.2	13.7	2.8	-	-	2
Forest	39.9212	-105.6737	3307	3.0	2.1	2.2	1.0	8.3	7.9	2.7	16.0	2
Frozen	40.2577	-105.6427	3529	27.0	3.5	2.7	0.8	8.9	4.9	4.9	-	2
GL1	40.0509	-105.6056	3425	7.0	9.8	4.0	0.4	13.2	1.9	7.0	49.2	2
GL4	40.0553	-105.6203	3550	13.0	1.9	4.1	2.2	10.8	3.1	4.5	14.8	2
Haiyaha	40.3046	-105.6622	3118	9.0	1.6	4.6	2.9	11.8	10.0	-	12.4	1
Isabelle	40.0693	-105.6185	3301	8.0	2.7	12.7	4.7	7.1	4.7	5.3	10.0	3
Jasper	39.9790	-105.6628	3301	10.0	2.9	7.6	2.6	6.1	2.8	3.5	11.5	2
Lion 1	40.2319	-105.6386	3373	1.8	0.7	2.0	3.0	11.8	0.6	-	-	2
Lion 2	40.2376	-105.6417	3478	11.4	0.8	1.5	1.8	10.6	4.2	5.0	6.3	5
Long	40.0723	-105.5923	3253	7.0	1.3	16.4	13.1	9.9	3.3	3.1	12.0	3
Lost	39.9496	-105.6165	2987	4.0	10.0	2.0	0.2	13.7	5.0	3.3	39.0	3
Mills	40.2895	-105.6416	3030	8.4	0.5	5.8	12.1	17.0	1.4	3.5	-	2
Pear	40.1767	-105.6267	3226	16.0	3.5	6.5	1.8	12.7	6.4	4.0	8.3	5
Red Deer	40.1427	-105.6101	3163	20.0	6.1	5.9	1.0	12.3	3.9	5.3	10.0	3
Sky	40.2781	-105.6683	3322	7.2	1.9	4.1	2.2	7.8	5.6	3.0	10.0	4
Snowbank	40.2402	-105.6452	3512	8.5	1.8	2.9	1.6	10.0	2.9	4.5	7.3	5
The Loch	40.2926	-105.6562	3048	5.0	0.8	5.3	6.8	10.0	2.1	4.4	13.1	5

Thunder	40.2222	-105.6472	3225	16.2	2.0	6.0	3.0	10.7	5.5	3.3	-	2
Upper Diamond	39.9882	-105.6612	3463	3.5	1.0	0.3	0.3	6.3	1.8	3.2	18.3	3
Upper Hutchenson	40.1738	-105.6477	3412	3.6	1.0	2.6	2.7	9.3	2.0	-	-	2
Yankee Doodle	39.9375	-105.6538	3261	7.5	4.0	1.4	0.3	12.1	4.8	3.0	10.5	2

B4. A table of variable importance values for each iteration of the best regional climate model. Columns depict the output after each addition of one or two environmental variables at a time. All environmental variables examined were ranked as the top two most important variables. However, the overall C.V. R^2 of the model decreased with each addition of environmental variables.

	Best Model		**add temp**		**add N:P & temp**		**add N:P**		**add TDP**		**add NO3**		**add TDN**		**add DOC**	
	CV R^2		**CV R^2**		**CV R^2**		**CV R^2**		**CV R^2**		**CV R^2**		**CV R^2**		**CV R^2**	
	0.38		0.34		0.35		0.34		0.25		0.26		0.36		0.31	
	R^2		**R^2**		**R^2**		**R^2**		**R^2**		**R^2**		**R^2**		**R^2**	
	0.83		0.91		0.91		0.84		0.84		0.86		0.83		0.85	
Variable	**Rank**	**V.I.**	**Rank**	**V.I.**	**Rank**	**V.I.**	**Rank**	**V.I.**	**Rank**	**V.I.**	**Rank**	**V.I.**	**Rank**	**V.I.**	**Rank**	**V.I.**
Weekly precip.	1st	25.1	2nd	16.0	3rd	14.7	1st	17.6	1st	18.5	2nd	17.3	1st	20.1	1st	20.8
Monthly mean temp.	2nd	14.1	3rd	10.4	4th	9.7	3rd	10.7	3rd	10.5	3rd	8.6	3rd	11.3	4th	9.8
Daily mean temp.	3rd	13.8	4th	9.1		6.6	5th	8.5	5th	8.0	5th	7.1		7.9	5th	8.5
DOY	4th	10.5		5.7		5.2		7.1		7.6		6.9	4th	10.8		6.8
Temp. % normal	5th	10.5	5th	8.5	5th	7.2		7.0	4th	9.5	4th	8.0	5th	8.1	3rd	9.9
Precip. % normal		8.6		6.2		4.1	4th	9.2		7.0		5.8		6.2		7.0

Daily mean precip.	8.1		3.9		3.3		6.3		6.1		5.0		6.1		4.8	
Max. SWE	5.1		2.0		1.8		2.7		2.7		4.3		3.0		2.2	
Measurement depth	4.2		1.8		1.3		0.8		1.7		1.9		1.9		1.6	
temp	-	1st	26.7	1st	19.8		-		-		-		-		-	
DIN:TDP	-		-	2nd	16.0	2nd	17.3		-		-		-		-	
TDP	-		-		-		-	2nd	15.9		-		-		-	
NO3	-		-		-		-		-	1st	23.4		-		-	
TDN	-		-		-		-		-		-	2nd	20.2		-	
DOC	-		-		-		-		-		-		-	2nd	14.3	

B5. Top predictors from the Regional WS model and Regional Envt models. Top predictors were produced from a backward-selection process, whereby variables of low importance were removed until cross-validation (C.V.) R^2 values were maximized. Since these models had lower C.VR^2 values than the Regional Climate and Regional Climate + WS models, we did not focus our discussion on interpreting these model results.

WS variables C.V. R^2 = 0.31	**V.I.** (%)	**Envt variables** C.V. R^2 = 0.15	**V.I.** (%)
DOY	22.8	DIN:TDP	22.7
Max. lake depth	12.6	TDP	19.2
Drainage ratio	8.5	NO3	17.2
Elevation	7.9	Lake temp.	15.7
Change in snow cover ('92-'11)	6.5	TDN	8.0
Shrub cover (2011)	5.7	DOC	6.9
Lake SA	5.3	DOY	6.7
Snow cover (2011)	5.0	Measurement depth	3.7
Summer radiation	4.8		
Biotite-gneiss (%)	4.6		
East mean	3.8		
Measurement depth	3.5		
Rock glacier area	3.3		
Change in water cover ('92-'11)	3.0		
Longitude	2.7		

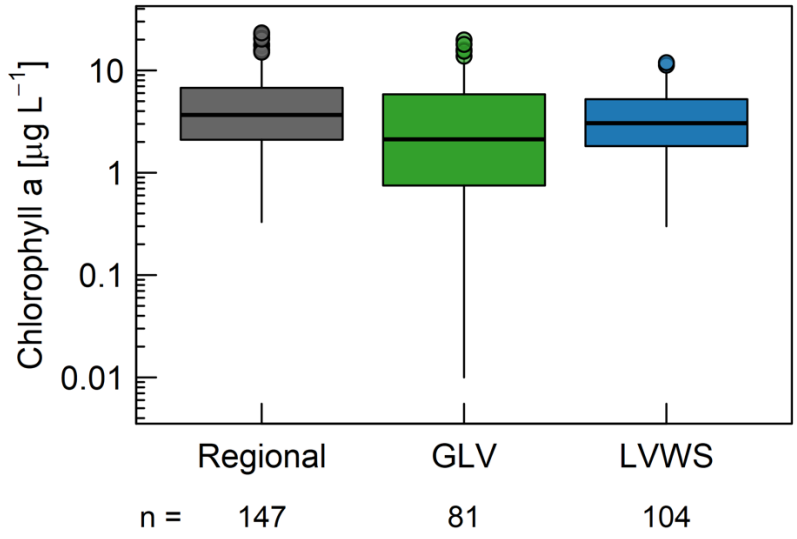

B6. Boxplot of measured chlorophyll a from each of the three datasets. The median of the Green Lakes dataset is significantly less than the Regional dataset, but no other differences are statistically significant. (p = 0.0016; Wilcoxon Rank Sum test with Bonferroni correction)

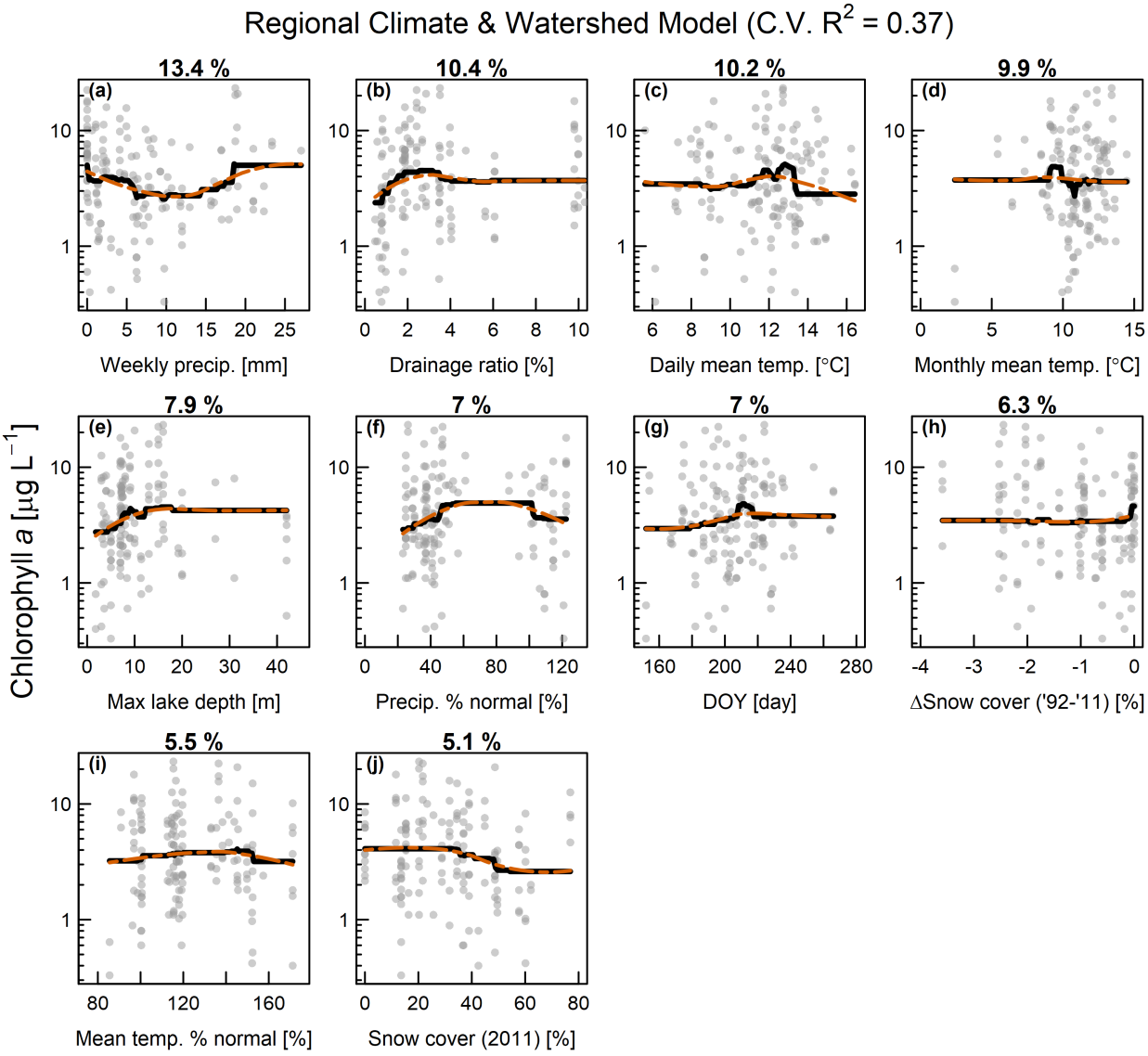

B7. Partial dependency plots of the predictor variables in boosted regression tree analysis from the best regional model with climate & watershed predictors (variable importance ≥ 5%) with the relative contribution of each variable printed at the top of each panel. The y-axis fitted function (black line) represents the effect of the selected variable on chl *a*, holding all other predictors at their mean value. The red dashed line is a loess curve fit to this relationship. Grey dots represent individual observations. Refer to Table 1 and Appendix B1 for predictor variable explanations.

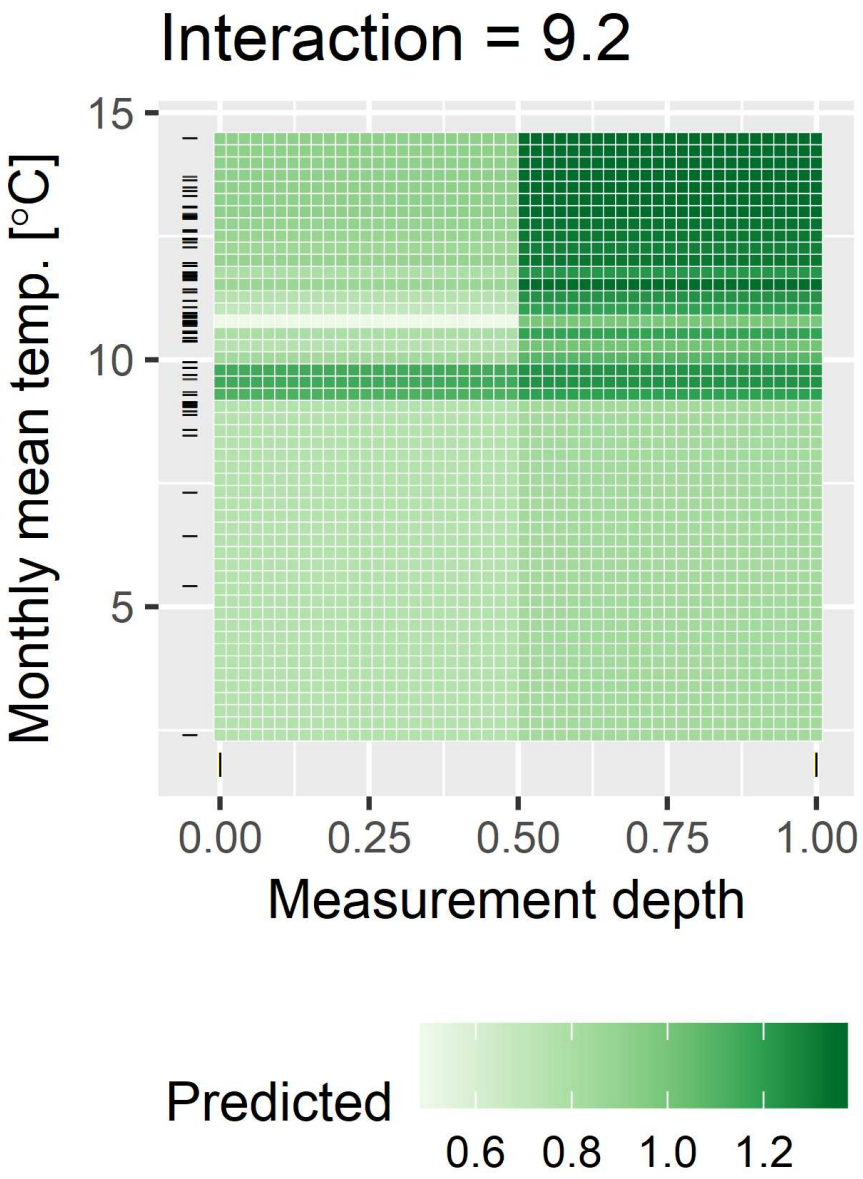

B8. Interaction plot from the best Regional Climate model for monthly mean air temperature and measurement depth (interaction strength = 9.2). Measurement depth is an indexing variable in which 0 = surface observations and 1 = hypolimnion observations. Colors are predicted log-chlorophyll *a* values. Hash marks along each axis indicate values of each variable from the regional lakes dataset.

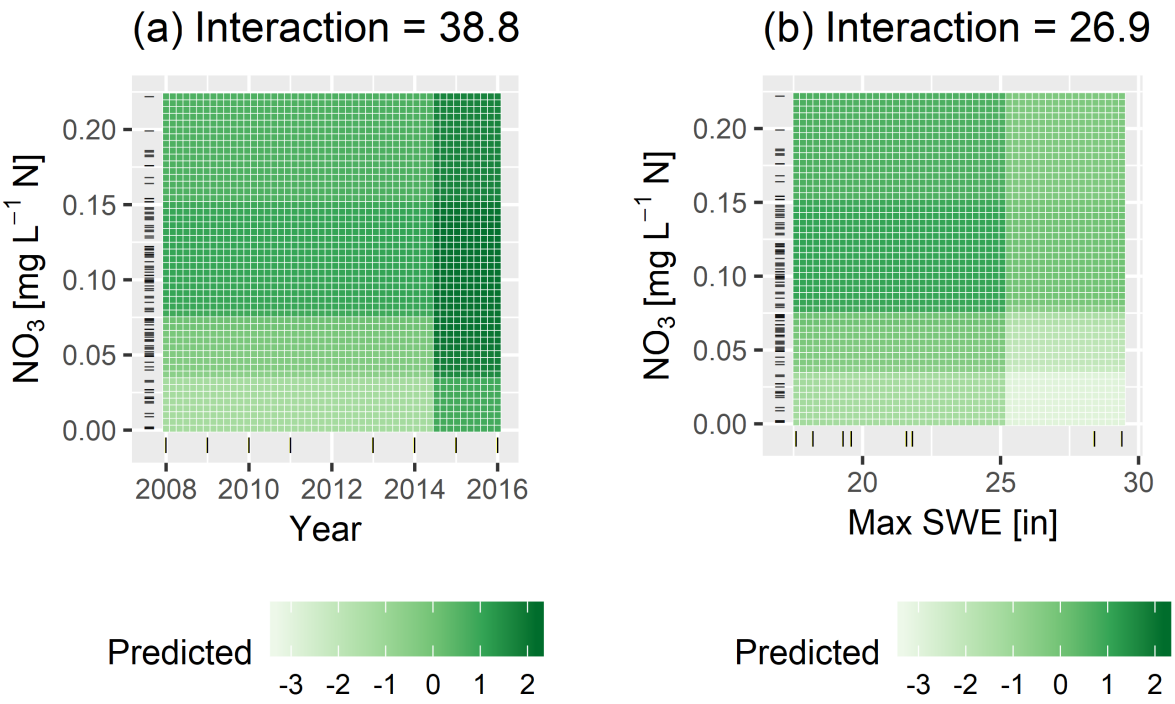

B9. Interaction plots from the best GLV model, ranked by interaction strength: (a) year and nitrate, (b) nitrate and maximum SWE. Colors are predicted log-chlorophyll *a* with darker shades corresponding to higher concentrations. Hash marks along each axis indicate values of each variable from the GLV dataset.

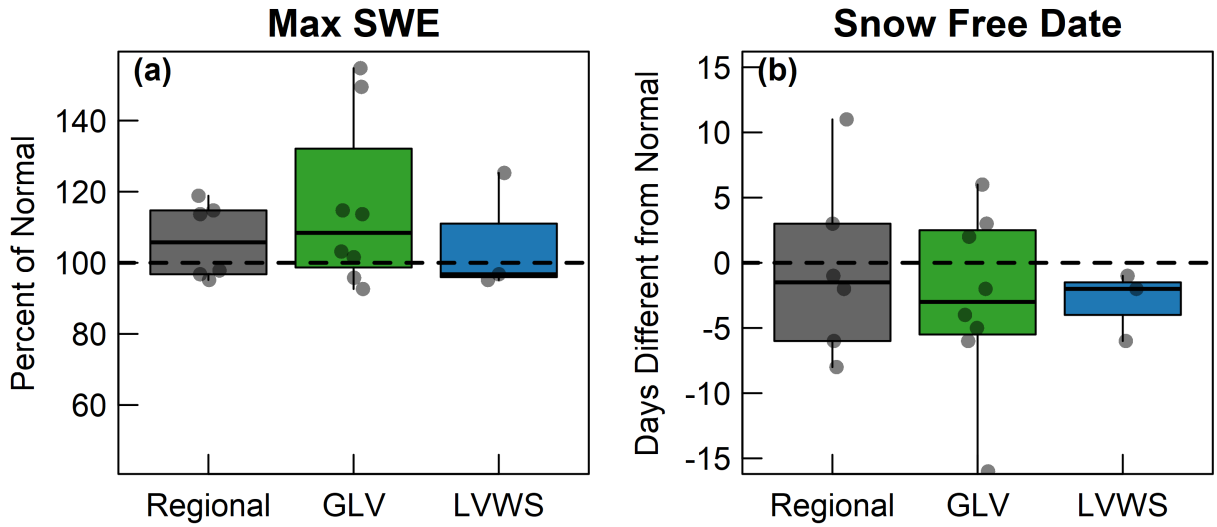

B10. Boxplots displaying maximum snow water equivalent (SWE) as a percent of normal (1980-2010) and the difference in the first snow free date as compared to normal (1980-2010). Data for the GLV and LVWS models were based on a single SNOTEL site for each model with data points representing a different year. Because many of the lakes in the All Lakes model are located close together, often times a single SNOTEL site represents multiple lakes. In general, the period of observation represented in these models had slightly above normal SWE but somewhat early melt-off.

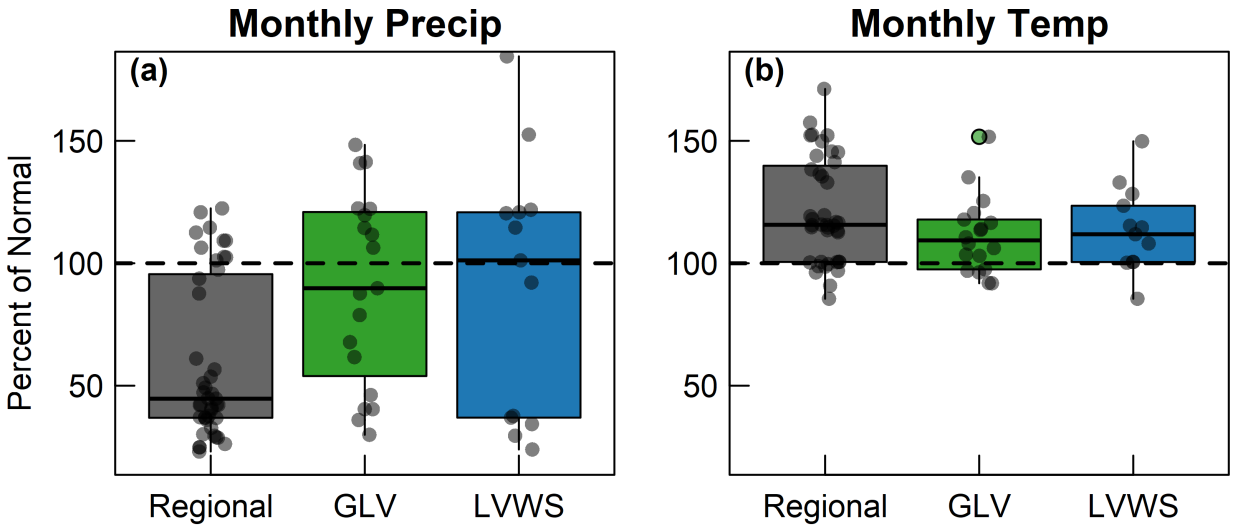

B11. PRISM climate data of monthly precipitation and temperature as a percent of normal (1980-2010). Generally, the period of observation was drier and hotter than normal.